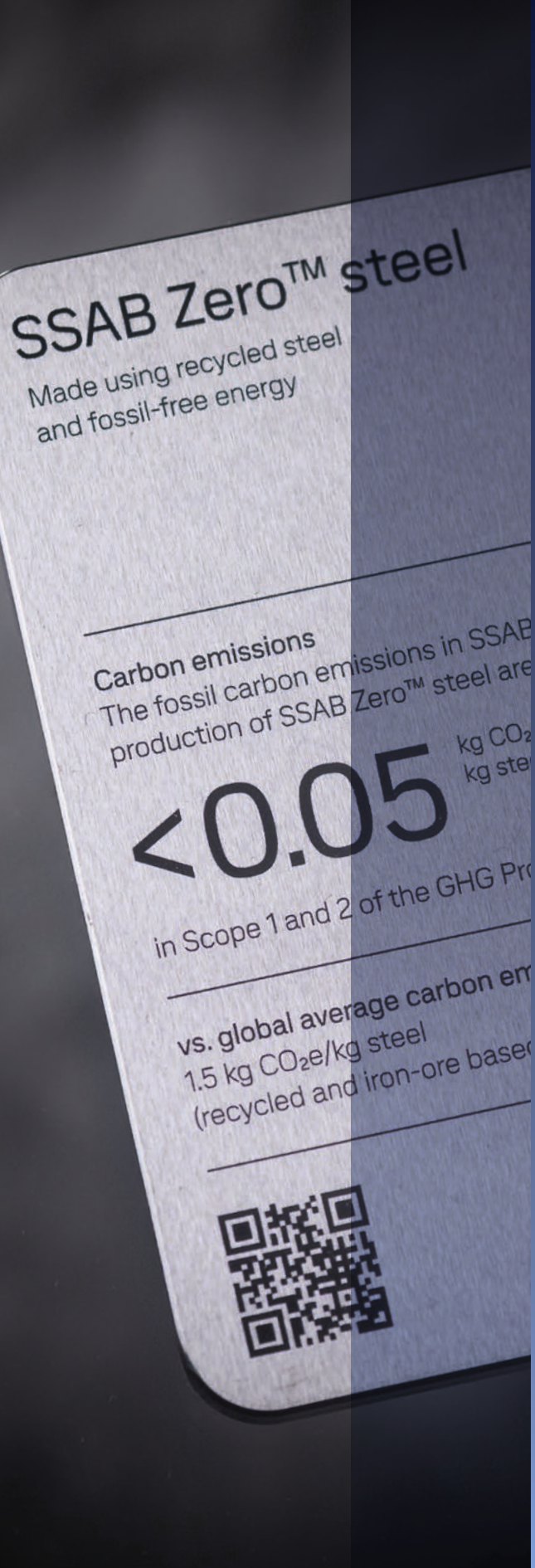

FOSSA2

FINAL REPORT 2026

FOSSIL-FREE STEEL APPLICATIONS

PHASE 2


FOSSA2

FOSSA2 - Fossil-free Steel Applications: Final report

Publisher and contact information
Macon Oy
Metsänkuninkaantie 3,
90250 Oulu, Finland
info@macon.fi

Editor
Maaru Moilanen, Macon Oy

Graphic design and layout
Sanni Salo, Muodo

Cover image
SSAB

Contents

Pasi Suikkanen
Chairman of FOSSA2 Steering Group
Product Development Manager
SSAB Europe Oy

INDUSTRY PREFACE

The FOSSA2 project was carried out during a period of major change in the industrial operating environment. Climate change mitigation, customers' growing demand for low-carbon products, and the need to safeguard the competitiveness of European industry created a strong need to renew material solutions and the manufacturing value chain. In this transformation, steel plays a central role: it remains a fundamental material for society and infrastructure, yet the steel industry is also among the world's most significant sources of industrial carbon dioxide emissions. FOSSA2 responded to this challenge by combining industrial practice, research, and application development into a single integrated effort.

The starting point of the project was the view that the transition to fossil-free steel was not only an environmental objective, but also a strategic opportunity to strengthen the position of Finnish and Nordic industry. SSAB's long-term goal of bringing fossil-free steel to market and achieving a phased renewal of production provided the project with a clear direction. In FOSSA2, this transition was advanced in practice by developing new fossil-free and low-carbon steel solutions, assessing their suitability for different applications, and building competence to support future industrial transformation.

A key strength of FOSSA2 was its broad and practical collaboration. In addition to SSAB, the project involved several industrial and research partners whose contributions were essential to the quality and impact of the results. Collaboration took place, for example, in the engineering workshop industry, maritime industry, and design sector, and participating partners included RMC, Ponsse, Hiab, John Deere, and Indalgo. In addition, universities and research organisations—such as the University of Oulu, Tampere University, and Lappeenranta University—provided deep expertise in metallurgy, modelling, and structural design. This cooperation ensured that the solutions developed in the project were concretely linked to industrial applications and customer needs.

During the project, it became increasingly clear that the fossil-free transition required more than the development of a new material. It required new thinking across the entire value chain: in design, manufacturing, material choices, energy efficiency, and end-use performance. In FOSSA2, this change was promoted by integrating material development, application development, and virtual design and modelling solutions. This created a foundation for an operating model in which new steels and their applications can be developed faster, in a more controlled manner, and more sustainably than before.

From the perspective of the final report, FOSSA2 was not only a single research and development project, but part of a broader industrial transformation in which the Finnish metal and mechanical engineering sector took concrete steps toward fossil-free value chains. The project strengthened cooperation between companies and research, expanded the shared competence base, and laid the groundwork for new products, applications, and future investments. At the same time, it demonstrated that ambitious climate action and industrial competitiveness can, at their best, reinforce each other.

From SSAB's perspective, FOSSA2 significantly supported the company's strategic renewal and reinforced the understanding that fossil-free steel and solutions based on it will constitute a future competitive advantage. At the same time, the project also created value for other participants by providing new knowledge and collaboration models, and by strengthening their capabilities to meet tightening sustainability and performance requirements.

I would like to express my thanks to all the companies, research organisations, experts, and individuals responsible for implementing the project. Special thanks go to the project's partners for their expertise, commitment, and practical perspective. The support of Business Finland was also crucial for the realisation of FOSSA2. The results of FOSSA2 created a strong foundation for further development, and the project's full impact will be seen in the work that continues afterwards in industry, research, and new forms of collaboration.

Antti Kaijalainen
Principal Investigator of University of Oulu FOSSA2 research
Associate Professor
Materials and Mechanical Engineering
University of Oulu

ACADEMY PREFACE

The Fossil-Free Steel Applications: Phase 2 (FOSSA2) project continued the uninterrupted transition towards fossil-free steel production and usage worldwide. This ambitious goal of anticipating and developing the use of fossil-free steel in Finnish industry has required extensive multidisciplinary metallurgical characterization and has also covered systematic research in regard to the usability of steels, enabling a new type of modeling utilization in the design and development of steels and steel applications. The project has further reinforced national competence in materials science, mechanical engineering, novel thermomechanical processing, and simulation-based design, while fostering deeper collaboration between universities, research organizations, and industrial partners beyond borders.

Based on its two-year achievements, FOSSA2 has strengthened both fundamental and applied research in several scientific disciplines and accelerated the process of green transition throughout the steel industry production value chain. The project has significantly expanded metallurgical characterization efforts quintessential to understanding the behavior of ultrahigh-strength steels, while also systematically investigating their usability in industrial processes. These include comprehensive research on forming behavior, weldability, and fatigue resistance properties that define the reliability, reproducibility, manufacturability, and long term performance of fossil-free steel in engineering applications. These research themes required not only advanced laboratory experimentation, but also unrelenting development and integration of new modeling tools to support material design and structural engineering.

FOSSA2 has also raised Finland’s position in international research networks related to sustainable steel production and applications. The consortium expertise has attracted collaborations in EU with research visits and exchanges, and joint use of specialized laboratory equipment across Europe and Asia. The impact on the academic world is huge: 25 master's and 13 doctoral theses and over 80 scientific publications and reports. These results highlight the strength of interdisciplinary collaboration, expanding the steel industry’s green transition while simultaneously confirming the importance of metallurgy and design within the academic research site.

Finally, I would like to thank the broader community of academics, researchers, students, and technical staffs, whose efforts have contributed to the desired goals and achievements of FOSSA2. Their passion and competence have invariably been vital to the success of this project.

How to read this report

- For the project background, structure and consortium, read **Project overview**.
- For a quick overview of the whole project, read **Project summary**.
- For work-package-specific achievements and their significance, read the **WP introductions**, **WP Key takeaways** and **Conclusions and next steps**.
- For more detailed descriptions of the research and company cases, read the main sections under **WP1**, **WP2** and **WP3**.
- For scientific outputs, see the **List of publications**.

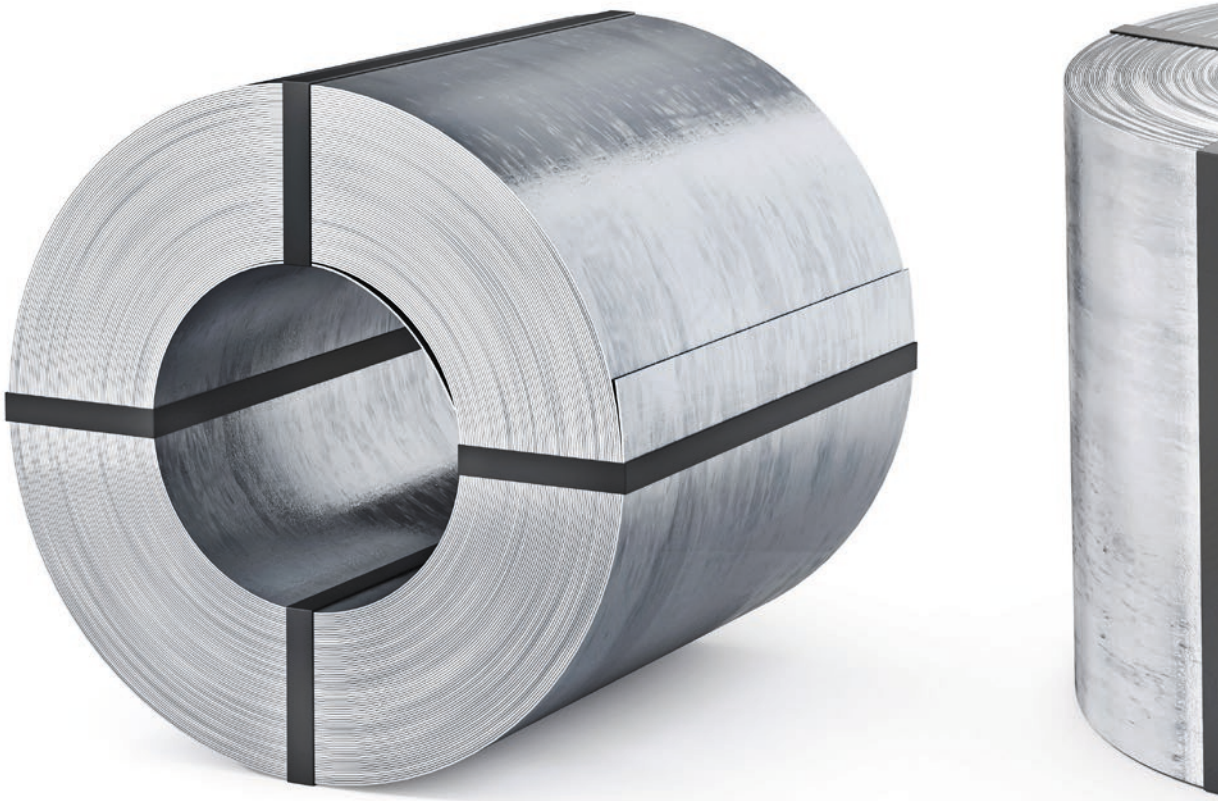

2. Project overview

FOSSA2 (Fossil-Free Steel Applications, Phase 2) was done in time when industry needed practical ways to reduce emissions, but still keep good performance and competitiveness. Steel is still basic material for many industries.

Main target of the project was to push fossil-free and low-emission steels to real applications, so that customers can use them without extra risk. Work was looking whole value chain. It looked how raw materials and recycling affect steel. It looked how chemistry and process affect properties. It checked how these things show in coating behaviour, formability and durability of product. At same time, project made better capability to predict results, so development work is more controlled and faster.

Important strength in FOSSA2 was cooperation. Beside SSAB, there were companies and research organisations, which brought practical needs and strong know-how in testing and modelling. Goal was to keep work close to real industrial questions, not only laboratory questions.

Work was divided to three parts. First part was focusing value chain of fossil-free steel and recycling. Second part was focusing applications and making sure fossil-free steel works in real products and supports business growth. Third part was focusing virtual steel production platform, meaning tools and models to understand and predict better how steel chemistry and process choices influence final properties.

Final result of FOSSA2 was clear. Project produced practical knowledge and tools, which help to take fossil-free steel to use in controlled way. It reduces technical risk in production and in customer interface. It makes development faster. And it gives good base for next steps and wider industrial use.

Pasi Suikkanen
Chairman of FOSSA2 Steering Group
SSAB Europe Oy

WP1:	WP2:	WP3:
Fossil-free steels' value chain and recycling	Fossil-free steel applications for economic growth	Virtual steel production platform

The FOSSA2 project consortium consists of six industrial partners and three research organisations. Industrial partners include: **SSAB Europe Oy**, **Hiab Finland Oy**, **Fortaco Ostrobothnia Oy**, **Ponsse Oyj**, **John Deere Forestry Oy** and **Indalgo Oy**, in addition to in-kind partners **Rauma Marine Construction Oy Ab**, **Kemppi Oy**, **Ramboll Finland Oy** and **Meyer Turku Oy**. The research organisations are **University of Oulu**, **LUT University** and **Tampere University**. **Macon Oy** acted as a project coordinator. The project was funded by **Business Finland** and the participating parties. The duration of the project was from 1/2024 to 4/2026.

3. Project summary

FOSSA2 advanced the transition toward fossil-free and low-emission steel applications by combining materials development, industrial usability and digital development tools. It addressed the wider conditions required for industrial use, including value-chain conditions, application performance, manufacturability, and the prediction of material and product behaviour. Across the project, the common outcome was a stronger foundation for introducing fossil-free and low-emission steels in a more controlled, reliable and industrially relevant way.

WP1 CLARIFIED THE ROLE OF FOSSIL-FREE STEEL IN THE VALUE CHAIN

The work strengthened the research and competence network around fossil-free steel and widened access to expertise in areas such as hydrogen technologies, steel metallurgy, value networks, weldability and steels in hydrogen environments. At the same time, the economic competitiveness of fossil-free ultra-high-strength steels was examined from the OEM perspective using AI-assisted information extraction and life-cycle cost modelling. This produced a preliminary value-chain model for forestry and marine case studies and an initial life-cycle cost framework for steelmaking and OEM applications. The results provide a clearer starting point for later feasibility and sensitivity analyses.

WP1 also made the product-level implications of lower-emission steel more concrete. Life-cycle work showed that steel with higher recycled content can reduce manufacturing-related emissions, while the overall environmental value still depends strongly on service life, maintenance, modernization and other lifecycle choices. The work also included a comparison of a lighter high-strength steel structure, which indicated clear potential to reduce product-level impacts. In load-handling equipment, the project translated this perspective into practical product-level work by producing Environmental Product Declarations, supporting eco-product development and creating an eco-calculator for product-level emissions assessment. Overall, WP1 clarified where fossil-free steel creates value, what still limits wider use, and how environmental and economic feasibility should be assessed across the value chain.

WP2 DEEPENED UNDERSTANDING OF HOW FOSSIL-FREE AND HIGH-STRENGTH STEELS PERFORM IN MANUFACTURING AND DEMANDING APPLICATIONS

WP2 produced important new knowledge on welding performance and welded-joint behaviour in demanding steel applications. The work showed that offshore welds met the required low-temperature toughness levels for arctic use and that beam-welded martensitic-austenitic AHSS retained very high fracture toughness at low temperatures. Research on TMCP steels showed that multiple steel grades can be produced from a single chemical composition by adjusting cooling conditions, while slower cooling was found to reduce HAZ toughness. Studies on dissimilar high-strength steel joints also clarified how HAZ softening, weld-bead geometry and residual stresses govern failure behaviour, while fatigue studies improved the assessment of welded components under variable loading and showed that weld extension techniques can further enhance fatigue strength. In addition, an industrially applicable adaptive robotic welding platform was developed, combining multisensor monitoring, synchronized data collection and digital shadow/twin functionality to support better traceability, control and future AI-based weld-quality prediction.

WP2 also made the forming and processing challenges of future high-strength steels more specific. In hot-rolled AHSS, good edge ductility was linked especially to a uniform grain structure. In medium-manganese steels, the best strength-ductility balance was reached only within a narrow intercritical annealing temperature range, which is directly relevant for industrial process control. The work also showed that rapid induction processing can create a hardened surface layer while retaining a softer core, offering an industrially feasible, energy-efficient way to improve bendability without reducing the overall strength of the steel. Rapid-annealing studies showed that copper and tin are unlikely to cause major property losses in future scrap-based sheet steels, although the highest copper level clearly increased strength. Overall, WP2 showed more clearly how processing route, local microstructure and residual elements shape the manufacturability of future low-emission high-strength steels.

WP2 also produced important results on hydrogen-related behaviour in high-strength steels. The hydrogen-related work on martensitic-austenitic AHSS showed that retained-austenite morphology, carbide structure and alloying all shape hydrogen diffusion, trapping and embrittlement resistance. It also showed that fine film-like retained austenite can act as a diffusion barrier rather than simply serving as a hydrogen trap. In welded pipeline steels, the work showed that hydrogen tolerance differs markedly between the base metal and the heat-affected zone, and that rapid cooling during welding produced microstructural features in the HAZ that modified hydrogen trapping behaviour and reduced the fraction of diffusible hydrogen. Together, these findings help define how steels and welded joints should be designed for hydrogen service.

WP2 also linked these technical results to industrial implementation. Company-level studies examined how fossil-free and high-strength steel solutions can be translated into product concepts, manufacturable structures and practical industrial use in vehicles, forestry machines and load-handling equipment. The work supported the development of low-CO_2 steel products, lighter structures and practical manufacturing concepts, and showed how the technical questions studied in WP2 connect to product development and manufacturability.

WP3 ADVANCED VIRTUAL TOOLS FOR MORE PREDICTIVE AND FASTER STEEL AND PRODUCT DEVELOPMENT

WP3 improved the use of modelling and virtual tools in steel and product development. In hot-strip processing, the work developed and validated an FEM model for induction heating that showed good agreement with dilatometry experiments. A dataset for future strip-thickness-profile prediction was created by using industrial data from more than 1000 coils from the SSAB Raahe finishing mill. This work provided a basis for future strip-thickness-profile prediction and for further development of hot-strip process modelling. Research on UHSS bendability showed that plane-strain tensile fracture strains correlated better with bending-derived fracture strains than conventional uniaxial tensile test fracture strains, and a new DIC-based method was developed for identifying fracture initiation in bending tests. These results improve bendability assessment before costly production trials.

WP3 also advanced simulation-based assessment of welded structures and welding processes. In fatigue assessment, the project further developed and validated a sequential finite-element

approach for welded high-strength steel joints. The results showed reasonable agreement with experiments for as-welded, overload and HFMI-treated conditions. In arc-welding simulation, new magnetohydrodynamic solvers were developed and validated as a basis for future three-dimensional prediction of weld geometry and temperature fields. This improves the ability to assess structural performance and welding outcomes virtually, before moving to expensive physical testing.

One result area was the development of practical virtual platforms and digital-service capabilities. A proof of concept for a virtual rolling platform, based on historical production data and coil-by-coil simulations, showed that simulation runs could be created, executed and reviewed in one environment. This is a concrete step toward faster development work, fewer production trials and better analysis of production deviations. In parallel, simulation and measured data were combined in equipment applications to support life estimation, fatigue evaluation and future digital services. Overall, WP3 produced tools that can speed up development, improve prediction of performance and support better industrial decision-making.

PROJECT IMPACT

FOSSA2 strengthened the expertise and collaboration base needed for fossil-free and low-emission steel applications in industry. The project expanded international research cooperation and competence networks, while producing new capabilities in metallurgical characterization, weldability, formability, bendability, fatigue and fracture assessment, hydrogen-related behaviour, value-chain analysis, and digital simulation environments.

The project clarified the conditions for wider industrial use across the value chain. It linked lower-emission steel not only to cleaner production, but also to manufacturability, product performance, life-cycle impacts and economic feasibility. This included results relevant to offshore and arctic steels, automotive and other high-strength steel applications, and overall lighter structures with lower material use and lower product-level environmental impacts.

Another important impact was the shift toward more predictive and controlled development. By combining AI, metallurgical knowledge and industrial data into digital solutions, the project created practical virtual and simulation-based capabilities for steel and product development. These support faster development work, fewer physical trials, better prediction of process and product behaviour, and more informed industrial decision-making.

The project also improved readiness for future steel applications in demanding conditions. Work on welded joints, fatigue resistance and bendability deepened understanding of how high-strength steels perform in manufacturing and in demanding use, and advanced further steel development for applications where reliability and long-term performance are critical. The project also produced new knowledge on hydrogen-related behaviour in high-strength steels and welded regions, helping to define how steels and welded joints should be designed for hydrogen service.

Overall, these results support industrial renewal and long-term competitiveness in the Finnish steel and metal industry, while also contributing to the wider green transition.

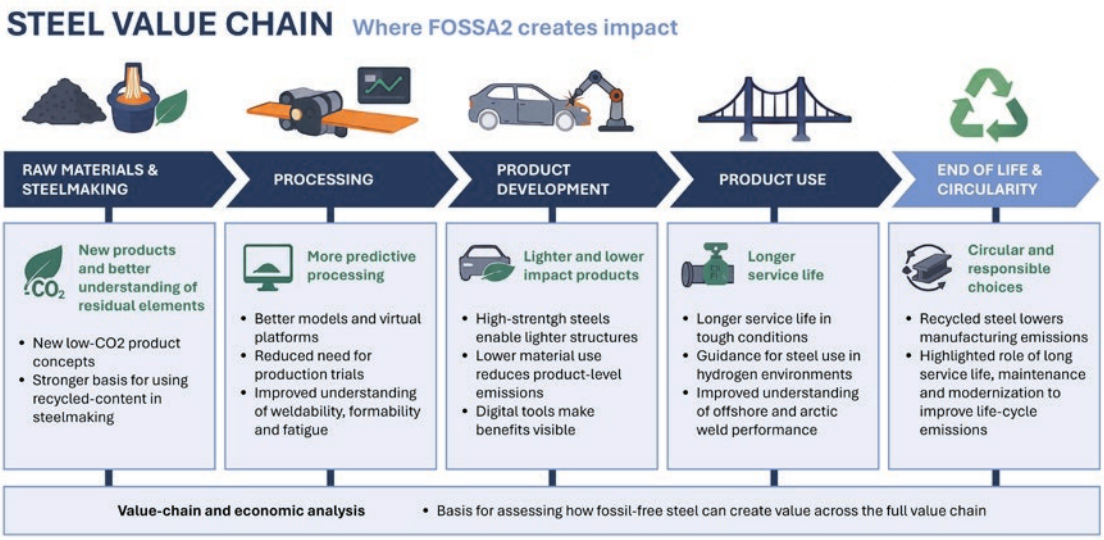

NEXT STEPS

The next phase should focus on validation, refinement and industrial scaling of the most promising results. Across the project, this means improving the reliability of economic and technical models, extending validation of welding, formability, hydrogen-related and simulation-based results, and continuing development of digital tools that support more predictive and controlled steel and product development. The next phase should also move the results further into industrial use, future investments and continued collaboration. This includes further development of fossil-free and low-emission steel solutions in real applications, stronger use of life-cycle and production data, and continued collaboration between research organisations and industry.

COMPANY HIGHLIGHTS

SSAB

- Proved fossil-free steel in real forestry-machinery and cargo-handling applications.
- Brought SSAB Zero products from development to launches and industrialised deliveries across several product families.
- Built new digital and tubular capabilities that support faster development and future hydrogen-infrastructure solutions.

HIAB

- Turned project results into three commercial eco-products: Performance package for Ultima, Ultima Zero and eUltima.
- Increased eco-portfolio sales from 8% to 34%, while tripling the number of eco-portfolio hooklifts sold.
- Delivered lighter hooklift concepts and digital tools that strengthen customer value, service business and future eco-product development.

FORTACO

- Showcased a fossil-free green-steel cabin concept at BAUMA.
- Built readiness to scale fossil-free steel into future serial production.
- Prepared next-generation investment plans for fossil-free high-strength cabins and structures.

PONSSE

- Built a fossil-free steel load-space demonstrator for the PONSSE Buffalo forwarder.
- Showed that SSAB's fossil-free steel performed flawlessly in Ponsse's supply chain, own production and in actual field tests.
- Strengthened readiness for future production use of fossil-free steel in forest machines.

JOHN DEERE

- Quantified how lower-impact steel choices can cut manufacturing emissions in forest-machine applications.
- Showed that advanced welding methods can support low-emission forestry-machine structures without compromising performance.
- Strengthened lifecycle-driven product development by linking sustainability, structural performance and machine data more closely together.

indalgo

- Created a working virtual steelmaking architecture in cooperation with partners, based on metallurgy, AI and real industrial data.
- Enabled faster, lower-risk and more energy-efficient steel development in a digital environment.
- Created a scalable foundation for future commercial deployment across multiple production sites.

Photo: Ponsse Plc

4. WORK PACKAGE 1
Fossil-free steels' value chain and recycling

Work Package 1 addresses fossil-free steels from the perspective of the steel value chain and recycling. Wider industrial use of fossil-free steels depends not only on material development, but also on economic competitiveness and on understanding their value in end-use applications. The reported work covers research cooperation on the fossil-free steel ecosystem, value-chain and cost-related analysis, and company-level application cases.

Fossil-free steel ecosystem and research cooperation	***What kind of research cooperation and expertise base supports fossil-free steel development?***

This section presents the wider fossil-free steel ecosystem and the research cooperation linked to it. The reported network brings together expertise in fields such as hydrogen technologies, steel metallurgy, energy systems, value networks, system analysis, weldability, and the behaviour of steels in hydrogen environments.

Economic competitiveness and value-chain conditions	*What conditions must be met for fossil-free ultra-high-strength steels to be used more widely in industry?*

Wider industrial use of fossil-free ultra-high-strength steels depends on economic competitiveness. Increased material costs may challenge the profitability of commercial applications. This section examines the issue from the OEM perspective, with particular attention to the mobile machinery and maritime industries. The reported approach combines AI-assisted information extraction with life-cycle cost modelling.

Practical product applications	*What role and value do fossil-free, recycled and high-strength steels have in practical product applications?*

Company cases address these questions at product level. SSAB's practical pilot cases show how fossil-free steel can be taken into practical use in the value chains of forestry machinery and cargo handling equipment. In the John Deere Forestry case, the work considers the environmental sustainability implications of changing the steel used in forest machines. Hiab investigates the customer value of fossil-free steel and its role in supporting eco-options for load-handling equipment. Ponsse participated by providing input to the work and by identifying useful findings and best practices related to fossil-free steel applications for future use.

Photo: SSAB

4.1 Fossil-free steel ecosystem

Contributors: **Jukka Kömi, Mahesh Somani,** University of Oulu

In globalized business, network economy expertise has become a critical success factor in all industries. It is an inevitable prerequisite for business success in a rapidly changing global situation and in a complex interaction context. International collaboration in FOSSA was a strategic approach adopted for improved competence and broad expertise available in relevant multidisciplinary fields to enhance project outcomes by leveraging diverse, cross-border skills, knowledge, and perspectives. As expected, such structured partnerships fostered new innovations, allowed for sharing of state-of-the-art equipment, cutting-edge tools and appropriate methodologies, and helped us address complex challenges as desired to meet the goals of the project, not to speak about the availability of resources and researchers, Figure 1.

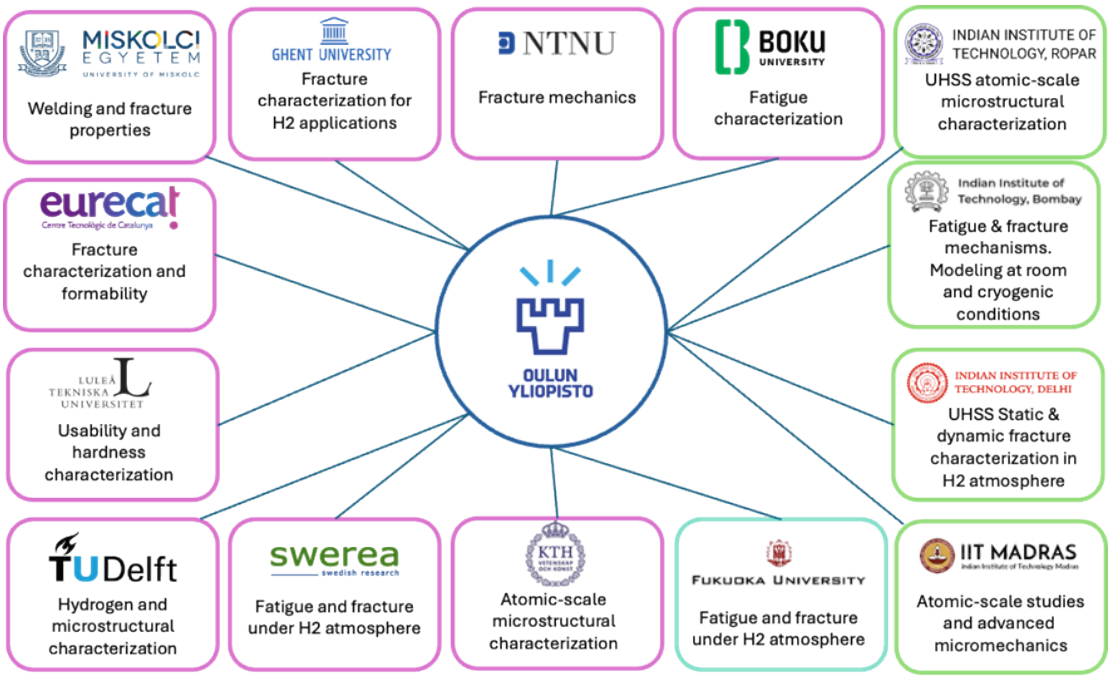

Figure 1. Cooperation network of University of Oulu Materials and Mechical Engineering (MME) in FOSSA projects.

The cooperation in Sweden is focusing to **Luleå Technical University (LTU)** and **KTH Royal Institute of Technology**. This research consortium brings together leading experts in Finland and Sweden, ensuring a multidisciplinary approach to fossil-free steels. It will be focusing on the whole value chain of steels, like hydrogen technologies, steel metallurgy and energy systems, value networks, system analysis and ecosystems. The consortium has the knowledge, infrastructure and collaboration networks needed to drive innovation and scale up sustainable solutions. The cooperation is now at the agreement phase.

As a part of the MME's International Strategic Partnership Development programme, **India** cooperation has started. The focus institutes are: Indian Institute of Technology (IIT) Madras, IIT Delhi, IIT Bombay and IIT Ropar, see Figure 1. The main idea was to promote research cooperation

in several strategic areas including Hydrogen future, Green Transition, Sustainable Steel and Clean Energy. Research collaboration has also been expanded with **University of Miskolc** and **TU Delft**. Miskolc research themes have focused on weldability, physical metallurgy of welding and the usability of steels, while Delft's main idea has been on the properties of steels in a hydrogen environment.

Photo: Ponsse Plc

4.2 Competence of FFUHS steel applications

Contributors: **Antti Ylä-Kujala[1], Toni Tani[1], Antti Ahola[2], Tuomas Skriko[3], Timo Kärri[1]**

[1] Industrial Engineering and Management, LUT University, Finland
[2] Steel Structures, LUT University, Lappeenranta, Finland
[3] Welding Technology, LUT University, Lappeenranta, Finland

Correspondence: **Antti Ylä-Kujala,** antti.yla-kujala@lut.fi

BACKGROUND

Extensive industrial utilization of novel fossil-free ultra-high-strength steels (FFUHSSs) requires economic competitiveness. In a previous interview and survey study, it was clearly indicated that in the current state, production costs are of vital importance for original equipment manufacturers (OEMs) in steel ecosystem (Kummala, 2021). Consequently, increasing material cost associated with newly developed fossil-free steel products challenges the economical profitability of commercial fossil-free steel applications, while technologically they provide substantial step towards green deal in steel production. In this task, the steel production ecosystem is identified from the OEM perspective, with a focus on the mobile machinery and maritime industries, to identify the barriers that hinder the breakthrough of fossil-free steel applications.

METHOD

AI-assisted information extraction

The primary aim of generating business ecosystem profiles and visualizations is to augment decision-makers' understanding of complex public narratives and provide a "critical strategic imperative" for navigating hypercompetitive environments (Basole et al., 2024; Tani et al., 2025). Data sources generally include public databases, press releases, news articles, company reports, social media, and other relevant private or open-source materials, which can be used in an AI-assisted information extraction process to identify, retrieve, and structure data.

AI tools were used to accelerate source screening, passage retrieval, and schema-based data extraction for life-cycle costing (LCC) and assessment (LCA) inputs. At the same time, all model-generated values remained subject to provenance checks and human validation before inclusion in the final assessment. This design follows AI-automated information extraction and a hybrid human-in-the-loop strategy that avoids treating the LLM as an ungrounded source of truth (Motamedi et al., 2026).

Life-cycle cost modelling

A life-cycle model (LCM) was created to better understand the competence of FSUHS steels from an economic perspective. LCM is based on life-cycle costing (LCC) approach and common investment appraisal methods (present value, discounted cashflow) that are designed to support sound capital budgeting decisions and cashflow analyses. A common criterion in LCC approaches is the consideration of the time value of money, which is achieved in the developed model by discounting annual cashflows to appraise cost and revenue items that occur in the future in relation to the actual decision-making point. The discounting of cashflows uses the weighted average cost of capital (WACC) method, reflecting organization’s preferred sources of funding (i.e., debt/equity).

A multi-actor modeling logic is also applied in the LCM in such a way that cashflows are formulated separately for a FSUHS steel manufacturer and its selected OEM customers from forestry and marine industries that utilize FSUHS steel in their products (e.g., forest harvesters, vessels). The cashflows are comprised of sales revenue, capital expenditure (CAPEX), and operational expenditure (OPEX), all itemized for each company separately. For the FSUHS steel manufacturer, the LCM considers, for instance, the cost and consumption of scrap steel, DR pellets, ferroalloys, and hydrogen as the reducing agent. It should be noted that CAPEX-related fields in the model can be omitted if investments in new manufacturing equipment are not required when moving from traditional steel to FSUHS steel. The net cashflow (NCF) for each company is formulated as follows:

$$NCF = CCF_{Revenues} - (CCF_{CAPEX} - CCF_{OPEX})$$

where CCF is the cumulative cashflow.

RESULTS AND FINDINGS

AI-assisted information extraction

Two case studies from two different industries were selected for a deeper analysis: forestry and marine. Using the human-in-the-loop AI strategy, we gathered over 200 input sources related to the fossil-free steel value chain and its business ecosystem, including mainly LCC data values, as well as some LCA data parameters. A preliminary structure of the steel production value chain was identified, after which the associated data were iteratively refined with AI to improve and expand the dataset.

Figure 2 presents the steel production value chain for the two case studies that were selected. AI-identified additional data mainly related to the HYBRIT scenario, based on the fossil-free steel value proposition were implemented in the analysis. In future research, the downstream ecosystems and value chains for both case studies can be further linked using these data, including their downstream effects on LCC results.

This research has already demonstrated meaningful productivity gains from using LLMs to integrate unstructured data into LCC semantics, although the process remains only semi-automated.

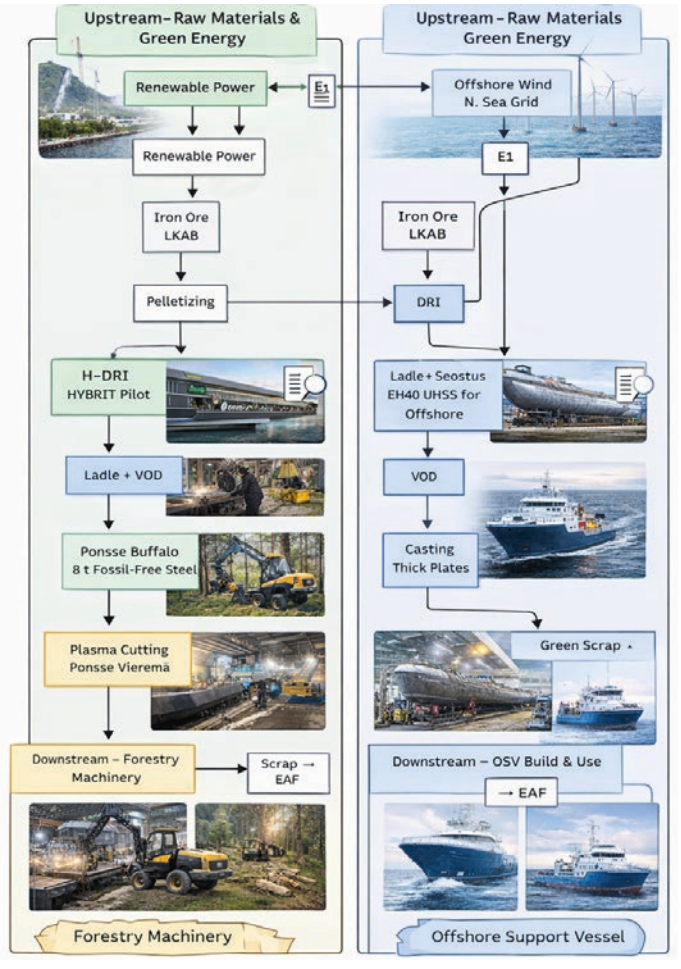

Figure 2. Fossil-free steel production ecosystem across the two case studies.

Life-cycle cost modelling

The developed LCM is comprised of three sheets, “UHSS LCC”, “OEM LCC” and “Dashboard”, where input parameters, model calculations and results are presented. UHSS LCC retains LCC calculations for the FSUHS steel manufacturer, while equivalent LCC calculations for the forestry and marine sector equipment manufacturers are contained in OEM LCC sheet. Dashboard compiles model results on one compact sheet in an understandable and visual format as illustrated in Figure 3. It should be stressed that the results depicted in the figure are preliminary and based on insufficient, non-uniform data that has been compiled with AI tools and therefore not yet verified manually. At this point, it can be concluded that the structure of the developed LCM is very close to final, and proper feasibility analyses for FSUHS steel will be carried out at a later stage. These analyses include proper sensitivity analyses on key modelling parameters, such as price data on FSUHS steel and hydrogen.

		End Value							
UHSS		**20**	*0*	*1*	*2*	*3*	*4*	*5*	*6*	*7*
Net cashflow	**TEUR**	-6 269 236	-2 419 864	-2 821 200	-3 187 383	-3 521 491	-3 826 334	-4 104 476	-4 358 255	-4 589 805
Lifecycle cost	TEUR	21 927 953	4 025 677	5 892 171	7 595 177	9 149 014	10 566 749	11 860 302	13 040 552	14 117 422
Accrued quantity	t	19 573 397	2 007 286	3 838 714	5 509 743	7 034 404	8 425 518	9 694 783	10 852 871	11 909 521
Cost price	**EUR / t**	1 120	2 006	1 535	1 378	1 301	1 254	1 223	1 202	1 185
Value add	EUR / t	-320	-1 206	-735	-578	-501	-454	-423	-402	-385
FOREST		**20**	*0*	*1*	*2*	*3*	*4*	*5*	*6*	*7*
Net cashflow	**TEUR**	74 279	-75 325	-61 674	-48 975	-37 162	-26 174	-15 952	-6 443	2 403
Lifecycle cost	TEUR	485 445	125 325	158 185	188 753	217 189	243 640	268 246	291 135	312 427
Accrued quantity	units	560	50	97	140	180	217	252	285	315
Cost price	**EUR / unit**	867 293	2 506 500	1 639 030	1 350 377	1 206 427	1 120 357	1 063 226	1 022 631	992 369
Value add	EUR / unit	132 707	-1 506 500	-639 030	-350 377	-206 427	-120 357	-63 226	-22 631	7 631
MARINE		**20**	*0*	*1*	*2*	*3*	*4*	*5*	*6*	*7*
Net cashflow	**TEUR**	83 479	-86 125	-52 474	-39 775	-27 962	-16 974	-6 752	2 757	11 603
Lifecycle cost	TEUR	636 245	276 125	308 985	339 553	367 989	394 440	419 046	441 935	463 227
Accrued quantity	units	513	3	50	93	133	170	205	238	268
Cost price	**EUR / unit**	1 240 911	92 041 667	6 240 665	3 659 837	2 766 285	2 313 888	2 041 196	1 859 274	1 729 557
Value add	EUR / unit	162 815	-22 041 667	-1 059 829	-428 711	-210 201	-99 572	-32 888	11 600	43 321

Figure 3. NCF and profitability of FFUHSS applications.

IMPACT OF THE WORK

Using AI approach, over 200 heterogeneous data sources were structured into a preliminary FFUHSS value chain model for forestry and marine case studies, enabling faster integration of unstructured LCC and limited LCA data. AI-assisted refinement expanded the dataset, including HYBRIT-related parameters, and supported development of a preliminary LCC model for UHSS steelmaking, OEM, and dashboard components. Although results remain preliminary due to non-uniform data, the work demonstrates notable productivity and economical possibilities, and establishes a robust foundation for future feasibility and sensitivity analyses.

NEXT STEPS

Data reliability and refinement of the LCC models and their outputs based on the validated data should be carried out. At the time this report being published, the task continues in LUT-FOSSA2 project with the finalization of the research actions and drawing the final remarks and conclusions from the findings.

REFERENCES

Basole, R. C., Park, H. & Seuss, C. D. (2024). Complex business ecosystem intelligence using AI-powered visual analytics. *Decision Support Systems*, 178, 114133. https://doi.org/10.1016/j.dss.2023.114133

Kummala, E. (2021) *Sustainability values in metal industry* (in Finnish). Bachelor's thesis, LUT University. Accessible: https://urn.fi/URN:NBN:fi-fe2021052131137

Motamedi, E., Novalija, I. & Rei, L. (2026). Semi-Automatic Hierarchical Taxonomy Creation from Existing Taxonomies with Large Language Models. *Business & Information Systems Engineering*, 68, 35–37. https://doi.org/10.1007/s12599-025-00982-y

Tani, T., Yläkujala, A., Metso, L., Sinkkonen, T. & Kärri, T. (2025). Prompt Engineering P2X Business Ecosystem with Generative AI. *Procedia Computer Science*, 256, pp. 20–27. https://doi.org/10.1016/j.procs.2025.02.091

4.3 Industry partner contributions

4.3.1 SSAB Europe Oy

Contributor: **Pasi Suikkanen,** pasi.suikkanen@ssab.com

Pilots for SSAB fossil-free steel (forestry machinery and cargo handling)

BACKGROUND

The target of task was that. Fossil-free steel must not stay only as a concept. It must be used in real products and real work. Because of this, SSAB supplied fossil-free steel to selected partners and the first pilots were done together.

In this work the focus was on two value chains. The first was forestry machinery, where loads are heavy and the equipment must last for a long time. The second was cargo handling, where strength and usability of structures are critical.

METHOD

The work was done through practical pilots with partners.

SSAB supplied fossil-free steel to Ponsse. The steel was used in a forestry machine structure, to confirm that the material works in demanding use in the same way as conventional steel. SSAB did a similar pilot in cargo handling together with Hiab. A hooklift component was made using fossil-free steel. This showed that the material can also be used in this type of structure and product.

RESULTS AND FINDINGS

Based on the pilots, fossil-free steel could be used in real products in forestry machinery and cargo handling. The cooperation with Ponsse gave a concrete example that fossil-free steel is suitable for forestry machinery use. The cooperation with Hiab gave a concrete example of a cargo handling product made using fossil-free steel.

IMPACT OF THE WORK

The main impact of WP1 was that fossil-free steel was taken to real use early. This reduced uncertainty and increased confidence that the material also works in demanding structures. At the same time, the pilots helped SSAB and the partners to understand what the use of fossil-free steel means in practice for the product, manufacturing, and the full value chain.

NEXT STEPS

The next step is to expand from single pilots to wider structural parts and more products. In addition, clear practical rules are needed on how fossil-free steel is taken toward stable supply and series production when availability grows.

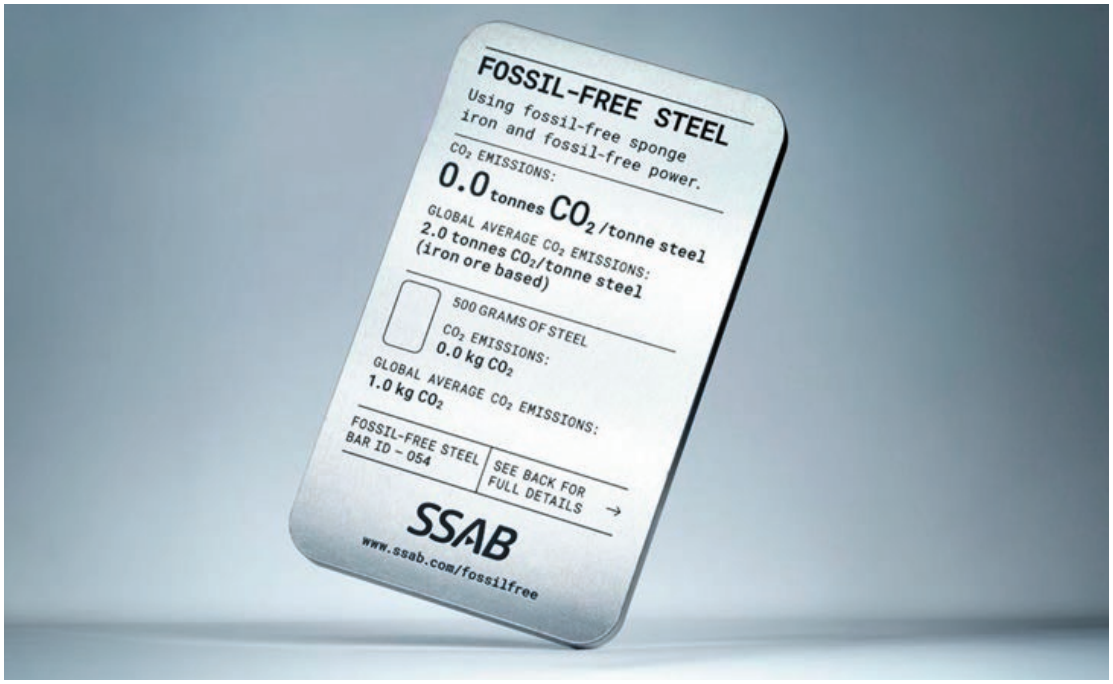

Figure 4. SSAB Fossi free steel using fossil free sponge iron and fossil free power.

4.3.2 John Deere Forestry Oy

Contributors: John Deere Forestry Oy, Comatec Mobility Oy

Correspondence: Aleksi Surakka, aleksi.surakka@comatec.fi

BACKGROUND

Fossil-Free Steel Applications – Phase 2 Work Package 1 (WP1) focused on the environmental sustainability possibilities related to changing the steel used in forest machines. The goal was to map out the environmental impacts related to new forest machine products and search for solutions to reduce the impact. Special steels, recycled steels and fossil-free steels were inspected as the key elements to address the impact.

Previous studies made at John Deere Forestry have revealed steel to be one of the major contributors to negative environmental impacts when looking at overall impacts related to the life cycle of forest machines. The main contributors to environmental impacts are the raw materials associated to the forest machine and the use phase diesel consumption. WP1 focused especially on the raw materials and more so to the steel used in the machine to better understand how changing the steel type or addressing steel life cycle could change the environmental impact of the forest machines manufactured by John Deere Forestry.

METHODS

To measure the effect when changing the used steel types, a Life Cycle Assessment (LCA) as guided by ISO 14040 and ISO 14044 was conducted for two different forest machine models. The goal was to map out the whole life cycle or Cradle-to-Grave impacts for 14 years of use.

Parallel to the LCA an End-of-Life (EoL) recyclability calculator was established in line with ISO 16714. The calculator was made for internal purposes to assess recyclability and reusability potential of forest machine materials at the end of its useful life.

Market research was done to find different steel possibilities. As John Deere Forestry mainly uses SSAB steel products, SSAB products available were more closely inspected. The Environmental Product Declarations (EPD) produced by SSAB were studied.

Interviews with and site visit at steel manufacturer were conducted to see current steel manufacturing practices and understand how the steel industry sees environmental matters developing in their sector.

Market research was also conducted to see how other circular practices such as modernization or remanufacturing are currently being adopted globally and in forest machine aftermarkets. Interviews were also done for forest machine users to raise awareness but also to understand the market readiness for circular practices.

Interviews with and site visit at EoL operator provided more context of how heavy machinery is currently being disposed of and what is the outlook for recycling in the future.

Indirectly linked to fossil free steels and their value chain, the possibilities related to Digital Product Passports (DPP) were recognized during WP1.

RESULTS AND FINDINGS

Majority of modern forest machines is built from steel. A material division was established during the LCA and the results are shown in Figure 5.

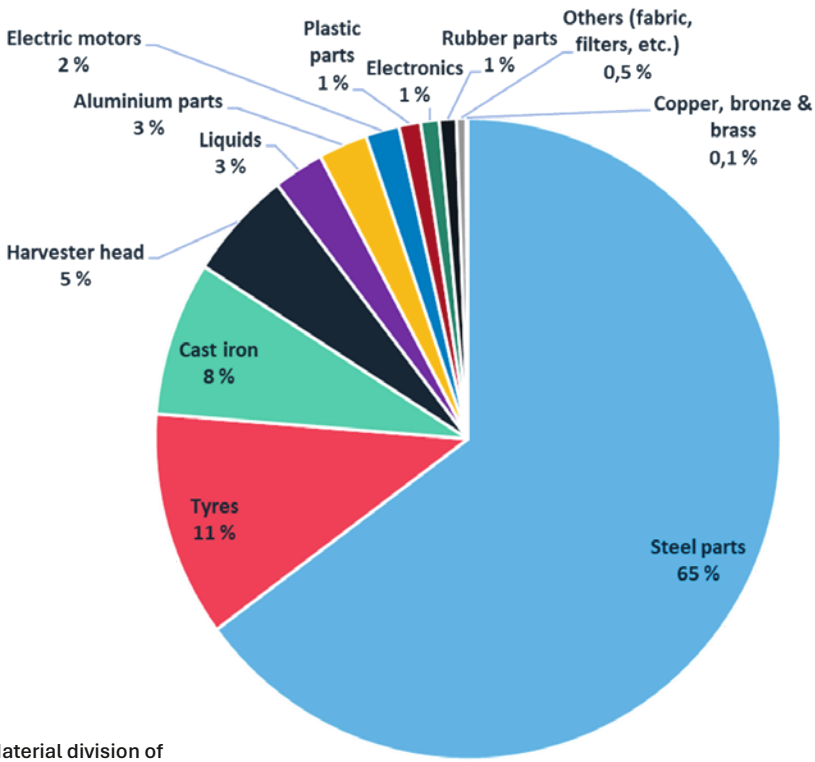

Figure 5. Material division of a forest machine

Addressing steel is an important factor. Using steel with more recycled inputs has good potential to reduce product manufacturing related emissions. When looking at Cradle-to-Grave emissions the reduction offered by switching to steel with less negative impact has seemingly marginal effect on a single product level. However, if looking at all forest machines manufactured on an annual basis, the reduction potential is promising. When compared only as a material, zero steel when compared to average steel, the reduction potential in Global Warming Potential (GWP) impact category is 60-75% less kgCO_2-eq per manufactured kg. Note that the GWP factor used for these studies was in line with IPCC 2021 and thus the potential benefit from biogenic carbon is not accounted for in the results.

One comparison was made where all used steel plates in one of the main components of the forest machine, the boom and frame, was replaced with SSAB Zero Steel Plates to see the effect on manufacturing environmental impacts. In GWP category the reduction was approx. 8% from the original result in Cradle-to-Gate or manufacturing related emissions which cover the raw materials, transportation of the raw materials and manufacturing activities. The components where the changes were applied and result comparison is shown in Figure 6.

SSAB Zero steel was used as an input for Front Frame, Rear Frame, Main Boom, and Extension boom in the LCA study

Impact category	Unit	1270H Assembly	1270H Assembly with SSAB Zero	Difference (compared to original)
Climate change - Fossil	kg CO2 eq	1,27E+05	1,16E+05	-8 %

Figure 6. Highlighted parts where SSAB Zero steel plates were used in the LCA model to replace current steel material. Table below the figure shows the results.

There was a goal to examine the fossil free steel possibilities as well but after searching and requesting related results the comparison could not be made as there were no verified or stated GWP results for fossil free steels. Fossil free steels are claiming to be close to zero result in GWP category, but no public information is yet available.

Another material-specific comparison made with special steels where the existing design was replaced with a lightweight version made from high-strength steel showed also good promise

on a smaller scale. Almost 50% of the impacts were reduced for this particular component by reducing the weight of it and by changing the logistics route to a nearer location. However, what was not and could not be assessed was the environmental impact associated with high-strength steels which according to interviewed steel manufacturers require a higher energy input during manufacturing as well as a different recipe to achieve the desired mechanical properties. Thus, the comparison is limited.

The request for fossil free steel specific information was also noted at the steel manufacturer's, SSAB, site. As publicly announced, the fossil free steel production is slowly ramping up, and investments are being made to both Finland and Sweden. However, as there is no actual data on fossil free steel production at scale, it is hard for SSAB to provide reliable results at this point. The showcased steel manufacturing plant offered a good insight into the steel making process and raised the understanding that current technology cannot fully support fossil free or recycled steel manufacturing. Future investments are made to increase the amount of recycled steel inputs use possibilities.

In both cases, the steel manufacturer and later with an EoL operator, a similar challenge was stated for steel recycling: Quality of the recycled input needs uniformity which is challenging to achieve. Highly contaminated steel or steel scrap with high copper inputs influence the end product quality and for example the mechanical properties desired could become compromised. Current EoL in Finland could follow the process as shown in Figure 7.

EoL operator did not see potential in steel sorting done by the product manufacturer as the scrapping process remains the same. The idea of retrieving important components during the EoL process was seen as doable but should be considered carefully from feasibility perspective. Overall, the EoL process is tied to geographical locations and readiness of the facility where the EoL could occur. When inspecting the EoL possibilities it became more clarified that the best environmental and economical impact is made by ensuring long life cycle with effective maintenance and modernization possibilities.

By searching information from forestry markets and heavy machinery industry it seems that forest machines are not heavily regulated from environmental perspective. Sustainability frameworks aimed to products currently focus more to the battery, textile and construction product industries. This was further backed up by arranging a user oriented live questionnaire at a forestry fair in Finland. The questionnaire provided an overview that sustainability is seen as a good thing, but it must be cost effective and more so reduce costs rather than increase them. Entrepreneurs and machine users stated in a conducted interview/questionnaire that they would be ready to invest in remanufactured components if the guarantee remains the same while the cost decreases. Otherwise, the importance of usability and availability were seen as important factors on a product level. Larger scale operators seemed to agree during an interview, and the new products sourced had relatively short operational lifespans before a switch to a newer model occurs.

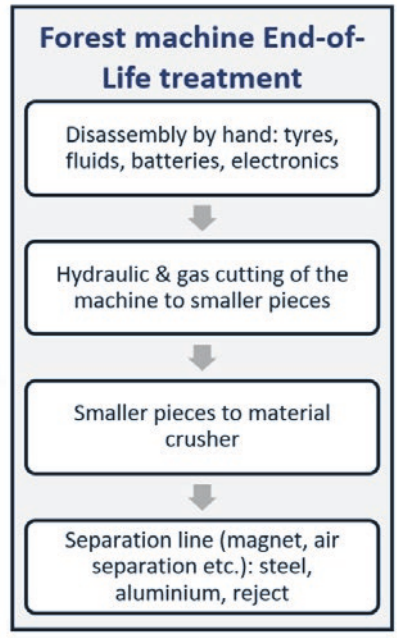

Figure 7. Forest machine End-of-Life flowchart.

IMPACT OF THE WORK

The work carried for WP1 has educated John Deere Forestry about the full steel value chain and its effect on life cycle impacts of a forest machine. As the knowledge of

low impact steel increases, John Deere Forestry is more capable to make meaningful changes in their product strategy when and if needed.

There seems to be a growing internal interest in testing low impact steel products for forest machines, and the measuring point and value chain mapping has now started effectively. The limitations regarding market availability and technical properties have been identified which make the communication between steel suppliers and the machine manufacturer easier. Using fossil free or low impact steels is not yet a clear priority in John Deere Forestry's customer base as the most relevant factors are related to the usage of the product. Steel therefore is a mean to ends product and the mechanical properties are seen more important than the environmental impact. Reducing steel impact is an important goal for John Deere Forestry to reduce organizational impacts.

John Deere Forestry recognized the importance of product level and especially life cycle data in environmental impact assessment during the project. Understanding full supply chain from single steel parts to complex welded or machined structures offers the best route to address environmental impact so that it will also serve economical interests.

NEXT STEPS

Next step for John Deere Forestry is to start assigning changes to steel components into the product and collecting the related digital data so it can be linked to the product. Main development routes are fossil free steels, recycled input steels and high-strength or special steels. Even though this type of data cannot be fully employed or is not in the full interest of the market, it opens the route for John Deere Forestry to enhance their product development efforts.

The importance of life cycle data is now highlighted and shown it's potential on a product level. Scaling from product level to the organizational level will be the next step for John Deere Forestry. Continuing developing product digital data collection and sharing methods will serve in a key position for this type of development. Circular steel has shown it's promise and circularity shall be inspected in a larger scale in the future.

As the EoL of a forest machine is now mapped out more carefully it has shown that the extension of the life cycle for machines is the best alternative for John Deere Forestry. The focus from this point forward will be on life cycle extension and working towards methods that avoid the final EoL processes.

REFERENCES

Ecoinvent. (2023). Ecoinvent database (Version 3.10). Ecoinvent Association.

Heikinmaa, L., & Surakka, A. (2025). *Life cycle assessment of John Deere 1270H harvester*.

Comatec Mobility Oy.

International Organization for Standardization. (2006). ISO 14040:2006 *Environmental management—Life cycle assessment—Principles and framework*. ISO.

International Organization for Standardization. (2006). ISO 14044:2006 *Environmental management—Life cycle assessment—Requirements and guidelines*. ISO.

SSAB Europe Oy. (2025). *Environmental product declaration: Hot rolled steel plates* (EPD IES 0022733).

SSAB Europe Oy. (2025). *Environmental product declaration: Hot rolled SSAB Zero™ steel plates* (EPD IES 0018716).

SSAB. (2026). *Fossil-free steel*. https://www.ssab.com/en/fossil-free-steel

4.3.3 Hiab Finland Oy

Contributors: **Matti Randelin, Lauri Era, Janne Enlund, Pauli Siivonen**
(Hiab Finland Oy, Demountables & Defence Division)

Correspondence: **Matti Randelin**, R&D Manager, Control Systems & Analytics
Hiab Finland Oy, Demontables & Defence Division
Pauli Siivonen, Product Manager
Hiab Finland Oy, Demontables & Defence Division

BACKGROUND

The purpose of this work was to investigate the customer benefits and value of fossil-free steel to promote the sale of eco-options for load-handling equipment. The market for on-road load-handling equipment is very cost-sensitive because the equipment itself is an additional component to the complete vehicle. Over the years, more advanced features—which increase safety, productivity, and the usability of the equipment—have become more standard and justified as value-adding features. Fossil-free steel, as an option, needs to follow the same path as other options because it will increase product costs, at least initially. To sell this kind of sustainable option, a proper study of value chain benefits must be conducted and customer selling arguments identified. Without a solid business case, sales cannot be made solely based on noble values. However, evolving climate legislation is increasing the demand for low-emission equipment and emission reduction options. The most relevant upcoming regulation for Hiab will be the EU's CountEmissionsEU act, which directly affects Hiab's customers (European Council, 2025).

METHOD

The work started by conducting an accurate cradle-to-grave Life Cycle Assessment (LCA). Significant background work had already been done in the FOSSA1 project, which provided a solid base for the final LCA calculation. The LCA was performed according to the ISO 14067 standard, which is recommended by the EU Taxonomy delegated acts (EU Regulation 2020/852, 2020). The target of the LCA was to verify new options to be categorized as eco-products, which would create additional value for Hiab's customers in public transport contracts. A certified eco-product shall have at least a 25% reduction in CO2-emissions during its life cycle compared to a standard product. The final LCA consisted of five parts: raw materials, transportation (during the life cycle), production (suppliers and own production), operation, and end-of-life. All components included in the hooklift product structure were analyzed, and CO2-emissions were determined for supplied components, equipment assembly, installation, and transportation. A complete LCA including operational emissions was possible by utilizing HiConnect data from the field and determining user profiles based on that data. With the complete LCA, Environmental Product Declarations (EPD) were developed for Multilift products.

The second phase of the project involved developing various ecometrics based on the data produced in the LCAs and field data collected via HiConnect. The purpose of the ecometrics was to create tools that calculate emissions in different manufacturing or operational phases. Based on these tools, the overall emission effects of the product can be shown, as well as the customer's cost-saving potential. The initial inputs for calculation are vehicle and hooklift information, descriptive parameters of the work performed, and the energy-saving options selected. The data can be entered manually or automatically from HiConnect if the customer is currently using a Multilift hooklift. With the HiConnect data connection, it is possible to compare current hooklift usage to the average usage of Multilift hooklifts or even to similar hooklift models in the field. With the eco-calculator, Hiab is able to present the benefits of

emission-reducing options and offer the customer the opportunity to utilize climate values in their own industry. Eco-calculator views are presented in Figure 8.

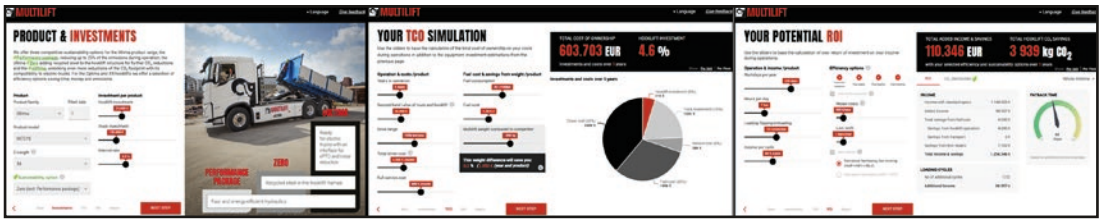

Figure 8. Multilift eco-calculator

RESULTS AND FINDINGS

The first results of the project involved creating the first-ever Environmental Product Declarations (EPD) for Multilift products. The Multilift Ultima 21S and 21S Zero were the first products to receive EPDs. The Ultima 21S Zero was presented at the IFAT exhibition in Germany in May 2024. Based on the work with EPDs, the effects of fossil-free steel in the product structure were very clear and, finally, led to the eco-product statement according to EU emission legislation. As a result of this work, Multilift now has three commercial eco-products:

- Performance package for Ultima
- Ultima Zero
- eUltima

The Performance package is an energy-efficient hydraulics option which can be selected for every Ultima hooklift. The Ultima Zero is a special version of the Ultima where a minimum of 25% of the steel structure is made with SSAB Zero recycled steel, and the Performance package is a standard feature. The eUltima is another version of the Ultima optimized for electric trucks (e.g., improved CAN connection, advanced ePTO installation, and silent performance options). The eUltima also uses recycled steel and includes the Performance package, like the Ultima Zero.

The first beta version of the Multilift eco-calculator was released in 2024. The official public version for customers was released in early 2025. The full version of the eco-calculator with all features is reserved for the use of Hiab's sales personnel.

IMPACT OF THE WORK

The work done in this work package has had a significant impact on the Multilift product line. Based on the studies and LCA calculations, Hiab has been able to classify and certify three products in the eco-product category according to the EU Taxonomy Act. During the project, eco-portfolio sales of Multilift hooklifts increased from 8% to 34%, and the number of eco-portfolio hooklifts sold tripled.

NEXT STEPS

Based on the created data models and achieved results, Hiab will study operational phase emissions more accurately and measure the effect of other hooklift options on CO_2-emissions to create further eco-option packages.

REFERENCES

European Council (2025). Passenger and freight transport: provisional agreement boosts transparency and comparability of data on greenhouse gas emissions, Press release, https://www.consilium.europa.eu/en/press/press-releases/2025/11/05/passenger-and-freight-transport-provisional-agreement-boosts-transparency-and-comparability-of-data-on-greenhouse-gas-emissions/ [Cited 11.3.2026]

European Union Eur-Lex (2020). Regulation (EU) 2020/852 of the European Parliament, https://eur-lex.europa.eu/legal-content/EN/TXT/?uri=celex%3A32020R0852 [Cited 11.3.]

Multilift Eco-calculator, https://multiliftcalculator.hiab.com/

Photo: Hiab Finland Oy

4.4 WP1 Key takeaways

Fossil-free steel ecosystem and research cooperation

- **International cooperation strengthened the fossil-free steel ecosystem.**

  University of Oulu built and expanded research collaboration with partners in Sweden, India, Hungary and the Netherlands in areas relevant to fossil-free steel development, including hydrogen technologies, steel metallurgy, energy systems, weldability and the behaviour of steels in hydrogen environments. **The work strengthened access to multidisciplinary expertise, research networks and shared methods needed to address complex fossil-free steel challenges and support future innovation.**

Economic competitiveness of fossil-free steel applications

- **Wider industrial use of fossil-free ultra-high-strength steels requires economic competitiveness across the value chain.**

  LUT examined the economic competitiveness of fossil-free ultra-high-strength steels and identified barriers that hinder the wider use of fossil-free steel applications in the mobile machinery and maritime industries from the OEM perspective. Using an AI-based approach, more than 200 heterogeneous data sources were structured into a preliminary FFUHSS value chain model and were used in the development of a preliminary LCC model for UHSS steelmaking, OEM, and dashboard components. This preliminary work established a foundation for future feasibility and sensitivity analyses. **This work provides a foundation for later economic evaluation of fossil-free ultra-high-strength steel use in industrial applications.**

Practical product applications

- **Practical pilot cases showed that fossil-free steel can be used in real products in forestry machinery and cargo handling.**

  SSAB supplied fossil-free steel to selected partners and carried out pilots with Ponsse and Hiab. In the forestry machinery pilot, fossil-free steel was used in a machine structure to confirm that it works in demanding use in the same way as conventional steel. In the cargo-handling pilot, a hooklift component was manufactured from fossil-free steel, likewise showing that the material can be used in a real product application. **These pilots reduced uncertainty, increased confidence in the material, and improved understanding of what the use of fossil-free steel means in practice for the product, manufacturing, and the full value chain.**

- **John Deere Forestry examined how material choices and end-of-life scenarios affect the environmental impact of forest machines.**

  John Deere Forestry mapped the cradle-to-grave impacts of forest machines and assessed how recycled steel, fossil-free steel and high-strength steel affect the result. Steel with more recycled inputs showed good potential to reduce manufacturing-related emissions: at material level, SSAB Zero steel showed a 60–75% lower GWP than average steel, and in one component-level comparison replacing the steel plates used in the boom and frame

with SSAB Zero plates reduced cradle-to-gate GWP by about 8%. A lightweight version made from high-strength steel also reduced impacts significantly in the component studied, although the comparison remained limited because the environmental impact of producing high-strength steel could not be assessed. The work also examined end-of-life options and showed the importance of long service life, effective maintenance and modernization. **The work improved the company's understanding of the full steel value chain and its effect on life cycle impacts of forest machines, and it identified limitations related to market availability and technical properties that make communication between steel suppliers and the machine manufacturer easier.**

- **Hiab investigated the customer benefits and value of fossil-free steel to promote the sale of eco-options for load-handling equipment.**

  The work produced the first Environmental Product Declarations (EPD) for Multilift products, and the effects of fossil-free steel in the product structure were clear enough to support an eco-product statement under EU emission legislation. As a result of this work, Hiab developed three commercial eco-products for the Multilift product line: Performance package for Ultima, Ultima Zero and eUltima. During the project, eco-portfolio sales of Multilift hooklifts increased from 8% to 34%, and the number of eco-portfolio hooklifts sold tripled. The work also led to the development of the Multilift eco-calculator, designed to present the benefits of emission-reducing options and offer the customer the opportunity to utilize climate values in their own industry. **The work gave Hiab stronger customer selling arguments and practical tools for presenting the benefits of emission-reducing options in their products.**

5. WORK PACKAGE 2
Fossil-free steel applications and economic growth

Work Package 2 examines the factors that affect the use of fossil-free and high-strength steels in end-products, structures and their manufacture. The work is set against the transition to carbon-free steelmaking, where the restructuring of the process chain, increasing electrification and growing use of recycled raw materials also change the cleanness, processing conditions and application requirements of steels. For high-strength steels, these changes are important because local weld behaviour, microstructure control and formability directly affect the performance of final products and structures. WP2 therefore combines materials research, welding and process studies and company-level application work.

Welding performance and welded-joint behaviour	***How do local changes in welded joints affect the performance of fossil-free and high-strength steels in demanding applications?***

In demanding steel applications, the critical limitations often arise in welded regions rather than in the base material alone. This is especially important in arctic and offshore applications, where the weldability and properties of welded regions are critical, as these may exhibit poor in-service performance due to limited low-temperature toughness. The most problematic regions are the coarse-grained heat-affected zones and the intercritically reheated coarse-grained heat-affected zones. WP2 addresses these issues through studies on multipass weld metal behaviour, fracture toughness, dissimilar HSS/UHSS joints, post-weld treatments and fatigue assessment. The work also examines how robotic welding can be supported by multisensor monitoring and synchronized data collection, together with digital shadow/twin functionality.

Formability and processing of AHSS and UHSS sheet steels	***How can advanced high-strength steels (AHSS) and ultra-high-strength steels (UHSS) retain good formability when heat treatment, microstructure and residual elements change?***

For advanced sheet steels, the challenge is not only to achieve high strength, but to do so without losing the formability required in manufacturing. This challenge becomes more important as scrap-based production increases, because future steels are expected to contain higher levels of scrap-derived residual elements. The work also considers industrial feasibility, including simple processing routes and induction-based approaches compatible with continuous production. WP2 examines these issues through studies on edge ductility of hot-rolled AHSS, intercritical annealing of medium-manganese steels, rapid induction-based microstructural modification, and the effects of rapid heating and residual elements in future scrap-based UHSS/AHSS steels. The common aim is to clarify how processing conditions shape microstructure and how that development affects mechanical behaviour in practice.

Hydrogen-related behaviour in high-strength steels	***What must be understood about hydrogen embrittlement and welded-region performance when developing high-strength steels for hydrogen environments?***

Hydrogen transport is becoming increasingly important for the development of the hydrogen economy, but hydrogen can significantly affect the performance of high-strength steels. In this work, hydrogen-related behaviour was studied in in martensitic-austenitic advanced high-strength steels and in welded pipeline steels. In martensitic-austenitic AHSS, the study addressed hydrogen embrittlement and examined how microstructural features influence hydrogen diffusion, trapping and HE resistance. In welded pipeline steels, the focus was on how weld-related microstructural changes influence hydrogen behaviour and the durability of welded regions in hydrogen-containing environments.

From steel solutions to industrial implementation	***How do fossil-free and high-strength steel solutions perform in practical applications and manufacturing?***

Successful material transition requires more than laboratory understanding. New steel solutions must also be translated into manufacturable products, production concepts and industrial launches. These questions are examined through company cases from SSAB, Fortaco, John Deere Forestry, Hiab and Ponsse. These cases examine the use of fossil-free and high-strength steels in vehicles, forestry machines and load-handling equipment. Together, they show how the technical questions studied in WP2 connect to product development, manufacturability and practical industrial use.

5.1 Fossil-free steels for smart applications

5.1.1 Simulation of multipass welding of 500 MPa shipbuilding and offshore steels

Contributors: **Henri Tervo, Antti Kaijalainen, Vahid Javaheri**, University of Oulu
Marcell Gáspár, Judit Kovács, Raghawendra Sisodia, University of Miskolc, Hungary
Johannes Sainio, SSAB Europe Oyj

Correspondence: **Henri Tervo** (henri.tervo@oulu.fi)

BACKGROUND

Demand for 500 MPa offshore and shipbuilding steels is rising for offshore platforms, wind turbines and ships operating in arctic conditions. Welded joints are typically the weakest locations because welding thermal cycles alter the steel microstructure near the weld. Thick-section welding often requires multiple passes, so subsequent thermal cycles also modify the first-pass weld metal. These altered regions, called heat-affected zones (HAZ), include coarse-grained (CGHAZ), intercritical (ICHAZ) and intercritically reheated coarse-grained (ICCGHAZ) subzones. Although HAZs in the base metal are well studied, the effect of additional thermal cycles on weld metal is less documented. This study investigates how multipass welding thermal cycles affect the microstructure and mechanical properties of earlier weld passes in 500 MPa steels

METHOD

The studied materials were welded joints of 500 MPa offshore steels. The filler metal was S3Ni1Mo0.2 (EN ISO 14171). The flux was EN ISO 14174: S A FB 1 55 AC H5. Welding was performed using submerged arc welding (SAW). Specimens were cut transverse from welded plate with the weld metal centered. Gleeble 3500 was used to reproduce HAZ cycles aiming for worst-case toughness microstructures: CGHAZ-W peak 1350°C, ICHAZ-W peak 815 °C ($A_{C1} \approx$ 765 °C; A_{C1}+50 °C used), and combined cycle for ICCGHAZ. Cooling times were $t_{8/5}$ = 5, 15, 30 s. Microstructural characterization was performed using light optical microscopy and scanning electron microscopy (SEM) with electron backscatter diffraction (EBSD) and energy dispersive spectroscopy (EDS). Mechanical testing included hardness, instrumented Charpy V-notch (CVN), and crack tip opening displacement (CTOD) fracture toughness.

RESULTS AND FINDINGS

Mainly acicular ferrite was observed in simulated HAZ subzones, with grain boundary ferrite and ferrite side plates also present (Figure 9). Ferrite laths were finer and carbon-rich constituents formed at prior austenite grain boundaries due to thermal cycles. Transformation within prior austenite grains consisted of acicular ferrite in both the original weld and simulated HAZ samples.

No significant hardening or softening was observed in CGHAZ-W, ICHAZ-W, or ICCGHAZ-W (Figure 10a). $t_{8/5}$ = 15 s produced hardness nearly equal to the original weld and base material. All tested zones and the original weld exceeded the base-material toughness requirement (>100 J at −40 °C), but each simulated subzone showed lower impact energy and CTOD than the original weld. ICHAZ-W exhibited the lowest toughness and larger unstable crack propagation; longer $t_{8/5}$ reduced impact energy in ICHAZ-W but not in CGHAZ-W (Figure 10b,c).

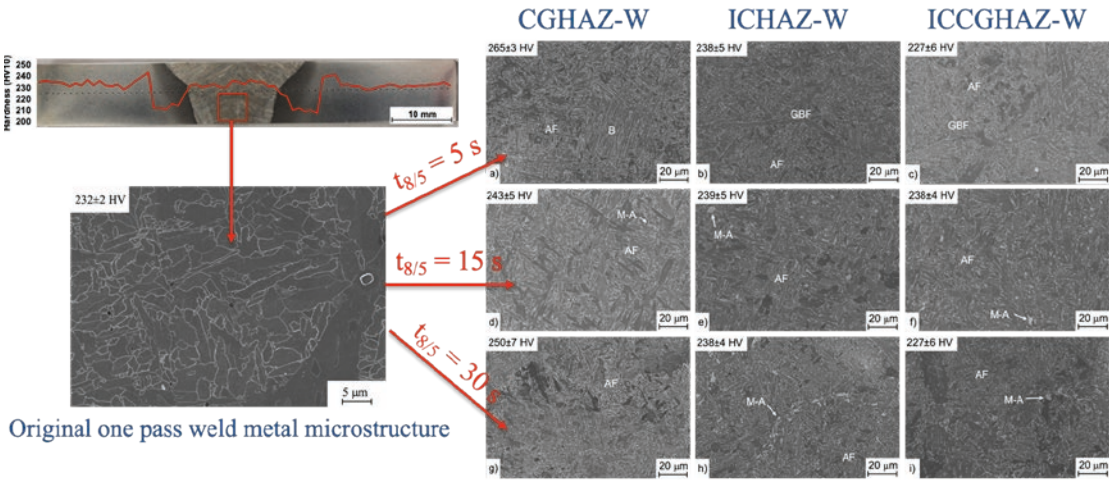

Figure 9. Microstructure of the before and after the HAZ simulations.

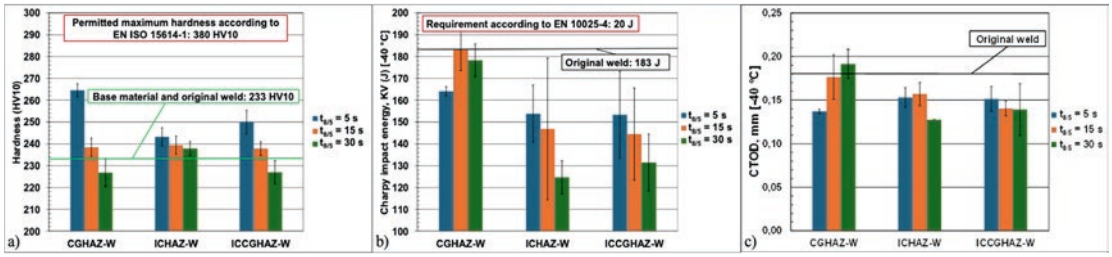

Figure 10. Hardness (a), impact toughness (b) and fracture toughness (c) results.

Simulated CGHAZ-W had higher inclusion number density and area fraction than the as-welded sample; inclusion area increased with longer cooling times. MnS area fraction was higher in simulated CGHAZ-W and grew with increasing cooling time.

Prior austenite grains in the original weld were refined by thermal cycles exceeding A_3. Effective grain sizes were comparable across samples; the cumulative 80% grain size was slightly larger in ICHAZ-W and tended to increase with longer cooling times. Austenite fraction decreased in simulated HAZs versus the original weld but increased with longer cooling times.

IMPACT OF THE WORK

These results provide valuable information about the behaviour of weld metal in the multipass welded 500 MPa offshore steels.

NEXT STEPS

The aim is to repeat the tests using different type of filler metal and compare the results to these ones. Additionally, similar type of research could be conducted to other type of steels too.

PUBLICATIONS

Gáspár, M., Kovács, J., Sainio, J., Tervo, H., Javaheri, V., & Kaijalainen, A. (2024) A többrétegű varratfelépítés hatásának elemzése fizikai szimulációval 500 MPa szilárdsági kategóriájú hajóacélnál. *Hegesztéstechnika*, XXXV (2), 37-42.

Gáspár, M., Kovács, J., Sainio, J., Tervo, H., Javaheri, V., & Kaijalainen, A. (2024) Effect of Welding Thermal Cycles on Weld Properties of 500 MPa Grade Offshore Steel. XXXII. *International Welding Conference: Proceedings* (Ed. J. Gáti & M. Gáspár), 88-94. https://www.researchgate.net/publication/387997965_The_effect_of_welding_thermal_cycles_on_weld_properties_of_500_MPa_grade_offshore_steel

Gáspár, M., Kovács, J., Sainio, J., Tervo, H., Javaheri, V., & Kaijalainen, A. (2025) Physical simulation-based analysis of multipass welding in S500 shipbuilding steel. *Welding in the World*, 69, 825-836. https://doi.org/10.1007/s40194-024-01908-0

Tervo, H., Gáspár, M., Kovács, J., Kaijalainen, A., Javaheri, V., Sainio, J., & Kömi, J. (2025) Physical Simulation of Heat-Affected Zones in a Weld Metal Used with 500 MPa Offshore Steel. Linköping Electronic Conference Proceedings 212; *Proceedings of the Second SIMS EUROSIM Conference on Modelling and Simulation, SIMS EUROSIM 2024* (Ed. E. Juuso et al.), 236-241. https://doi.org/10.3384/ecp212.033

Gáspár, M., Kovács, J., Tervo, H., Kaijalainen, A., Javaheri, V., Sainio, J., & Kömi, J. (2025). The microstructure and fracture mode of physically simulated heat-affected zones of a weld metal used with 500 MPa offshore steel – Part 1: Impact toughness test results. *Procedia Structural Integrity*, 68, 500–505. https://doi.org/10.1016/j.prostr.2025.06.088

Tervo, H., Gáspár, M., Kovács, J., Kaijalainen, A., Javaheri, V., Sainio, J., & Kömi, J. (2025). The microstructure and fracture mode of physically simulated heat-affected zones of a weld metal used with 500 MPa offshore steel – Part 2: Fractographies, inclusions and microstructures. *Procedia Structural Integrity*, 68, 506–512. https://doi.org/10.1016/j.prostr.2025.06.089

Tervo, H., Gáspár, M., Kovács, J., Javaheri, V., Sainio, J., Alatarvas, T., Kömi, J., & Kaijalainen, A. (2026). Evolution of inclusions in physically simulated heat-affected zones of a weld metal used with a 500 MPa offshore steel. *Key Engineering Materials*, 1040, 47–53. https://doi.org/10.4028/p-KPi3DF

Tervo, H., Gáspár, M., Kovács, J., Javaheri, V., Sainio, J., Kömi, J., & Kaijalainen, A. Electron Backscatter Diffraction Characterization of Physically Simulated Heat-Affected Zones of a Weld Metal Used with 500 Mpa Offshore Steels, presented in TIMA25 conference in November 2025, to be published by Trans Tech Publications in 2026.

Gáspár, M., Kovács, J., Sisodia, R. P. S., Sainio, J., Tervo, H., Javaheri, V., Kaijalainen, A., & Lukács, J. CTOD examination of physically simulated heat-affected zones in S500 shipbuilding steel welds, to be published in 2026.

5.1.2 Low-temperature fracture toughness of welded structural steels

Contributors: **Laura Autio and Sakari Pallaspuro**, University of Oulu
Johannes Sainio, SSAB Europe Oyj
Sebastian Lindqvist, VTT Technical Research Centre of Finland, Finland
Ann-Christin Hesse, Tamás Tóth, Klaus Dilger, Technical University of Braunschweig, Germany

Correspondence: **Sakari Pallaspuro**, sakari.pallaspuro@oulu.fi

BACKGROUND

Good toughness, which means resistance against crack propagation, is one of the main properties at low temperatures that is required from steels and their welds used in arctic and offshore environments. Welding causes local heterogeneities to the structures, which will inevitably yield differing mechanical behaviour, which must be addressed in structural design and design of optimal welding practices. With multi-pass welded thick plates of moderately strong offshore steels, the challenge is the produced local brittle zones in the complex heat affected zones (HAZ). With modern single-pass welding practices, for example with thermally metastable phases like as-quenched martensite and retained austenite, the challenge is how to retain the exceptional base-material properties with minimal heat-input. In this subtask, these two extremes of weldability were studied. First study considered MAG and SAW welding of 65 mm thick offshore steels, and the second electron-beam welded martensitic-austenitic advanced high-strength steels. Both materials were subjected to fracture mechanical testing to quantify the low-temperature properties, and to identify the weakest links in the welded joints.

METHOD

Two steel types were considered. First is a S420 grade offshore steel with a plate-thickness of 65 mm, which has been designed for cold weather applications. This was produced via thermomechanical rolling, which yields a fine-grained base-material with high fracture toughness. Plates were butt-welded with a half V-groove parallel to the rolling direction with two different methods; low heat-input MAG welding, and higher heat-input SAW welding. 20 mm thick single-edge notched bend specimens (SENB) were extracted both from upper and lower quarter-thickness and centreline to sample representable fractions of intercritical coarse-grained heat-affected zone (ICCGHAZ) and centreline segregation. Fracture toughness tests were done at -80 °C according to the standard ISO 12135:2021 Metallic materials — Unified method of test for the determination of quasistatic fracture toughness, and SFS-EN ISO 15653:2018 Metallic materials — Method of test for the determination of quasistatic fracture toughness of welds.

The second study utilised low-carbon laboratory hot-rolled, direct-quenched and partitioned (DQP) steel with CEIIW = 0.74 and CET = 0.44, which indicate need for pre-heating and post-weld heat treatment (PWHT). This DQP steel with 7 % of retained austenite (RA) has base-material yield strength of ~1130 MPa and hardness of 455 HV1, and it is compared against an essentially martensitic direct-quenched (DQ) state, which has yield strength of ~1360 MPa and hardness of 494 HV1. The plates were electron-beam welded transverse to the rolling direction with 120 kV voltage and 37 mA beam current at a speed of 10 mm/s using figure-8 pattern beam oscillation. The resulting weld seam hardness is 460 HV1, essentially the same with the base material, but hardness drops at the fusion line to 338 HV1. Some plates underwent PWHT treatment trials at the partitioning temperature of 275 °C, which should retain the base-material properties. PWHT treatment lowered hardness values of all the cases with about 20 HV1. Fracture toughness testing was done according to the standard ASTM E1921 at room temperature and at low temperatures

of -40 °C and -60 °C. Both studies included detailed microstructural characterisation of the base materials and their welds, which were investigated with a range of hardness profiling techniques, and fractography was an essential method in identifying the consequent failure mechanisms.

RESULTS AND FINDINGS

CTOD testing of the offshore steels showed some differences between different heat inputs, and fracture behaviour seemed more brittle with the lower heat-input MAG welding than with the high heat-input SAW welding, which had over twice as high average CTOD values. 86 % of the low heat-input specimens showed unstable crack propagation during the testing, whereas only approx. ¼ of high heat-input specimens showed the same. Location-wise the centreline appeared less tough than the quarter-thickness specimens, which was attributed to the centreline segregation present in the thick plate. Despite these observations, all the tested joint types and their CTOD values complied with the offshore standard that was used to evaluate the usability of these welded joints.

In the AHSS study, the electron-beam welded weld seam retained 3 vol.% of RA, ~half of that of the base material. Despite a short t8/5 time of 2.2 seconds, measured near the fusion line, this RA content is substantial when compared to the DQ state content below the quantification limit. Both the fracture toughness values and the provisional reference temperature T0Q indicate that PWHT treatment impairs toughness properties in all the conditions (base material, weld seam, HAZ / notch position at the fusion line). This can be due to partly lost RA in the PWHT treatment, resulting in detrimental high-hardness fresh martensite and cementite clusters.

The fracture toughness test results of the base materials, EB-welded weld seam and the HAZ show that both the chosen alloy is clearly robust, having high fracture toughness both at room temperature and at -40 °C, and that the resulting fracture toughness reference temperature T0 are around -40 °C, the weld seam having marginally lower KJc levels than HAZ and the base material. The base materials (DQP and DQ) have impact toughness transition temperatures T28J below -100 °C, and the highest T28J of -66 °C is for the weld seam (Pallaspuro et al., 2022). All these results can be considered excellent for the given strength level, demonstrating great potential for high-toughness welded AHSS components.

IMPACT OF THE WORK

Considering the offshore steels targeted for arctic applications, both weld types exceeded the required CTOD levels, and the steel shows robustness even at very low temperatures. This indicates good potential for arctic applications, and identified weakest links of ICCGHAZ and centreline segregation pave way to further in-depth studies.

The results acquired with the 0.2 wt.% C martensitic-austenitic DQP steel shows that the alloy is very tough, and that these kind of steels with metastable microstructures are weldable. Most importantly, the welds and HAZ show really high fracture toughness even at low temperatures, which should promote industrialisation and utilisation of these kind of novel 3rd gen. AHSSs for automotive components that are weldable with beam welding techniques. Surprisingly, PWHT reduced toughness, which indicates possibilities to omit it completely, making the manufacturing process faster and cheaper.

NEXT STEPS

Further studies could focus on sampling the centreline segregation with smaller size specimens to enable accurate identification of local weakest links when compared to their immediate vicinity without segregation. Given the positive results of the first electron-beam welding trials, further optimisation of the welding parameters should provide even better toughness properties.

PUBLICATIONS AND THESES

Autio, L. (2025) *Fracture toughness and crack initiation of welded S420 offshore steels at a low temperatures -80 C* [Master´s thesis, University of Oulu]. Accessible: https://urn.fi/URN:NBN:fi:oulu-202503192100

Pallaspuro, S., Hesse A-C., Tóth, T., Aho, N., Mirshekari, B., Ghosh, S., Lindqvist, S., Dilger, K., Kömi, J. (2024) Low-temperature fracture toughness of electron-beam welded low-carbon martensitic-austenitic steel. *Procedia Structural Integrity*,68, 802-808. https://doi.org/10.1016/j.prostr.2025.06.133

REFERENCES

Pallaspuro, S., Hesse A-C., Engelke, T., Sainio, J., Ghosh, S., Javaheri, V., Dilger, K., Kömi, J. (2022) Impact toughness of an electron-beam welded 0.2C direct-quenched and partitioned steel. *Procedia Structural Integrity*, 42, 895-902.

5.1.3 Effect of residuals on microstructure, mechanical properties and weldability on TMCP steels

Contributors: **Tommi Hintsala, Henrik Auvinen, Anttu Hoikkaniemi, Henri Tervo, Antti Kaijalainen**, University of Oulu
Johannes Sainio & Ville Ritola, SSAB Europe Oyj

Correspondence: **Tommi Hintsala** (tommi.hintsala@oulu.fi),
Henrik Auvinen (henrik.auvinen@oulu.fi)

BACKGROUND

As the steel industry moves towards greener production technologies, manufacturing routes are increasingly shifting to continuous processes. This transition limits the feasibility of producing numerous steel grades with widely varying chemical compositions, making it necessary to reduce the number of slab grades while still maintaining the required material properties. At the same time, greener steelmaking, especially scrap based production, introduces challenges, as tramp elements accumulate over multiple recycling cycles and influence both processing and final steel behavior. The research aims to determine how alloying design, tramp elements from scrap based production and welding, interact and influence the final microstructure and mechanical properties on TMCP steels.

METHOD

The materials examined included three structural steel compositions and two compositions alloyed with Ni and Mo. In the structural steels, the chemical composition was modified by adjusting the manganese (Mn) content, while in the Ni–Mo steels, the silicon (Si) content was varied. For each chemical composition, three plates were rolled, and each plate was subjected to a different cooling method. The cooling methods consisted of air cooling to room temperature (AC), interrupted accelerated cooling (IC), and direct quenching (DQ). All rolling operations were carried out using a laboratory rolling mill in University of Oulu.

Materials were mechanically tested for hardness, tensile properties and instrumented impact toughness. Tensile tests were performed using Zwick Z100 tensile test machine, instrumented impact toughness testing was performed on Zwick/Roell HIT750P and hardness measurements

were conducted using Zwick ZHU 2.5 hardness measurement machine. Microstructural characterization was performed using field emission scanning electron microscopy (FE-SEM) and electron backscatter diffraction (EBSD).

Weldability of the materials manufactured using the interrupted accelerated cooling method was studied. Materials were subjected to simulated welding using Gleeble 3800. CGHAZ, ICHAZ and ICCGHAZ were simulated with t8/5 cooling times of 7 seconds and 30 seconds. Microstructure, hardness and impact toughness of HAZ was studied, using same equipment as mentioned above.

RESULTS AND FINDINGS

Figure 11 illustrates how the different cooling methods typically influenced the microstructures of the structural steel compositions. In the AC condition, the microstructure consists of polygonal ferrite and pearlite. The IC condition is characterized primarily by quasi-polygonal ferrite, while the DQ condition produces a granular bainitic microstructure. The DQ condition also contains a high fraction of M/A constituents, whereas their amount is noticeably lower in the IC condition. Among the cooling methods, DQ resulted in the highest tensile strength and hardness, while AC produced the lowest values. The IC condition achieved the highest yield strength when the interrupted cooling process was successful, due to the formation of fully bainitic microstructures.

The microstructures of the Ni and Mo alloyed steels differed from those of the structural steels due to their higher hardenability. In the AC and IC conditions, the Ni–Mo steels exhibited quasi polygonal ferritic and granular bainitic microstructures, while in the DQ condition they developed lath like bainitic structures. These microstructural differences resulted in significantly higher yield and tensile strengths, as well as reduced elongation, compared to the structural steels.

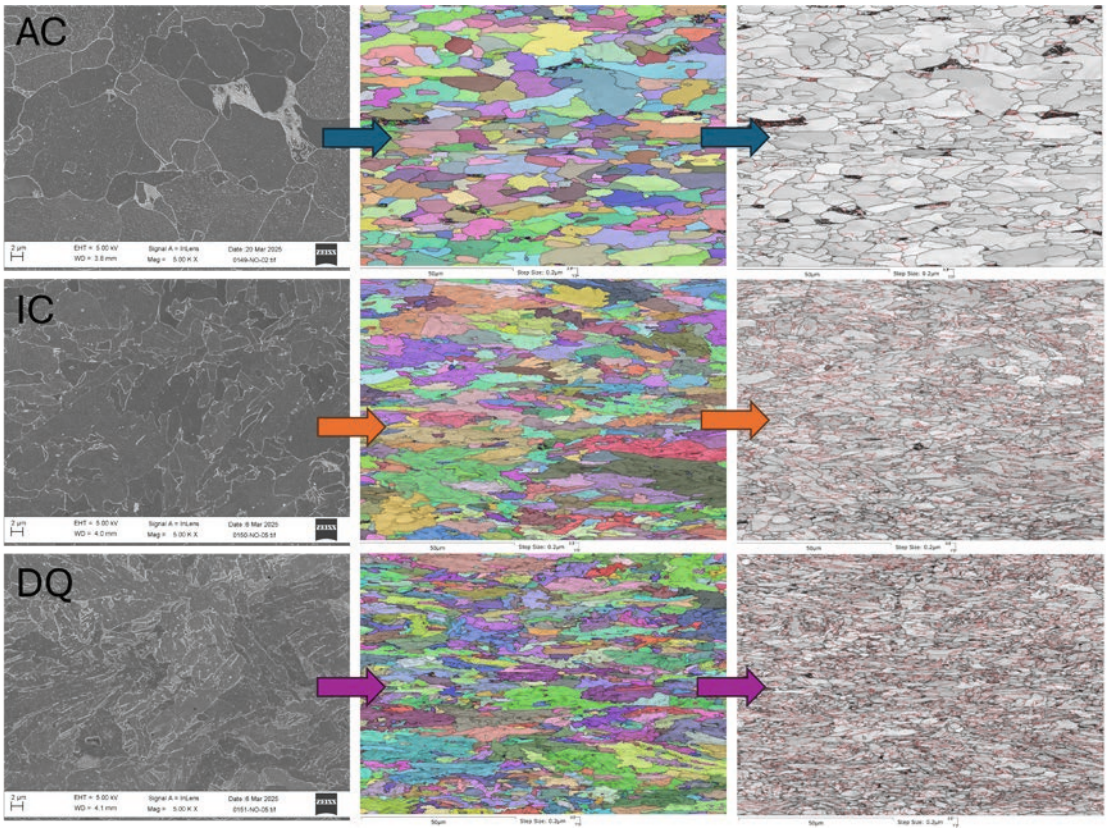

Figure 11. FE-SEM and EBSD images of 0.05C-1.1Mn-0.3Cu composition base metal in different conditions.

The physical simulations of heat-affected zone of IC condition specimens resulted in upper bainitic microstructures, granular bainitic microstructures and lath-like microstructures with features of lower bainite and bainitic ferrite in CGHAZ and ICCGHAZ. ICHAZ simulations resulted in granular bainitic microstructures with all chemical compositions. HAZ specimens with upper bainitic microstructure with coarsened grain size exhibited poorest toughness properties and the best results were obtained with granular bainitic microstructures.

Toughness properties of the physically simulated HAZ of the IC condition specimens are displayed in Figure 12. In contrast to the expectations, good Charpy V – notch impact toughness results were obtained with microstructures filled with M-A constituents. Fine grain size was found to have more influence on crack propagation resistance compared to the fraction of high-angle boundaries. Slower cooling time was found to reduce HAZ toughness in both CGHAZ and ICCGHAZ regions of the structural steel specimens. In contrast, the shipbuilding steels showed consistently good toughness across all HAZ variants. Since the t8/5 cooling time corresponds to heat input, the results would suggest that lower heat input would be more suitable for welding of the structural steels examined in this study.

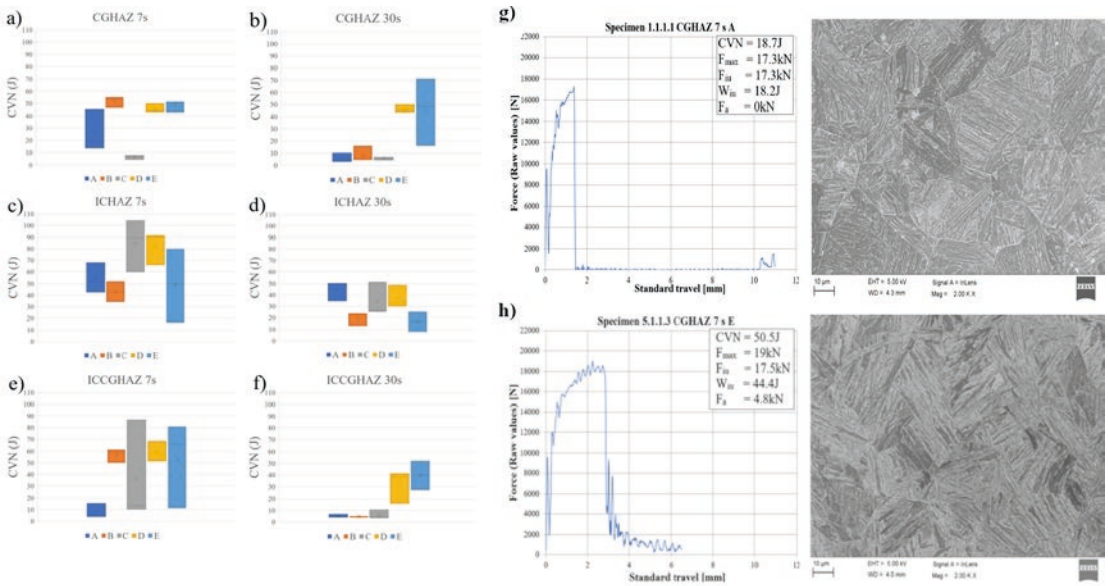

Figure 12. a–f) Instrumented Charpy V-impact toughness test results of all HAZ variations and g–h) instrumented Charpy V-impact toughness curve and corresponding microstructure of CGHAZ of 0.05C-1.6Mn-0.1Ni- 0.3Cu and 0.05C-1.6Mn-Ni-Mo-0.3Cu material.

IMPACT OF THE WORK

These results provided valuable information about manufacturing different steel grades from same chemical compositions by varying cooling method and about the influence of the tramp elements from scrap-based steelmaking to microstructures and mechanical properties of base metal and heat-affected zone. These base material test results demonstrate that multiple steel grades can be produced from a single chemical composition. By adjusting the cooling process, the mechanical properties can be tailored to meet the requirements of different steel grades.

NEXT STEPS

The aim is to gather more information and investigate the materials even more to answer risen questions from the master's theses in form of journal and conference articles in IIW conference. Research on the topic will be continued in doctoral dissertation.

PUBLICATIONS AND THESES

Auvinen, H. (2026). *Microstructure and toughness properties of physically simulated heat-affected zone of 500 MPa low-carbon bainitic steels* [Master's thesis, University of Oulu]. Accessible: https://urn.fi/URN:NBN:fi:oulu-202601211321

Hintsala, T. (2025). *Effect of alloying content and cooling parameters on mechanical properties of low carbon bainitic steel* [Master´s thesis, University of Oulu]. Accessible: https://urn.fi/URN:NBN:fi:oulu-202509175890

Hoikkaniemi, A. (2024). *Effect of EAF impurities on microstructure and mechanical properties of low-carbon steels* [Master's thesis, University of Oulu].

Auvinen, H., Tervo, H., Sainio, J., Kömi, J., & Kaijalainen, A. (To be published). *Microstructure and Toughness Properties of Physically Simulated Heat-Affected Zone of 500MPa Low-Carbon Bainitic Steels*.

Hoikkaniemi, A. J. T., Haiko, O., & Kaijalainen, A. (2026). Effect of EAF Impurities on Microstructure and Mechanical Properties of Low-Carbon Steels. *Solid State Phenomena*, 383, 13–18. https://doi.org/10.4028/p-s1q3hn

5.2 Multi-resistivity of fossil-free steels

5.2.1 Edge ductility of advanced high-strength automotive steel

Contributors: **Pekka Plosila, Henri Tervo, Olli Nousiainen, Jaakko Hannula, Antti Kaijalainen,** University of Oulu
Vili Kesti, SSAB Europe Oy
Raimo Vierelä & Päivi Juntunen, Lapland University of Applied Sciences
John Joy, Luleå University of Technology

Correspondence: **Pekka Plosila** (pekka.plosila@oulu.fi)

BACKGROUND

Manufacturing advanced high-strength steel (AHSS) components for automotive industry applications require the material to have sufficient formability due to complex geometries and blanked holes. AHSS can be susceptible to cracking of the sheared edge during the forming process. To increase utilization of high-strength steels in the applications, development of new steel grades with improved edge ductility and stretch-flangeability are of an interest. Sheared edge formability is most often evaluated by the ISO 16630 hole expansion test, where a 10 mm diameter punched hole is expanded with a conical tool until a through-thickness failure in the edge is observed. The result of the test is the limiting hole expansion ratio (HER), which describes an overall performance of the material in stretch-flanging. The research of the work package investigated hole expansion behaviour of hot-rolled AHSS focusing on material microstructural features and mechanical behaviour during the expansion process.

METHOD

The research continued the investigation of 3 mm thickness low-carbon hot-rolled 800 MPa tensile strength grade steels previously studied in FOSSA1 project. The tensile and hole expansion properties were evaluated during the former project, and a journal paper discussing the results (Plosila et al., 2024) was published during the FOSSA2 project. A summary of the properties of the test materials is presented in Table 1.

Table 1. Microstructures and mean mechanical properties of the investigated steels. Microstructure: F = ferrite, B = Bainite, and M-A = martensite-austenite constituent. Tensile strengths and total elongations are given in the material rolling direction.

Steel	Microstructure	Tensile strength [MPa]	Total elongation [%]	Planar anisotropy Δr [-]	Hole expansion ratio [%]
CP1	F + B + M-A	846	11.5	-0.66	38
CP2	F + B + M-A	834	15.4	-0.50	47
PF	F	845	16.4	-0.54	33
QF1	F + M-A	835	16.3	-0.38	66
QF2	F	828	17.4	-0.21	106

Different microscopy methods were utilized at University of Oulu to investigate base material microstructure. Scanning electron microscopy (SEM) was used in microstructure imaging and electron backscatter diffraction (EBSD) scans were performed at different material depths to investigate grain structure. Additionally, deformation areas in cross-sections of punched and

expanded hole edges were examined by SEM. X-ray diffraction (XRD) analysis was done at the base material centerline to measure volume fraction of retained austenite. Nanoindentation measurements were performed at Luleå University of Technology to investigate hardness inhomogeneity of the base material microstructure.

Three of the five steels (CP1, PF, and QF2) were selected for more detailed investigation of mechanical behaviour during the hole expansion testing. Interrupted ISO 16630 hole expansion tests with various test discontinuation points during the expansion were performed at Lapland University of Applied Sciences for test specimens with punched and wire electrical discharge machined (W-EDM) hole edges. After the test discontinuation, the different test specimens were 3D scanned and thinning of the hole edge was determined in three sheet principal directions (0°, 45°, and 90° relative to the rolling direction) around the expanded hole to investigate localization of deformation during the expansion process.

RESULTS AND FINDINGS

A journal paper discussing the microstructure – mechanical properties relationships is to be published during 2026 (Plosila et al., 2026). A summary of the different microstructures present in the steels can be found in Table 1. The ferrite morphologies were observed to be polygonal in PF and quasi-polygonal in QF1 and QF2. Retained austenite volume fractions measured by XRD were 1.3%, 4.8,% and 1.2% for CP1, CP2, and QF1, respectively. Complexity of the microstructure was reflected well in the nanoindentation hardness deviations, supporting the observation of the presence of harder (M-A, martensite-austenite) constituents also in QF1. EBSD grain size measurement results from material quarter thickness are presented in Figure 13a and measured number fractions of large inclusions in Figure 13b. There were no clear trends observed between HER and the presented parameters.

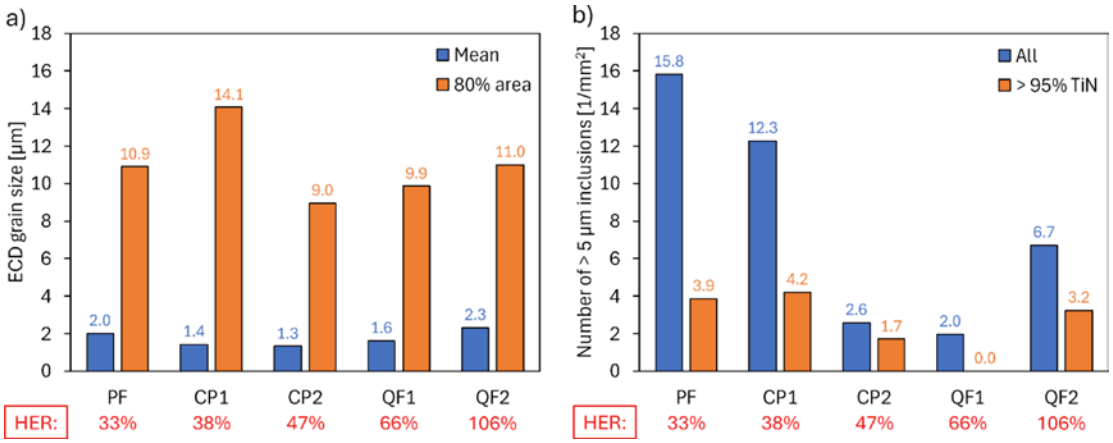

Figure 13. a) Mean equivalent circle diameter (ECD) grain size and ECD grain size at 80% cumulative area distribution measured at material quarter thickness, and b) number density or all large inclusions and large titanium nitride inclusions (consisting of > 95% TiN) through the material thickness. The hole expansion ratios of the steels are presented below.

For the grain morphologies, elongated and/or banded grains were observed in CP1, CP2, and PF, whereas in QF1 and QF2, the grain structure was overall equiaxed and more consistent through the material thickness and between the rolling and transversal directions. Example EBSD grain maps illustrating the difference between the grain morphologies between steels PF and QF2 are presented in Figure 14, showing the elongated and banded ferrite grains in PF.

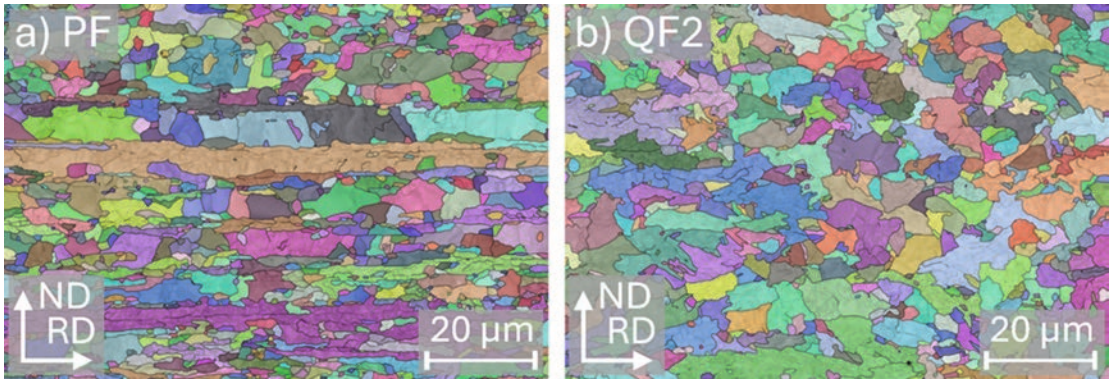

Figure 14. EBSD grain maps at quarter thickness of a) PF and b) QF2. The maps are constructed from band contrast and random colour grain maps, and ≥ 10° grain boundaries are highlighted in black.

In investigations of the deformed edge areas, void formation was primarily observed to occur around inclusions and interfaces between highly deformed ferrite and M-A constituents. Microcracks were also seen to propagate along the grain boundaries. Example micrographs from punched and expanded hole edge cross-sections are presented in Figure 15.

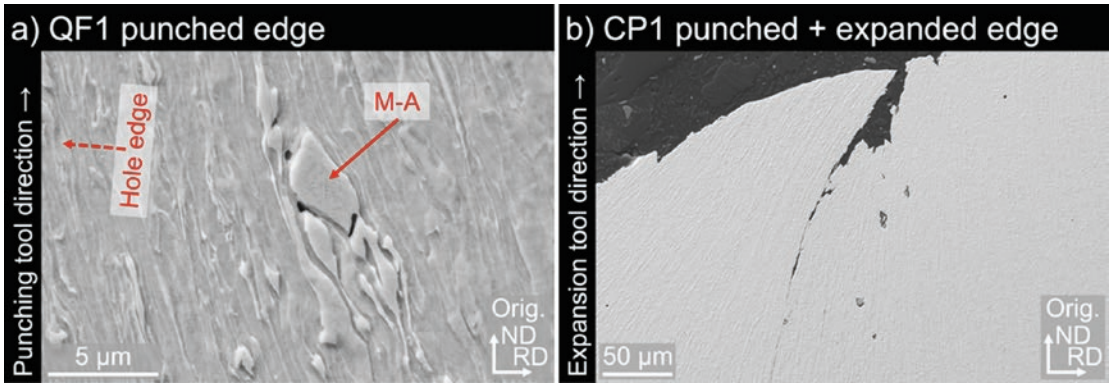

Figure 15. SEM images of microstructure from Nital-etched cross-sections near a) punched hole edge of QF1 showing void formation on M-A constituent interfaces, and b) punched and expanded edge of CP1 showing crack propagation along the elongated microstructure.

Overall, the results show that presence of M-A constituents, number of large TiN inclusions, or large grain size is not a sole determining factor for the hole expansion performance of similar-strength steels. Out of the investigated factors, the uniformity of the grain structure seems to have the strongest connection to high HER values. For improved performance, it would be desirable to have homogeneous microstructure combined with uniform grain structure (non-banded, non-elongated) and a low overall inclusion content.

A paper discussing the interrupted hole expansion testing was published at the IDDRG2025 conference (Plosila et al., 2025). The drawing force – expansion stroke data showed similar behaviour between the materials at the initial phase of the expansion and more deviation near the through-thickness failure. In the W-EDM specimens, a sudden drop of the drawing force at failure could be observed, indicating a more abrupt fracture. Drawing force – expansion stroke curves from ISO 16630 tests with punched and W-EDM holes are presented in Figure 16a. Example thinning measurement results from punched edges are presented in Figure 16b.

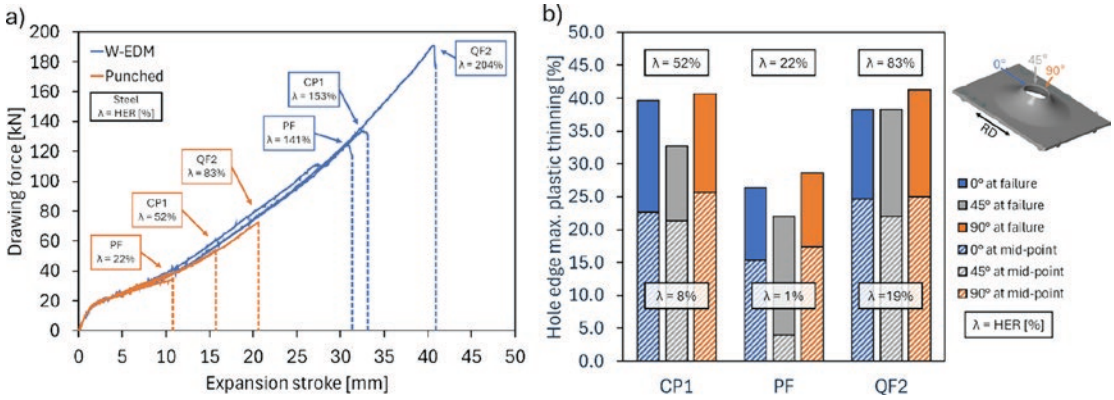

Figure 16. a) Drawing force compared to expansion stroke during hole expansion testing until a through-thickness failure appearance in punched and W-EDM specimens, and b) punched hole edge maximum thinning measurement results in different sheet directions in through-thickness failure specimens and specimens expanded until the middle-point of the expansion stroke of a through-thickness failure specimen. Hole expansion ratios (λ) of the individual tests are presented.

Localization of thinning in the different sheet directions (0°, 90°) was observed in punched specimens, and the behaviour was more pronounced in the W-EDM specimens due to the higher deformation level. Lesser amount of thinning localization was observed QF2, which was consistent with the material having the least degree of planar anisotropy.

IMPACT OF THE WORK

The research results provide valuable information on hole expansion behaviour of hot-rolled AHSS, which can assist in future steel development. The research results may also assist manufacturers to decrease issues with edge cracking during component production.

NEXT STEPS

The aim is to extend the investigations to a broader selection of steels, especially to ultra-high tensile strength grade steels. Additionally, damage propagation and fracture behaviour during cut-edge forming will be examined more in-detail.

PUBLICATIONS

Plosila, P., Kesti, V., Hannula, J., Kömi, J. & Kaijalainen, A. (2024). A comparison between tensile and hole expansion properties in 800 MPa tensile strength grade hot-rolled steels. *Materials Today Communications*, 40, 109521. https://doi.org/10.1016/j.mtcomm.2024.109521

Plosila, P., Vierelä, R., Juntunen, P., Kesti, V., Kömi, J. & Kaijalainen, A. (2025). An investigation on behaviour of 800 MPa grade hot-rolled steels in interrupted ISO 16630 hole expansion testing. *MATEC Web of Conferences*, 408, 01073. https://doi.org/10.1051/matecconf/202540801073

Plosila, P., Kesti, V., Nousiainen, O., Tervo, H., Joy, J., Hannula, J., Kömi, J. & Kaijalainen, A. Characterization of microstructural features and their contribution on mechanical properties of hot-rolled advanced high-strength ferritic and complex-phase steels. To be published 2026.

5.2.2 Effect of intercritical annealing treatment on hot-rolled Med-Mn steels

Contributors: **Tuomas Perkiö, Pekka Kantanen, Pekka Plosila, Vahid Javaheri, Antti Kaijalainen,** University of Oulu

Correspondence: **Tuomas Perkiö** (tuomas.perkio@oulu.fi)

BACKGROUND

The pursuit of increased fuel efficiency and reduced CO_2 emissions through weight reduction has driven the development of next-generation steel grades for the automotive industry. Among these, medium manganese steels (MMnS) have emerged as one of the most promising candidates. The combination of high strength and good ductility in these steels arises from a sufficient fraction of retained austenite (RA) with appropriate stability. RA in MMnS can trigger transformation induced plasticity (TRIP) and in some cases also twinning induced plasticity (TWIP). Achieving the desired mechanical properties and microstructure requires an appropriate annealing treatment. Intercritical annealing treatment (IAT) is the most widely used processing route for MMnS. In this study, the effects of IAT temperature and holding time on the microstructure and mechanical properties were investigated for different chemical compositions.

METHOD

The studied materials were MMnS with varying Mn and C compositions (0.3–0.4C and 6–8Mn). Also, the effect of niobium (Nb) on the mechanical properties has also been examined, but its influence appears to be relatively minor. Materials were hot-rolled at the University of Oulu using a laboratory rolling mill. IAT was simulated at different temperatures and holding times (650–725 °C, 3–30 min). The simulations performed with the Linseis dilatometer provided dilatometric data for determining phase transformation temperatures and produced samples for microstructural analysis. Electron backscatter diffraction (EBSD) and X ray diffraction (XRD) were used to determine phase fractions. Samples etched with 2% Nital were examined using scanning electron microscopy (SEM) for microstructural characterization. Macrohardness measurements were also performed on these samples. Gleeble 3800 was used to simulate IAT for tensile specimens. Tensile tests were conducted to determine optimal combination of strength and ductility.

In addition to the previous IAT simulations, chamber furnace IATs (650 °C & 700 °C, 10 min) were carried out for a laboratory hot-rolled 0.3C-6Mn steel with 4 mm thickness to further investigate formability of the MMnS material. Effects of shear cutting were evaluated by comparing punched and wire electrical discharge machined (W-EDM) hole edges through microhardness measurements, laser and scanning electron microscopy, and EBSD scans. To investigate stretch-flangeability of the materials, hole expansion tests according to the ISO 16630 standard were performed at Lapland University of Applied Sciences.

RESULTS AND FINDINGS

Based on the results, the optimal combination of strength and ductility was achieved with the 0.4C–6Mn variant within a narrow annealing temperature range around 700 °C, clearly standing out from the other compositions. Holding time between 3–30 min had minor effect compared to annealing temperature. (Figure 17).

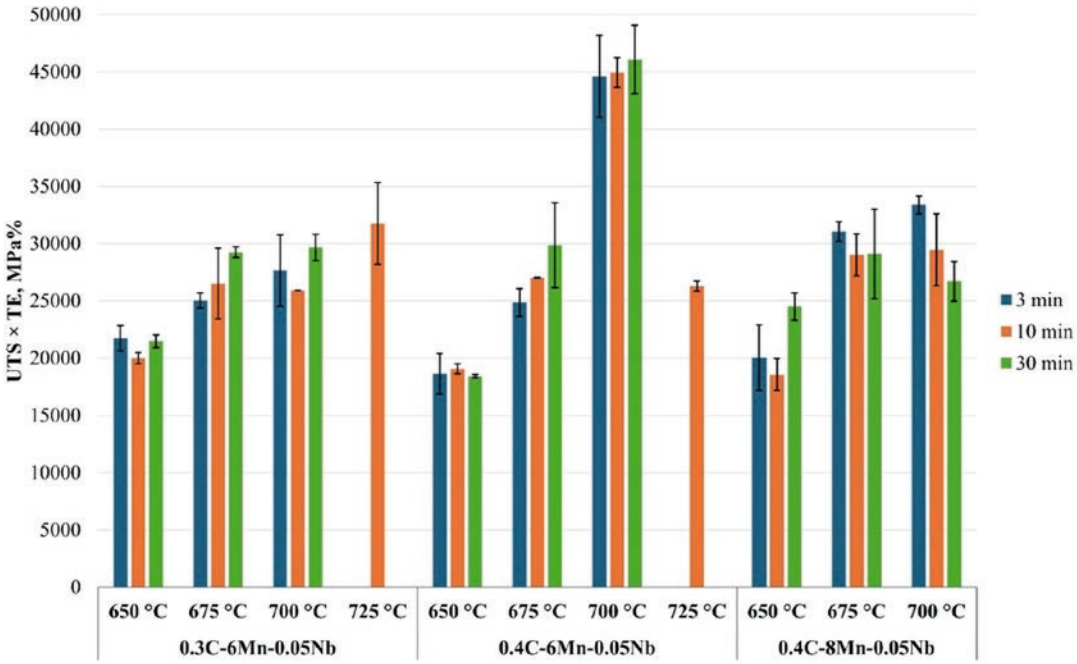

Figure 17. Average product of strength and elongation of each IAT variation.

Above mentioned variant showed favourable strain hardening, resulting in improved elongation. This was attributed not only to the fraction and chemical composition of the retained austenite, but also to the influence of its effective grain size and morphology on mechanical stability. (Figure 18).

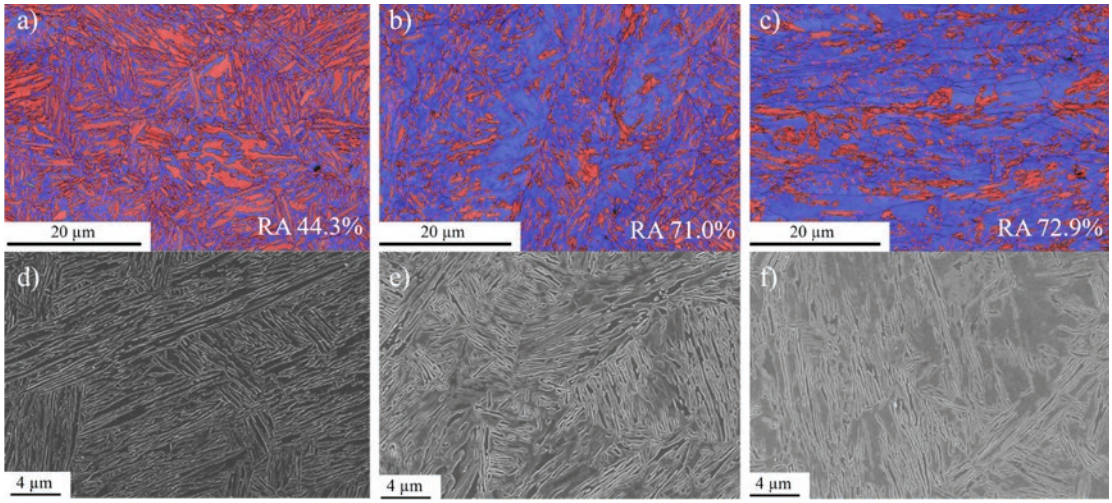

Figure 18. IAT at 700 °C, holding time 10 min. EBSD phase maps, with band contrast and grain boundaries for a) 0.3C-6Mn b) 0.4C-6Mn and c) 0.4C-8Mn. Red corresponds to bcc, and blue to fcc. FESEM micrographs of d) 0.3C-6Mn e) 0.4C-6Mn and f) 0.4C-8Mn after 2% Nital etching.

The IAT conditions that produced the highest fractions of retained austenite also led to reduced austenite stability. As a result, the TRIP effect was exhausted at lower strains, which resulted in diminished elongation. 0.4C-6Mn variant was particularly sensitive to the annealing temperature, which could pose challenges for large scale industrial production.

In the furnace IAT experiments, materials with 1027 MPa and 911 MPa tensile strength and 7.3% and 43.3% RA volume fraction were obtained for the IAT temperatures of 650 °C and 700 °C, respectively. Hole expansion ratios (HER) with punched edges were found out to be poor for both IAT temperatures (Figure 19a), and the higher RA content of the IAT 700 °C material did not drastically improve the stretch-flangeability. This behaviour was attributed to the high hardness increase towards the punched hole edge (Figure 19b), which resulted from strain-induced martensite formation due to high local deformation induced by the hole punching process. As the retained austenite close to the hole edge is already transformed into martensite during the punching, the local formability potential of the microstructure is then decreased for the flange formation during the expansion testing.

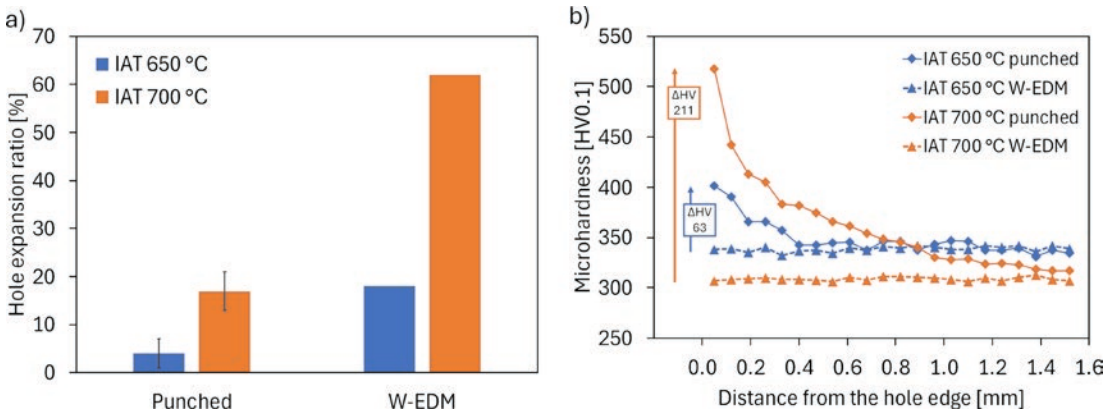

Figure 19. Hole expansion testing results (a) and non-expanded hole edge microhardness profile measurement results (b) for the furnace IAT test materials with punched and W-EDM holes.

For the W-EDM edge condition, where the shear-affected zone of the punching process is not present, more significant increase in HER was achieved with the higher RA volume fraction material. However, the increases in HER levels due to the improvement of the edge quality were not as substantial as expected considering the material tensile strengths. It was concluded that the rather poor rolling surface quality of the hot-rolled MMnS material may have affected the results by promoting the failure to occur earlier during the forming.

IMPACT OF THE WORK

MMnS are potential candidates for the next-generation steel making. This work provides valuable insight into the intercritical annealing behaviour of hot rolled medium carbon, medium manganese steels, using a processing route kept as simple as possible to maintain industrial feasibility.

NEXT STEPS

Based on these results, suitable material variants and intercritical annealing (IAT) parameters can be selected for more detailed investigation. The next steps include fatigue testing and studying the effect of the heating rate. For the possible formability testing of hot-rolled MMnS in the future, more consideration should be given to material surface quality.

PUBLICATIONS AND THESES

Perkiö, T. (2024). *Optimizing intercritical annealing treatment for hot-rolled medium-manganese steels* [Master´s thesis, University of Oulu]. Accessible: https://urn.fi/URN:NBN:fi:oulu-202412187424

Plosila, P., Kantanen, P., Hannula, J., Javaheri, V., Kömi, J. & Kaijalainen, A. (2024). Hole expansion performance of a medium manganese advanced high-strength steel after hot rolling and intercritical annealing, *Materials Research Proceedings*, 44, 358–367. https://doi.org/10.21741/9781644903254-38

Kantanen, P., Plosila, P., Javaheri, V., Perkiö, T. & Kaijalainen, A. (2025). Strain-induced martensite formation during punching of a medium manganese advanced high-strength steel. *Procedia Structural Integrity*, 69, 53–60. https://doi.org/10.1016/j.prostr.2025.07.008

Perkiö, T., Kantanen, P. & Kaijalainen, A. (2026). Effect of intercritical annealing temperature to mechanical performance of hot-rolled medium manganese steel. *Materials Science Forum*, 174, 83–88. https://doi.org/10.4028/p-kG28cH

5.2.3 Rapid induction based microstructural modification of steel

Contributors: **Ahmed W. Abdelghany, Terho Iso-Junno, Oskari Haiko, Antti Järvenpää, Antti Kaijalainen, Anttu Hoikkaniemi, Aki-Petteri Pokka,** University of Oulu

Correspondence: **Antti Kaijalainen** (antti.kaijalainen@oulu.fi)

BACKGROUND

This work package addresses rapid induction-based heat treatments as a route to tailor microstructure and strengthen steel components by applying fast, localized heating and controlled cooling schedules. In the published 51CrV4 study, the core purpose was to evaluate whether a continuous high-speed induction line can create a hardened surface layer while maintaining a softer core response through a short quench-and-temper route (rapid austenitisation, water quench, short temper).

In parallel, the induction surface heat treatment study on ultrahigh-strength steel was motivated by the known sensitivity of bendability to near-surface and subsurface properties. Prior work shows that bendability of ultrahigh-strength structural steels is strongly influenced by the mechanical properties of the sheet surface, and that a relatively soft surface/subsurface layer can suppress strain localization that otherwise develops into shear bands and fracture. These established relationships provide a clear rationale for using induction as a targeted surface-modification tool: the objective is not only "high strength," but a controlled property gradient that supports forming operations (especially cold bending) where the surface region experiences the highest tensile strains.

METHOD

The induction-quench-and-temper case study focused on 51CrV4 spring steel processed on a continuous high-speed induction heating line. The material was supplied as 8 mm thick sheets (reported composition Fe–0.5C–0.9Mn–1Cr–0.16V in wt.%). The processing route consisted of rapid austenitisation at 900 °C with an approximate heating rate of ~200 °C/s, followed by water quenching and tempering at 300 °C. This system was selected to replicate continuous and controlled feed industrial processing, as shown in Figure 20. After processing, the outcomes were evaluated by a combination of optical microscopy for microstructure overview, hardness profiling across the section to quantify surface-to-core gradients, electron backscatter diffraction (EBSD) to resolve the transformed surface-layer structure and prior-austenite grain scale, and field-emission SEM (FESEM, including carbide assessment) to examine tempering-related microstructural features.

For the bendability-driven induction surface treatment work, the experimental approach aligns with established bending characterization practices in UHSS research, where bending tests are paired

with digital image correlation (DIC) to measure surface strain evolution during forming. A detailed example of this approach (bending tests with DIC-based optical strain measurement) is documented in related UHSS bendability research from the same research environment. The induction surface heat treatment concept itself is consistent with peer-reviewed findings that surface/subsurface mechanical response governs bendability and that a softer subsurface layer can enable better strain distribution across the bend.

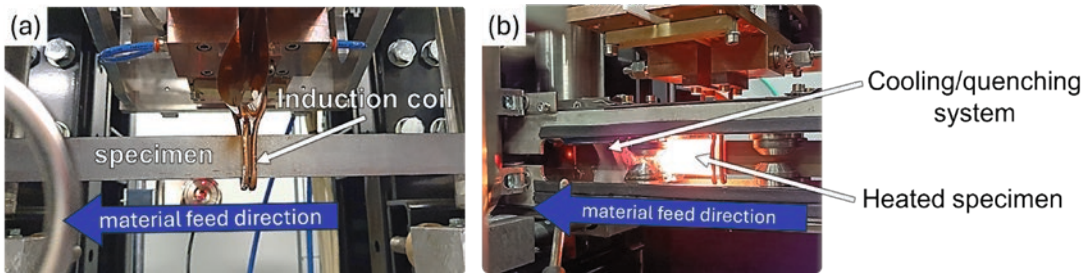

Figure 20. Photographs of the high-speed induction heating of steel specimens using a continuous pilot-scale axial inductor system at Nivala, Finland.

RESULTS AND FINDINGS

In the continuous induction line study on 51CrV4, the key metallurgical outcome was the formation of a uniform, crack-free martensitic surface layer extending to approximately ~1.2 mm from the surface after the rapid quench-and-temper route, as shown in Figure 21. This microstructural gradient was reflected directly in the measured hardness distribution: the surface hardness was reported at 590 ± 20 HV, decreasing into the core region to approximately 240–330 HV. EBSD analysis confirmed that the surface layer was fully martensitic and reported a refined prior-austenite grain scale on the order of ~3.2 µm. SEM-based observations further indicated minimal carbide coarsening, supporting the interpretation that the short-time tempering step was sufficient to modify the martensitic structure without extensive carbide growth. Taken together, these measurements demonstrate that, within the studied processing window, "flash" induction processing can create a hardened shell while retaining a notably lower-hardness core, which is the central design outcome for many surface-engineered components.

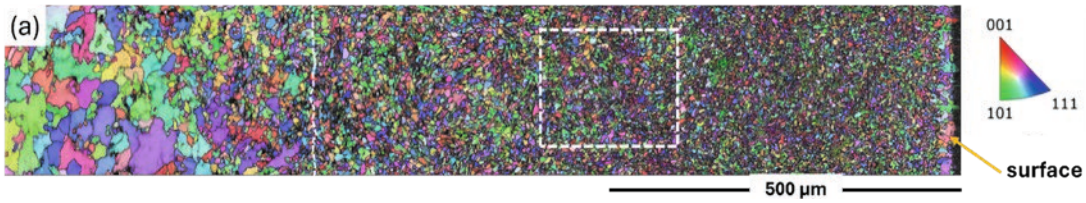

Figure 21. Multi-scale microstructural characterization of the tempered surface region in 51CrV4 steel after rapid induction heat treatment (A9-T3 condition).

For the induction surface heat-treatment study on 1300 MPa steel, the objective was to modify the near-surface/subsurface hardness and microstructure to improve bendability without relying on bulk softening. This direction is expected to enhance the UHSS bendability which is highly dependent on the mechanical properties of the sheet surface, Also, excellent bendability can be achieved when the subsurface region is relatively soft down to a depth scale corresponding to a small fraction of the sheet thickness.

IMPACT OF THE WORK

The 51CrV4 outcomes provide peer-reviewed evidence that a continuous, high-speed induction route can deliver a controlled surface-hardening response (martensitic shell) together with a measurable surface-to-core hardness gradient under rapid processing conditions. From a manufacturing perspective, the publisher's abstract explicitly frames the process as an energy-efficient and scalable alternative to conventional furnace-based treatments, which is an important impact statement for industrial translation because it connects the metallurgical result (shell hardening + retained core response) with processing efficiency and scalability.

The surface-engineering direction for bendability improvement is also of practical significance because it targets the location that governs bending failure in UHSS forming: prior work indicates that bendability is governed by subsurface hardness and crystallographic texture, and that the surface mechanical response can control whether deformation spreads smoothly or localizes into shear bands and fracture (Figure 22). Consequently, induction-based surface modification provides a technically grounded pathway to address forming limitations through microstructure/property gradients rather than by lowering the overall strength level.

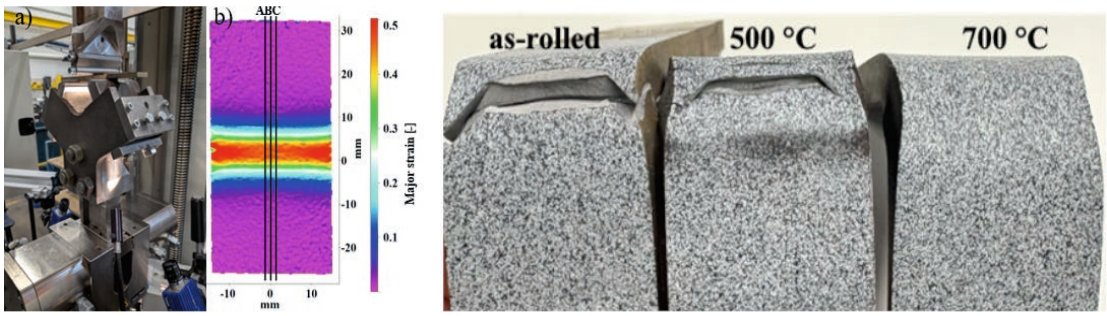

Figure 21. Multi-scale microstructural characterization of the tempered surface region in 51CrV4 steel after rapid induction heat treatment (A9-T3 condition).

NEXT STEPS

For the continuous induction processing of 51CrV4, the next research phase should expand from microstructure–hardness characterization into structure–property performance mapping that explicitly links the hardened surface layer and the softer core to mechanical response under relevant loading modes.

On the other hand, for induction surface heat treatment aimed at bendability improvement, next steps should continue with detailed microstructure quantification of the modified layer (including crystallographic characterization and precipitate/carbide assessment where relevant), while maintaining a direct connection to bending performance metrics.

PUBLICATIONS

Abdelghany, A. W., Haiko, O., Järvenpää, A., & Kaijalainen, A. (2026). Revealing the Microstructure and Mechanical Properties of Rapidly Quenched and Tempered 51CrV4 Steel Processed Via a Continuous Induction Line. *Solid State Phenomena* 383 (2026) 7–12. https://doi.org/10.4028/p-69oURO

Kaijalainen, A., Abdelghany, A., Haiko, O., Hoikkaniemi, A., & Pokka, A.-P. Microstructural Modification and Bendability Improvement in 1300 MPa Steel via Induction Surface Heat Treatment. ESAFORM 2026.

5.2.4 Hydrogen embrittlement of martensitic-austenitic AHSS steels

Contributors: **Renata Latypova, Vahid Javaheri, Sakari Pallaspuro**, University of Oulu
Lisa Claeys, Kim Verbeken, Tom Depover, Ghent University, Belgium
Poulumi Dey, Delft University of Technology, The Netherlands
Eric Fangnon, Yuriy Yagodzinsky, Aalto University, Finland
Graham King, Canadian Light source, Canada.

Correspondence: **Renata Latypova** (renata.latypova@oulu.fi),
Sakari Pallaspuro (sakari.pallaspuro@oulu.fi)

BACKGROUND

Martensitic high-strength steels are widely used, e.g., in the automotive industry, and martensitic-austenitic advanced high-strength steels (AHSS) are making their way into products. Especially these AHSS are appealing solutions for producing combinations of high strength, deformability achieved via enrichment with retained austenite (RA), and toughness. However, both of these are susceptible to hydrogen embrittlement (HE). This susceptibility of martensitic steels origins commonly from the relatively low macroscopic deformability, which combined with high operational (tensile) stress levels exposes these steels to high concentrations of hydrogen. Additionally, recrystallised prior austenite grains are more susceptible to intergranular cracking, which can be mitigated via processing methods like direct-quenching (Latypova et al., 2023). With martensitic-austenitic AHSSs, larger less stable RA cause these materials to become brittle, as larger high-carbon RA grains transformed into brittle martensite create potent microcracks, which accelerate the damage processes. A method to overcome this challenge is to produce sufficiently fine film-like retained austenite morphology, e.g., via direct-quenching and partitioning (DQP) process (Kantanen P. et al., 2019, Wang S. et al., 2021).

Evaluating HE susceptibility requires a thorough understanding of how hydrogen diffuses in these microstructures, gets trapped in tailored microstructural features like carbides and RA, and finally concentrates on highly stressed areas. This study investigates how different heat treatments and alloying affect carbide formation in martensitic steels, specifically iron carbides such as cementite and eta carbides, and how these factors influence H diffusion and trapping properties. Furthermore, the same is investigated in detail with martensitic-austenitic steels, showing that significant mitigation of HE can be achieved by limiting RA size to nanoscale, tailoring the RA film-thickness and bcc-alloying.

METHOD

The materials studied were medium-carbon direct-quenched (DQ) and direct-quenched and partitioned (DQP) AHSSs with 0.3 C and 0.4 C (wt.%). The tempering study included DQ steels that were rapidly tempered at 420 °C and 720 °C. The resulting variants, T420 and T720, have lath-martensitic microstructures with different fractions and morphologies of cementite, reflecting the effect of tempering temperature. T420 has cementite with a continuous rod-like structure, whereas in T720 it occurs in higher fractions, exhibiting a more fragmented, discontinuous, and globular morphology. With the DQP steels, Al and Si alloying were used to study the suppression of cementite formation and how bcc-alloying can help driving hydrogen into RA. With the 0.4 wt.% C DQP variant, Si alloying resulted in a significant fraction of η-carbides in lath-martensitic matrix. This DQP was subsequently tempered to eliminate η-carbides for trapping comparison. The effect of highly stable retained austenite (RA) films was thoroughly investigated combining microstructural and electrochemical characterisation, density functional theory calculations, and in situ hydrogen-charged slow strain rate tensile (SSRT) tests. Electrochemical H permeation (EP) experiments

were performed to determine the H diffusion coefficients (D) of the test materials, while thermal desorption spectroscopy (TDS) was employed to quantify H concentrations, and analyse the various H trapping sites within the materials. Microstructural characterisation utilised various techniques, including DSC, SEM, XRD (both lab-scale and high-energy synchrotron HE-XRD), and TEM.

RESULTS AND FINDINGS

The results with the 0.4 wt.% C steels show that both cementite and η-carbides act as weak traps, with rod-like cementite increasing trapping of hydrogen with increasing interface area. However, η-carbides contribute to weak H trapping with higher activation energies than other typical weak traps in the martensitic matrix, such as dislocations, grain boundaries, or cementite. Figure 23 shows H desorption curves for DQP (H-Si) and its tempered variant (H-Si-T), illustrating the significance of η-carbide trapping. After tempering, high-angle grain boundary trapping remains similar, dislocation trapping is reduced, and eta carbide trapping is eliminated, shifting the maximum peak temperature to lower values in the H-Si-T condition.

With 0.4 C DQP, RA is acting as H diffusion barrier and not a trap as demonstrated in Figure 24. RA nanofilms are embedded in harder martensite, and are thus subjected to compressive stresses, creating an unfavourable stress state at the martensite/RA interface, suppressing H transport. This stress state can be partly influenced with the chosen partitioning/tempering T.

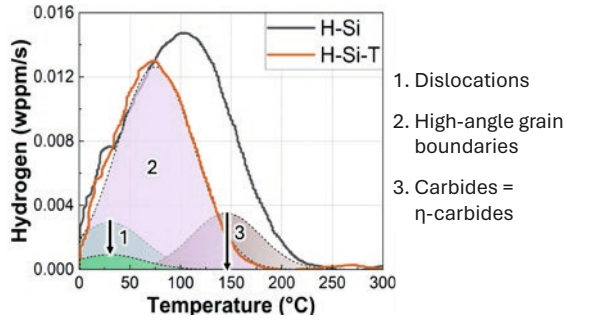

Figure 23. H desorption curves of DQP and its tempered variant with illustration of H trapping sites.

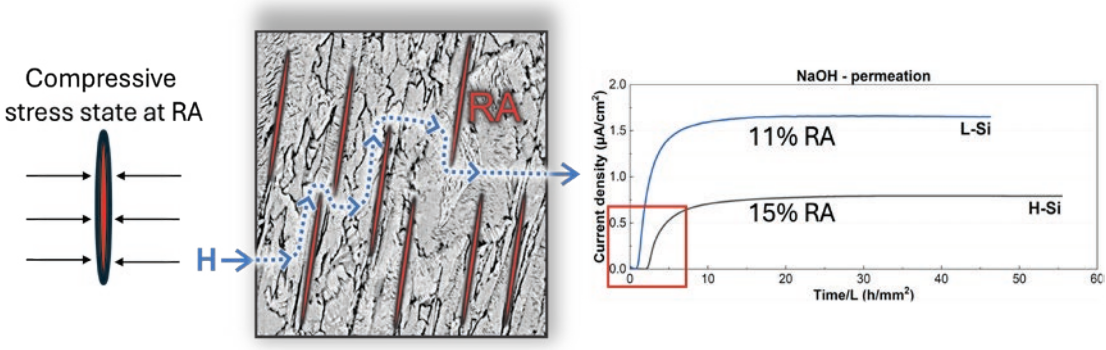

Figure 21. Multi-scale microstructural characterization of the tempered surface region in 51CrV4 steel after rapid induction heat treatment (A9-T3 condition).

The SSRT study with 0.3 wt.% C Al- and Si-alloyed DQP steels show that HE resistance increases with higher bcc-phase enrichment and larger retained-austenite (RA) film thickness. DFT results show that H is less soluble in Al-alloyed bcc-Fe than Si-alloyed bcc-Fe, which helps pushing H into RA, and that the solubility of H increases significantly in C-enriched RA. These theoretical findings account for the experimentally observed reductions in hydrogen diffusivity and increase in trap density, explaining the superior HE resistance of Al-DQP with thicker nanoscale RA-films when compared with Si-DQP and DQ steel.

IMPACT OF THE WORK

This research provides new insights into the H-trapping properties of cementite and η-carbides, which are important for tailoring the microstructures of next-generation steels for increased tolerance to residual H, and towards developing ultrahigh-strength steels for H applications. The prevailing assumption that RA is a strong trap is challenged by showing that highly compressed film-like RA can facilitate faster H diffusion. Nevertheless, Pallaspuro et al. (2024) provided novel insights into the interplay of hydrogen with bcc and fcc, pushing the boundaries of how relatively low level of embrittlement can be achieved with DQP steels up to 800 MPa higher tensile strength level when compared to traditional quenched and partitioned steels.

NEXT STEPS

Further research will focus on RA films examined using TEM to characterise the dislocation distribution at RA interfaces, enabling evaluation of interface deformation, and the HE mechanisms with RA transformation into martensite. Different RA morphologies should be investigated to determine the specific conditions under which RA switches from a beneficial hydrogen trap to a diffusion barrier, guiding hydrogen-resistant steel design.

PUBLICATIONS AND THESES

Pallaspuro, S., Fangnon, E., Aravindh, S.A., Claeys, L., Latypova, R., Yagodzinsky, Y., Aho, N., Kantanen, P., Uusikallio, S., Depover, T., Huttula, M., Dey, P. & Kömi, J. (2024). Mitigating hydrogen embrittlement via film-like retained austenite in 2 GPa direct-quenched and partitioned martensitic steels. *Materials Science and Engineering*: A, 908, 146872. https://doi.org/10.1016/j.msea.2024.146872

Latypova, R., Javaheri, V., Claeys, L., Verbeken, K., Depover, T., Kömi, J. & Pallaspuro, S. (2025). Effect of rapid tempering and cementite morphology on hydrogen diffusion and trapping in a medium-carbon advanced high-strength steel. *Engineering Fracture Mechanics*, 326, 111376. https://doi.org/10.1016/j.engfracmech.2025.111376

Latypova, R., Fangnon, E., Ghosh, S., Pallaspuro, S., Claeys, L., Verbeken, K., Depover, T., & Kömi, J. (2025) Effect of silicon alloying on hydrogen diffusion and trapping in medium-carbon DQ&P steels, 5th International Conference on Metals and Hydrogen 2025.

Latypova, R., Nyo, T. T., Seppälä, O., Ruoppa, R., Kauppi, T., Singh, H., Huttula, M., King, G., Pallaspuro, S., & Kömi, J. Low-temperature tempering for improving hydrogen embrittlement resistance in direct-quenched steel, Under review.

REFERENCES:

Latypova, R., Seppälä, O., Nyo, T.T., Kauppi, T., Mehtonen, S., Hänninen, H., Kömi, J., Pallaspuro S. (2023) Influence of prior austenite grain structure on hydrogen-induced fracture in as-quenched martensitic steels. *Engineering Fracture Mechanics*, 281, 109090. https://doi.org/10.1016/j.engfracmech.2023.109090

Kantanen, P., Somani ,M., Kaijalainen, A., Haiko, O., Porter, D., Kömi, J. (2019) Microstructural characterisation and mechanical properties of direct quenched and partitioned high-aluminium and high-silicon steels. *Metals*, 9, 259 https://doi.org/10.3390/met9020256

Wang, S., Kistanov, A.A., King, G., Ghosh, S., Singh, H., Pallaspuro, S., Rahemtulla, A., Somani, M., Kömi, J., Cao, W., Huttula, M. (2021) In-situ quantification and density functional theory elucidation of phase transformation in carbon steel during quenching and partitioning. *Acta Materialia*, 221, 117361. https://doi.org/10.1016/j.actamat.2021.117361

5.3 Hydrogen-induced fatigue

Contributors: **Mahdieh Safyari, Masoud Moshtaghi**, Mechanics of Materials Lab, LUT University

Correspondence: mahdieh.safyari@lut.fi; +358 50 342 4568
masoud.moshtaghi@lut.fi, +358 50 565 0973

BACKGROUND

A reliable and efficient method for transporting large volumes of hydrogen is essential for the development of the hydrogen economy (Moshtaghi et al., 2024). Among the available options, pipelines are considered the most economical and safest solution for long-distance and large-scale hydrogen distribution (Safyari and Moshtaghi, 2025). However, constructing new pipelines specifically designed for hydrogen requires substantial investment. Therefore, repurposing existing natural gas pipeline networks for hydrogen transport has been proposed as a practical and cost-effective strategy.

Despite these advantages, blending hydrogen into existing pipeline systems introduces important technical challenges related to the integrity and durability of pipeline materials. One of the main concerns is hydrogen embrittlement. When hydrogen atoms enter the steel matrix, they can significantly reduce key mechanical (Moshtaghi and Safyari, 2023; Moshtaghi et al., 2022) properties such as ductility, fracture toughness, and fatigue life of pipeline steels and their weldments that otherwise perform well in natural gas environments (Nguyen et al., 2020). This issue is particularly critical for ferritic pipeline steels, which are widely used due to their lower cost but are more susceptible to hydrogen-related degradation (Pichler et al., 2023).

METHOD

In this project, we investigated an API 5L X70 pipeline steel with a nominal thickness of 12 mm. The welded pipeline samples were received from SSAB. The pipes were produced using high-frequency induction (HFI) welding, a common industrial process for manufacturing longitudinally welded pipelines. The chemical composition of the material (wt.%) was approximately 0.073 C, 1.44 Mn, 0.197 Si, 0.045 Nb, 0.070 V, 0.104 Mo, 0.304 Cr, and 0.042 Ni, while the phosphorus and sulfur contents were about 0.011.

We characterized the microstructure using several advanced techniques. Electron backscatter diffraction (EBSD) was performed to analyze the grain structure and crystallographic orientation. The samples were first mechanically polished and subsequently electrochemically polished to remove residual surface deformation. EBSD measurements were carried out using a Hitachi SU6600 scanning electron microscope. To investigate fine-scale microstructural features, thin lamellae were prepared using a plasma-focused ion beam (FIB) for transmission electron microscopy (TEM). Site-specific specimens containing cementite particles were extracted from the steel matrix. In addition, needle-shaped tips with a radius of approximately 50–100 nm were prepared for atom probe tomography (APT) analysis. APT measurements were conducted in laser-pulsing mode at a specimen temperature of approximately 50 K with a pulse repetition rate of 250 kHz and a pulse energy of 40 pJ, maintaining a detection rate of about 0.5–1.0%.

To evaluate the mechanical performance of the material, the tests were carried out both in laboratory air and in 100 bar ultra-high-purity hydrogen. After testing, the fracture surfaces were examined using SEM.

To investigate hydrogen/microstructure interactions, specimens extracted from the weld region were electrochemically charged with hydrogen. After charging, thermal desorption spectroscopy (TDS) was then carried out to measure hydrogen release during heating.

In addition, density functional theory (DFT) calculations were performed to evaluate hydrogen trapping energies in cementite (Fe_3C). The calculations considered hydrogen interaction with carbon vacancies, vacancy clusters, and α-Fe/Fe_3C interfaces. All experiments were repeated three times to ensure the reproducibility and reliability of the results.

RESULTS AND FINDINGS

In this study, we demonstrate that faster cooling of the heat-affected zone (HAZ), compared to the thermomechanically controlled processed (TMCP) base metal, significantly improves resistance to hydrogen embrittlement. To understand the underlying mechanisms, we combined TEM, APT, TDS, mechanical testing in hydrogen, and DFT calculations.

Microstructural analysis revealed that the rapid cooling experienced during welding produces a refined ferrite–bainite lath structure in the HAZ, accompanied by inter-lath cementite films and a high dislocation density. In addition, the welding thermal cycle promotes the formation of a significant population of carbon vacancies within the cementite phase. These microstructural features play a key role in modifying the hydrogen trapping behavior of the material.

TDS results showed clear differences in hydrogen release behavior between the base metal and the HAZ. The base metal exhibited a single dominant low-temperature desorption peak, indicating that most of the hydrogen is weakly trapped and can diffuse relatively easily. In contrast, the HAZ showed a smaller low-temperature peak together with an additional high-temperature peak. This indicates that a larger fraction of hydrogen in the HAZ is trapped at stronger trapping sites and is released only at higher temperatures, reflecting slower hydrogen diffusion and a reduced fraction of diffusible hydrogen compared to the base metal.

DFT provided further insight into the origin of these trapping sites. The calculations showed that hydrogen is energetically unfavorable in regular interstitial sites of cementite (Fe_3C), with a solution energy of approximately +0.35 eV. However, hydrogen becomes strongly stabilized at carbon vacancies within the cementite structure. Additional stabilization occurs near α-Fe/Fe_3C interfaces and in vacancy clusters. The calculated incremental solution energies for multiple hydrogen atoms (1–5 H) demonstrate both the depth and capacity of these traps, explaining the high-temperature TDS peak observed experimentally and the reduced diffusible hydrogen fraction in the HAZ.

Although both the HAZ and the base metal satisfy the acceptance criteria defined by standard, mechanical testing conducted in hydrogen revealed notable differences in performance. Under identical loading conditions, the HAZ exhibited greater resistance to hydrogen-assisted cracking than the base metal. These results indicate that the microstructural modifications introduced by faster cooling during welding can significantly improve hydrogen tolerance in the HAZ, which is critical for the safe operation of hydrogen transport pipelines.

IMPACT OF THE WORK

The findings of this study provide valuable insights for SSAB in the development and optimization of pipeline steels for hydrogen transport. By showing that faster cooling of the HAZ during welding significantly enhances resistance to hydrogen embrittlement, the results demonstrate how welding parameters can be adjusted to improve the durability of ferritic pipeline steels in hydrogen service. Advanced characterization using TEM, APT, TDS, and DFT revealed that the refined ferrite–bainite lath structure, inter-lath cementite films, high dislocation density, and carbon vacancies in cementite act as strong hydrogen traps, slowing hydrogen diffusion and

reducing the fraction of diffusible hydrogen. These microstructural modifications allow the HAZ to exhibit greater resistance to hydrogen-assisted cracking than the base metal, while still meeting standard acceptance criteria. For SSAB, this knowledge provides a clear strategy to optimize welding processes and tailor steel microstructures for hydrogen applications, supporting the safe and cost-effective repurposing of existing pipelines and strengthening the company's position in supplying hydrogen-compatible steel solutions for the emerging hydrogen economy.

NEXT STEPS

Building on the data generated in this work, the next step of the project will be to integrate experimental results with new simulation studies to develop predictive models for pipeline steel performance under both hydrogen and air environments. By combining microstructural characterization, hydrogen trapping behaviour, and mechanical performance (fatigue data) with computational modeling, it will be possible to quantify how different microstructural features affect hydrogen diffusion, trapping, crack initiation, and propagation. The models will be designed to predict fracture toughness and fatigue life under varying hydrogen pressures as well as standard air conditions, providing a comprehensive understanding of performance under service-relevant environments. Integrating simulations with experimental data will increase insight into the mechanisms controlling hydrogen embrittlement while also capturing baseline behavior in air. This combined approach will allow optimization of welding parameters and microstructures, enabling the design of pipeline steels with enhanced durability and safety for both hydrogen and conventional natural gas service. Ultimately, these predictive models will improve the ability to anticipate long-term performance, reduce experimental effort, and accelerate the development of steels tailored for safe, reliable, and cost-effective hydrogen transport.

PUBLICATIONS AND THESES

Horváth, D. Hydrogen embrittlement of welded steels. [Doctoral thesis, LUT University]. On-going.

Horváth, D., Safyari, M. & Moshtaghi, M. (2026) Hydrogen embrittlement in welded pipeline steels: Fundamentals, mechanisms, testing, mitigation and welding processes. Submitted, under review.

Ghasemi, A. (2026) *Simulation of hydrogen TDS peaks and ML-based prediction of desorption energies (SimuTDS) from experimental data* [Master's thesis, LUT University]. Accessible: https://urn.fi/URN:NBN:fi-fe2026030718761

Safyari, M. & Moshtaghi, M. (2025) Welding design of API 5L X65 pipeline steel: Effects of robotic hybrid laser arc welding versus GMAW on fracture toughness evaluated by SENT tests in air and hydrogen. *Materials & Design*, 254, 113950. https://doi.org/10.1016/j.matdes.2025.113950

Safyari, M., Kivimäki, M., Tulonen, J., Virolainen, E., Suikkanen, P. & Moshtaghi, M. (2026) Enhancing fracture toughness of the heat-affected zone in welded X70 pipeline steel under hydrogen gas. Submitted, under review.

Safyari, M., Horváth, D. & Moshtaghi, M. (2025) Enhancing hydrogen embrittlement resistance in steel pipelines through hybrid welding. *Welding in the World*. https://doi.org/10.1007/s40194-025-02071-w

Safyari, M., Ahmad, M. & Moshtaghi, M. (2026) Insights into gaseous hydrogen permeation behavior in welds of X65 pipeline steel. *Welding in the World*. https://doi.org/10.1007/s40194-026-02362-w

REFERENCES

Moshtaghi, M., Safyari, M. (2023) Different augmentations of absorbed hydrogen under elastic straining in high-pressure gaseous hydrogen environment by as-quenched and as-tempered

martensitic steels: combined experimental and simulation study. *International Journal of Hydrogen Energy*, 48(70), 27408–27415. https://doi.org/10.1016/j.ijhydene.2023.03.396

Moshtaghi, M., Safyari, M., Khonsari M. M. (2024) Hydrogen-enhanced entropy (HEENT): A concept for hydrogen embrittlement prediction. *International Journal of Hydrogen Energy*, 53, 434–440. https://doi.org/10.1016/j.ijhydene.2023.12.068

Moshtaghi, M., Safyari, M., Mori, G. (2022) Combined thermal desorption spectroscopy, hydrogen visualization, HRTEM and EBSD investigation of a Ni–Fe–Cr alloy: The role of hydrogen trapping behavior in hydrogen-assisted fracture. *Materials Science and Engineering*: A, 848, 143428, https://doi.org/10.1016/j.msea.2022.143428.

Nguyen, T. T., Tak, N., Park, J., Nahm S. H., Beak, U. B. (2020) Hydrogen embrittlement susceptibility of X70 pipeline steel weld under a low partial hydrogen environment," *International Journal of Hydrogen Energy*, 45(43), 23739–23753. https://doi.org/10.1016/j.ijhydene.2020.06.199

Pichler S., Bendo, A., Mori, G., Safyari, M., Moshtaghi, M. (2023) Inhibition of grain growth by pearlite improves hydrogen embrittlement susceptibility of the ultra-low carbon ferritic steel: the influence of H-assisted crack initiation and propagation mechanisms. *Journal of Materials Science*, 58, 13460–13475. https://doi.org/10.1007/s10853-023-08856-y

Safyari, M., Moshtaghi, M. (2025) Welding design of API 5L X65 pipeline steel: Effects of robotic hybrid laser arc welding versus GMAW on fracture toughness evaluated by SENT tests in air and hydrogen. *Materials & Design*, 254, 113950. https://doi.org/10.1016/j.matdes.2025.113950

5.4 High-performing high-strength FFHS steel components

5.4.1 Mechanical performance of dissimilar welded joints

Contributors: **Shahriar Afkhami[1,2], Janak Devkota[2], Antti Ahola[2], Vahid Javaheri[3], Johannes Sainio[4], Tuomas Skriko[1]**

[1]Welding Technology, Mechanical Engineering, LUT University
[2]Steel Structures, Mechanical Engineering, LUT University
[3]Microstructure and Mechanisms, Materials and Mechanical Engineering, University of Oulu
[4]SSAB Europe Oy, Knowledge Service Center

Correspondence: **Shahriar Afkhami** (shahriar.afkhami@lut.fi)

BACKGROUND

Thermomechanically-processed (TMCP) high-strength steels (HSSs) and ultra-high strength steels (UHSSs) are widely used in steel structures for their excellent strength-to-weight ratios and cost savings. However, their welded joints can suffer from heat-affected zone (HAZ) softening due to microstructure evolution during welding. This issue complicates the prediction of joint failure, especially between steels with similar strength but different degrees of HAZ softening. Microstructural changes in the HAZ also alter the distribution of residual stress: martensite and bainite encourage compressive stress, while post-weld cooling induces tensile stress. Accordingly, the resulting balance affects joint mechanical behavior and fatigue failure.

METHOD

This study experimentally investigated two types of dissimilar welds: S500MCD to S700MC (HSS with different strengths) and S960MC to S960QT (UHSS with similar strengths, different TCMP). Steel plates were 6 mm (single-pass) and 8 mm (double-pass), welded with recommended parameters. After welding, microstructure, Vickers hardness, residual stress, and quasi-static mechanical properties (by tensile tests and DIC) were evaluated.

RESULTS AND FINDINGS

The results showed that single-pass welding caused up to 15% softening in S500MCD-S700MC welds, and this softening increased to 24% on the lower side of the double-pass welds (reheating effect on the first pass) (Figure 25). However, for S960QT-S960MC welds, there was no noticeable difference in the highest detected softening between single-pass and double-pass welds. S960QT experienced the most severe softening in its HAZ. Microstructural analysis identified the formation of coarse bainitic/ferritic features as the main reason for softening in all welded steel variants, regardless of whether the weld was single- or double-pass.

Regarding the tensile tests, welded S500MCD-S700MC joints failed from their S500MCD base metal, regardless of the welding approach. The dominant influence of S500MCD base metal on the mechanical performance of the welded joint is well reflected in the stress-strain curves (Figure 26a). However, S960MC-S960QT (Figure 26(b)) welds failed from their fusion line, as shown in Figure 27. In this case, the failure appears to be governed by a combination of HAZ softening and weld-bead geometry. Finally, multi-pass welding alleviated the residual stress near the fusion line and even transformed it from tensile to compressive for S960 variants (Figures 26(c) and (d)).

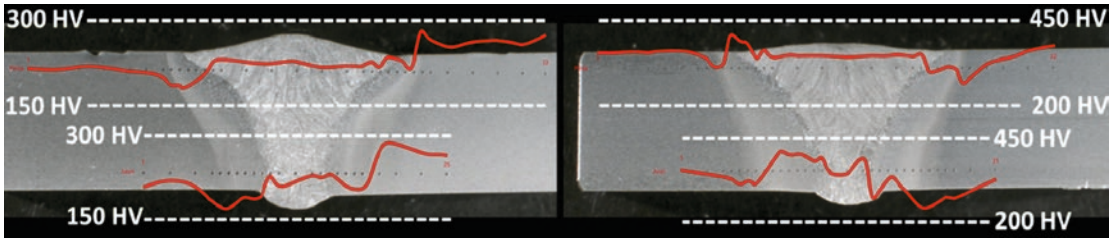

Figure 25. Hardness profiles of S500MCD-S700MC and S960MC-S960QT.

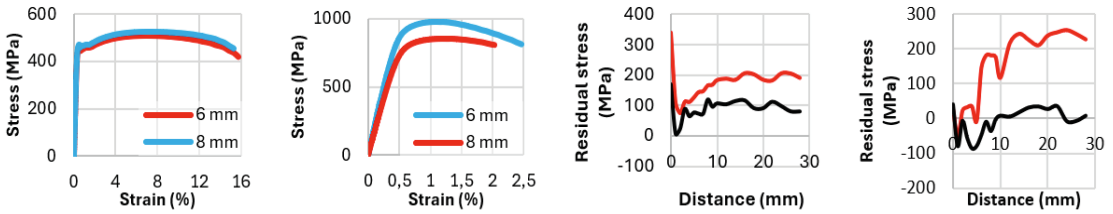

Figure 26. Engineering stress stain curves of S500MCD-S700MC (a) and S960QT-S960MC (b) welds. Residual stress distribution based on the distance from the fusion line in single-pass (c) and double-pass (d) welded S960QT-S960MC joints.

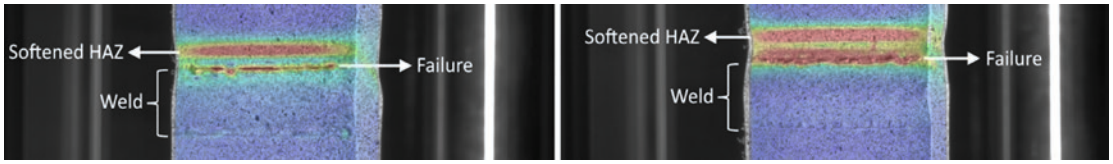

Figure 27. Strain distribution of S960QT-S960MC: 8 mm (left) and 6 mm (right) before their failure.

IMPACT OF THE WORK

The research promotes the application of TMCP HSS and UHSS to improve sustainability in steel structures and construction. Further, it addresses mechanical failures of such components to improve safety evaluations and predictions for contemporary steel structures.

NEXT STEPS

Given the greater influence of weld bead geometry and residual stress on the fatigue performance of welded HSS and UHSS, the next steps of this research will focus on the mechanical failure of welded components under cyclic loads.

PUBLICATIONS AND THESES

Devkota, J. (2025). Mechanical performance and fracture behaviour of dissimilar welds made of thermo-mechanically rolled steels: a study of dissimilar steel grades weld joint between S700 MC Plus, and Domex 500 D [Master's thesis, LUT University]. Accessible: https://urn.fi/URN:NBN:fi-fe2025061871725

Ayub, H. (2026). Effect of arc welding on microstructure and mechanical properties of S960 MC to S960 QT Ultra-High Strength Steel (UHSS) dissimilar joints [Master's thesis, LUT University]. (To be published).

Garabics, B. (2026). Residual stresses in welded ultra-high-strength steels and their correlation with microstructure [Bachelor's thesis, LUT University] (to be published).

5.4.2 Fatigue performance of post-weld-treated high-strength steel joints

Contributors: **Antti Ahola[1], Kalle Lipiäinen[1], Martin Leitner[1,2,*]**

[1]Steel Structures, Mechanical Engineering, LUT University
[2]Institute of Structural Durability and Railway Technology, TU Graz, Austria
*Visiting professor of LUT University (2023-2025)

Correspondence: **Antti Ahola** (antti.ahola@lut.fi), +358 50 475 2825

BACKGROUND

It is well-known that as-welded high-strength steel (HSS) joints suffer from the lack of improved fatigue resistance, specifically in cyclically loaded welded structures prone to fatigue failures. To overcome these drawbacks associated with as-welded joints, post-weld treatments (PWTs) are a robust solution to locally enhance the fatigue strength of welded joints by modifying the residual stresses and/or local weld toe geometry. Although these methods have been recognized already for some decades, the lack of proper design data and methodologies prevents the full utilization of the benefits gained by PWTs. This task contributed to understanding the fatigue performance of high-frequency mechanical impact (HFMI)-treated and clean-blasted joints, and use of a novel weld extension technique for enhancing the fatigue strength of longitudinally reinforced joints. 4R method applications were developed for HFMI-treated joints, subjected to variable amplitude loading (see also Section 6.3 for the simulation-based prediction model). In addition, the stress gradient effects were studied in bending-loaded HFMI-treated joints with the aim of validating the existing fatigue design guidelines for HFMI-treated joints (Marquis and Barsoum, 2016) and bending correction factors (BS7608, 2015).

METHOD

The task utilized experimental fatigue data for the model development and validations. For the HFMI studies, literature data was obtained. In the 4R applications for the HFMI-treated joints under VA loading, the developed 4R-VA equivalent stress concept, Figure 28 (Rohani Raftar et al., 2024; Grönlund et al., 2024) was extended:

$$\Delta\sigma_{\mathrm{k,eq,ref}} = \sqrt[m]{\frac{1}{D}\frac{\sum_i \left(n_i \left(\frac{\Delta\sigma_{\mathrm{k},i}}{\sqrt{1-R_{\mathrm{local},i}}} \right)^m \right)}{\sum_i n_i}}$$

In Eq. $\Delta\sigma_{k,eq,ref}$ is the mean-stress-corrected equivalent effective stress range, D is the linear damage sum, $\Delta_{\sigma k,i}$ is (individual) i^{th} effective stress range, $R_{local,i}$ is i^{th} local stress ratio, m is the slope parameter of the S-N curve, and ni is the number of ith load cycles. The effective stresses were computed using the numerical finite element models, employing the effective notch stress concept (Hobbacher and Baumgartner, 2024). For the HFMI stress gradient study, the combined thickness-bending correction factor k^{tb} and IIW thickness correction factor *f(t)* were validated (BS7608, 2014; Hobbacher and Baumgartner, 2024). In the weld extension study, an experimental fatigue test campaign was carried out to study different options to enhance fatigue strength of welded-around gusset joints (as-welded, HFMI-treated and specimens with weld extensions).

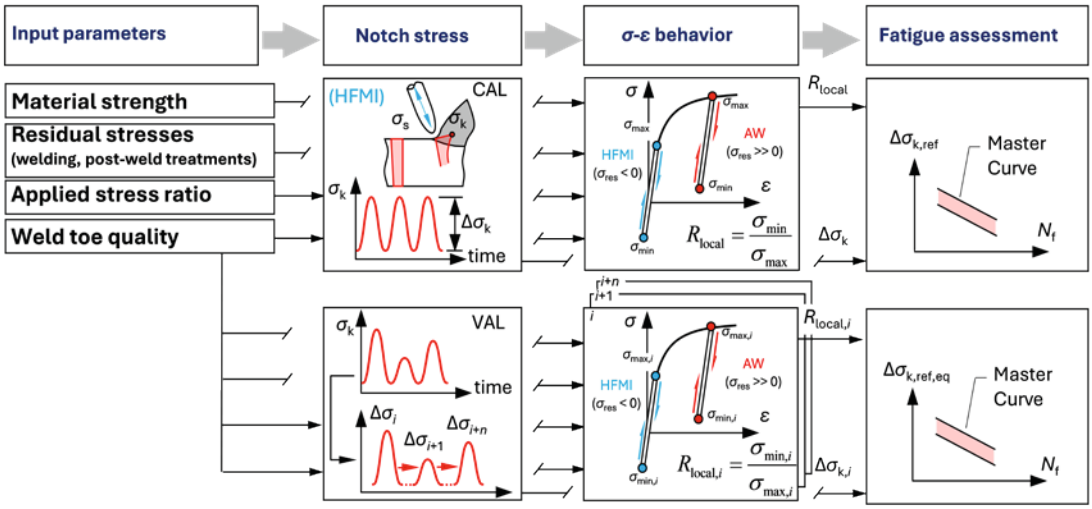

Figure 28. Workflow and principles of the master curve approach of the 4R method (Ahola et al., 2025).

RESULTS AND FINDINGS

The VA fatigue data evaluation indicated that the 4R method is capable of capturing the sequential load effects, and the master curve methods also work for HFMI-treated joints, Figure 29a. Specifically, the 4R method provided increased accuracy compared to other effective stress methods in joints subjected to reversed cyclic stresses (applied stress ratio of -1), and demonstrated load configuration-specific damage sum parameters, that the conventional stress-based approaches could not capture. Figure 29b exemplifies the experimental fatigue data validation of k_{tb} and *f(t)*-corrected results in the bending-loaded HFMI joints. In general, k_{tb} was found to provide more accurate results than the *f(t)* thickness correction suggested by IIW. For welded-around longitudinal reinforcements, Figure 29c demonstrates that weld extension techniques can provide further enhanced fatigue capacity, even compared to the HFMI-treated joints in S420 steel components.

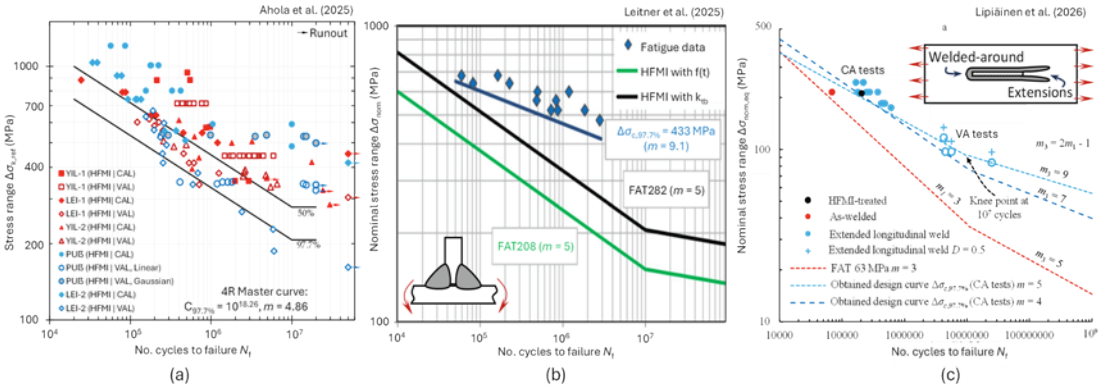

Figure 29. Result summary of the task B: (a) 4R applications for HFMI-treated HSS joints, (b) thickness- and bending stress-corrected design curves with respect to fatigue data, and (c) benefits gained by the weld extension techniques.

IMPACT OF THE WORK

This work advanced fatigue design principles for lightweight high-strength steel welded structures by extending the 4R method to HFMI-treated joints under variable-amplitude loading, enabling

more accurate accounting of sequential load effects than conventional stress-based approaches. Validation of stress-gradient correction factors provides new experimental evidence supporting refinement of current IIW and BS7608 fatigue design guidelines, with ktb shown to outperform existing thickness corrections in bending. Additionally, weld extension techniques were demonstrated to further enhance fatigue strength in longitudinally reinforced joints. Together, these findings support more reliable fatigue assessments, leading to complete utilization of steel capacity enabling lightweight steel solutions with reduced in-service emissions.

NEXT STEPS

Next steps include extending the 4R effective stress methods to thin-walled joints by incorporating real weld geometries, enabling more accurate fatigue assessment in geometrically sensitive configurations. The work will also support the development of harmonized international design guidelines that reflect the improved understanding of HFMI performance. In addition, further studies will focus on applying HFMI treatments to novel high-strength and ultra-high-strength steel materials to broaden their industrial use and optimize structural fatigue resistance.

PUBLICATIONS

Ahola, A., Leitner, M., Grönlund, K., Brunnhofer, P., Buzzi, C., Moshtaghi, M., Björk, T. (2025). Fatigue assessment of as-welded and HFMI-treated high-strength steel joints under variable amplitude loading using local approaches. *Welding in the World*, 69, 687–700. http://dx.doi.org/10.1007/s40194-024-01919-x

Leitner, M., Ahola, A., Moshtaghi, M., Björk, T., Brunnhofer, P., Buzzi, C. (2025). Fatigue strength assessment of HFMI-treated steel joints under bending loading. *Welding in the World*, 69, 243–2441. https://doi.org/10.1007/s40194-025-02100-8

Lipiäinen, K., Heinilä, S., Ahola, A., Skriko, T. (2026). Fatigue strength improvement of gusset end detail with welding techniques. Revision submitted to journal (ref. background IIW document: XIII-3163-2025)

REFERENCES

BS7608 (2014) *Guide to fatigue design and assessment of steel products*. British Standards Institution (BSI).

Grönlund, K., Ahola, A., Riski, J., Pesonen, T., Lipiäinen, K., Björk, T. (2024) Overload and variable amplitude load effects on the fatigue strength of welded joints. *Welding in the World*, 68, 411–425. https://doi.org/10.1007/s40194-023-01642-z

Hobbacher, A., Baumgartner, J. (2024) *Recommendations for Fatigue Design of Welded Joints and Components*. 3rd edition, Springer.

Marquis, G., Barsoum, Z. (2016) IIW *Recommendations for the HFMI Treatment*. 1st edition, Springer.

Rohani Raftar, H., Ahola, A., Lipiäinen, K., Björk, T. (2024) Fatigue behavior of load-carrying cruciform fillet weld joints under variable amplitude load. *Journal of Constructional Steel Research*, 215, 108559. http://dx.doi.org/10.1016/j.jcsr.2024.108559

5.5 Quality leap in welding of FFHS steels: Adaptive robotic welding with multi-sensor feedback control

Contributors: **Humza Wali, Tuomas Skriko**, Welding Technology, Mechanical Engineering, LUT University

Correspondence: **Humza Wali** (humza.wali@lut.fi)

BACKGROUND

Robotic arc welding is widely used in manufacturing industries, as it can do repetitive tasks economically within acceptable quality standards. Typically, a robotic welding process consists of two tightly coupled subsystems: the robotic motion system and welding power source. However, these two systems are controlled by separate loosely coupled controllers and it becomes difficult to maintain and control the quality requirements in case of occurrence of inaccuracies or disturbances in the process. (Pires et al., 2006; Tarn et al. 2015)

Adaptive robot welding with multi-sensor feedback control is motivated by the gap that exists between what is defined in Welding Procedure Specification (WPS) and what off-line programmed (OLP) robotic welding can achieve under varying joint and process conditions. A WPS is a formal document that provides necessary welding process parameters and guidelines to produce acceptable welds that meet applicable codes and standards. Welding robots can repeat a programmed path and execute preset process parameters reliably but without sensing and feedback control they cannot detect or compensate for actual joint geometries having misalignments, gaps, distortions, etc. (Pires et al., 2006; Tarn et al. 2015)

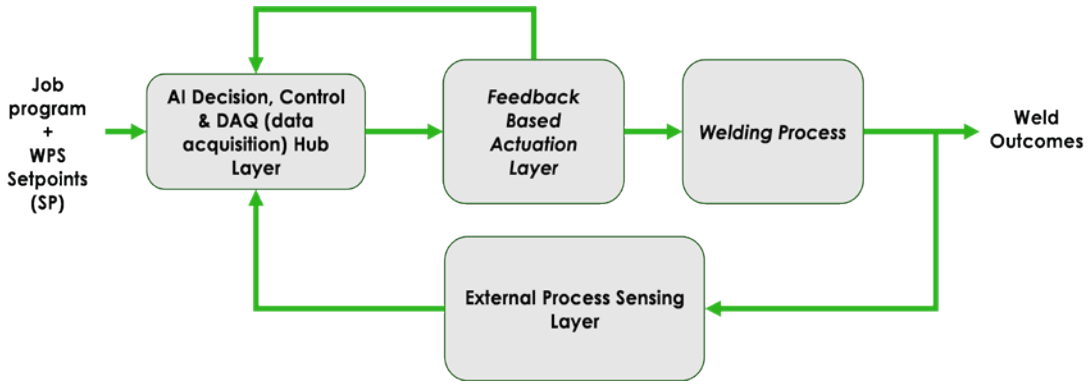

Figure 30. System architecture for adaptive robotic welding process.

Arc welding is a complex dynamic process that generates a lot of data having significant variability under harsh and challenging conditions such as intense arc radiation, high temperature, electromagnetic interference, acoustic disturbances, mechanical vibrations, etc. Practically, most of the process relevant data can be measured in real-time by utilizing the inherent sensors of the robotic motion system (torch speed, joint values, poses, etc.) and power source (voltage, current, wire feed speed, etc.) which can be complimented by the utilization of external sensors such as non-contact optical sensors which operate in visible (high-speed arc filtered welding camera) and infrared (thermal camera and pyrometer) spectral ranges, as well as laser line scanners to extract geometric features. Process relevant features and parameters are extracted and processed by synchronizing these multiple sensors to predict and estimate the weld quality. This is utilized in

closed loop control (Figure 30) of the welding process which adjusts the robot motion and welding power source parameters to keep weld quality stable under joint and process variability. (Pires et al., 2006; Tarn et al. 2015)

METHOD

The task focused on implementing a modular architecture for AI enabled adaptive robotic welding. This required integration of hardware via industrial communication links to support synchronized multi-sensor data collection. Multi-layer architecture for adaptive robotic welding is given in Figure 31. The system consists of 4 layers: XR (extended reality) HMI Layer, AI-enabled control & integration layer, external process sensing layer, and feedback-based actuation layer.

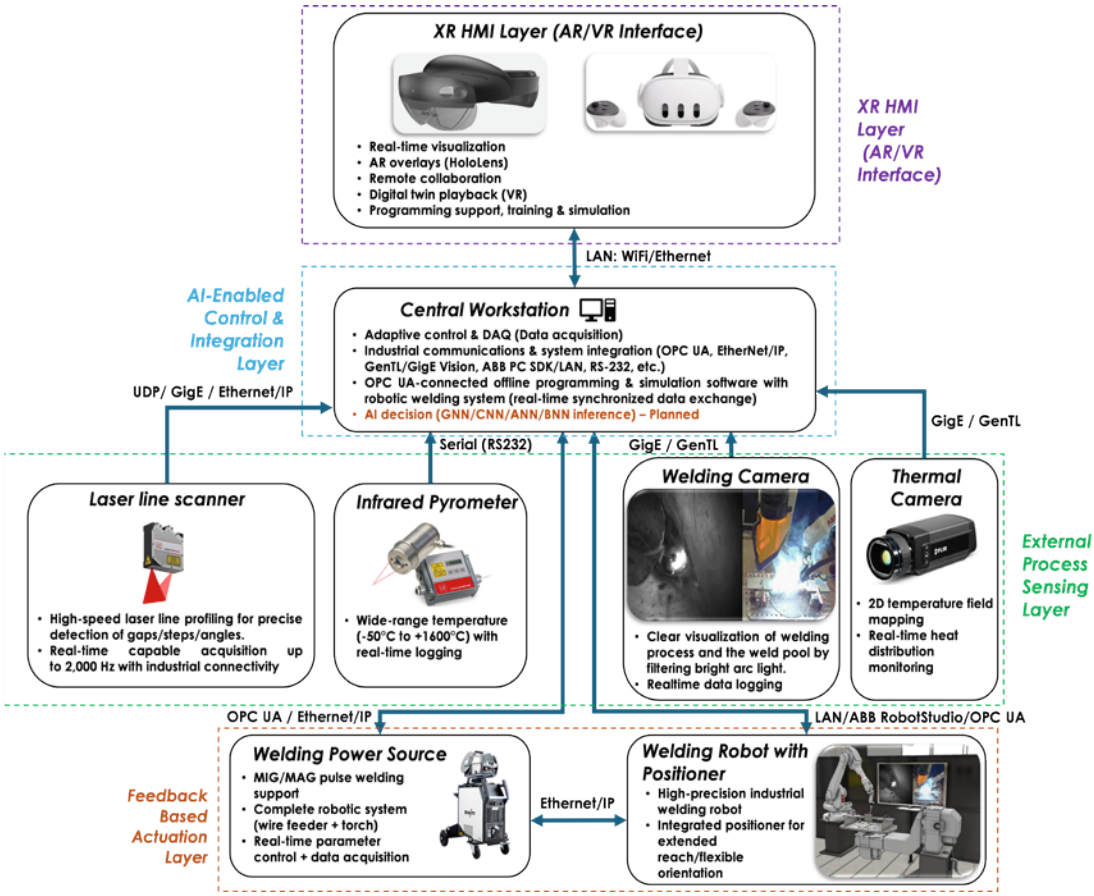

Figure 31. System overview at LUT robotic welding unit developed in FOSSA2.

The central workstation coordinates and integrates all the system layers, with ongoing development of deep learning capabilities (GANs - generative adversarial for data augmentation, and CNNs/ANNs/BNNs - convolutional, artificial neural, and Bayesian neural network models for weld quality prediction and uncertainty-aware decision support) to enable automated weld quality prediction and AI enabled adaptive control. It implements the data acquisition (DAQ), real-time monitoring and control involving online welding power source parameter tuning. Key functions include welding job program transfer via LAN (ABB Robot Studio for ABB and FTP

for Yaskawa robot system respectively), OPC UA communication with multibody dynamics and simulation software (Visual Components and MATLAB Multibody Dynamics software) for digital shadow implementation thus enabling real-time data exchange between physical system and digital model, custom MATLAB programs for real-time monitoring and tuning of welding parameters thus implementing digital twin of welding power source, multi-sensor synchronization, and real-time data logging and visualization from pyrometer, thermal camera, specialized arc-filtered laser illuminated welding camera, and laser line scanner. External process sensing layer consists of synchronized sensors communicating via industrial interfaces such as GigE Vision, EtherNet/IP, and Serial/RS-232. These include laser line scanner, welding camera, pyrometer, and thermal camera. Laser line scanner collects data regarding joint geometry, bead geometry, gaps, offset, etc. Whereas, welding camera is utilized for observing and collecting data regarding surface defects, droplet transfer, spatter, arc/melt pool stability, asymmetry/fusion detection, etc. Infrared pyrometer is utilized for measurement of localized temperature at a specific point of the weld zone.

Feedback based actuation layer consists of industrial welding robotic system and a welding power source integrated via IIoT (industrial internet of things) enabled communication. The welding power source enables real time monitoring and tuning of process setpoint parameters i.e. current/wire feed speed, voltage, and arc dynamics. The robotic motion system consists of six-axis industrial manipulator complemented by a two-axis positioner allowing real-time control based on multi-sensor feedback, operated under real-time control. The implemented framework primarily reflects the properties of a digital shadow with partial bidirectional communication towards digital twin functionality. The extended reality (XR) based human-machine interface (HMI) layer offers augmented reality (AR) and virtual reality (VR) interfaces for real-time visualization and interaction with the robotic welding setup with some applications shown in Figure 32. This layer offers AR overlays to support remote collaboration, digital twin playback, programming assistance, and operator training.

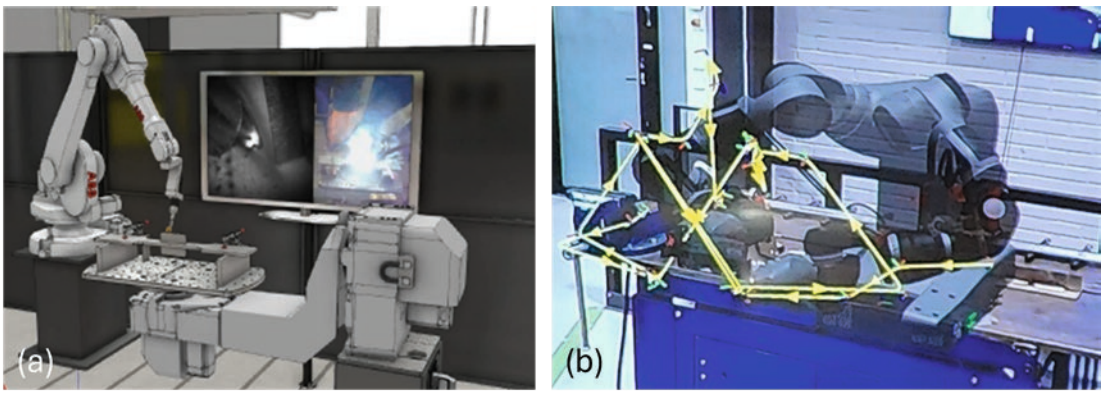

Figure 32. Extended reality applications in welding. (a) Welding camera and RGB camera feed in VR environment with digital representation of welding robot system, and (b) AR overlay showing robot and path plan.

RESULTS AND FINDINGS

A layered, adaptive control based robotic welding framework was developed and implemented to enable the application development of AI-driven multi-sensor weld quality monitoring, prediction, and closed-loop control. Multi-sensor integration, data acquisition and synchronization were achieved by utilizing industrial communication interfaces (OPC UA, Ethernet/IP, GigE Vision/ GenTL, etc.) resulting in a centralized data acquisition (DAQ) system.

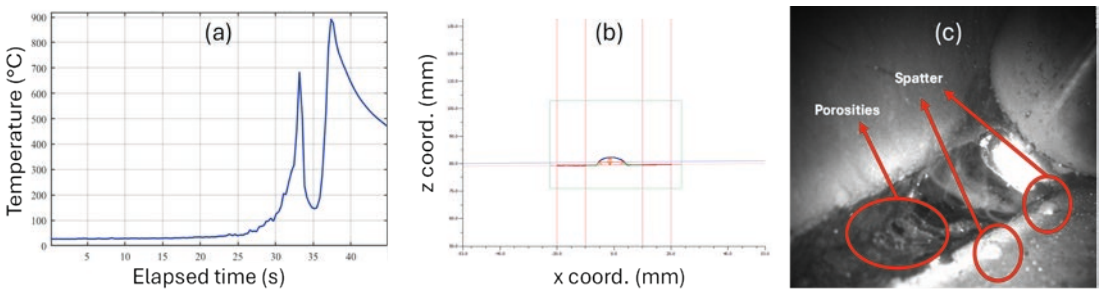

Figure 33. (a) Temperature versus time data from pyrometer, (b) weld bead measurement data from 3D line scanner, and (c) welding camera feed showing defects during welding process.

Custom acquisition programs were developed for the pyrometer and the laser line scanner using industrial interfaces (i.e. serial, Ethernet/IP, GigE Vision, and UDP/IP) enabling real time data logging of temperature and joint/bead geometry measurements within a unified workstation-based data acquisition pipeline as shown in Figure 33a-b. Welding camera with the capability to filter arc radiation and laser-based illumination of the region of interest was integrated via custom MATLAB program through GigE vision. This enabled real-time data logging, visualization, and dataset generation for subsequent welding process feature extraction and CNN model development. Figure 33c shows visual surface defects captured by welding camera which are critical for weld quality analysis. Thermal monitoring capability was implemented using the manufacturer's software development kit (SDK) and dependencies, and a digital shadow was created through OPC UA connectivity interface to enable real-time data exchange between the physical robot motion system and its digital representation in multibody simulation environments.

IMPACT OF THE WORK

This task delivered an end-end, industrially scalable platform that embodies unified multisensory data acquisition, synchronized logging and streaming, and real-time process monitoring and control within a single architecture, thereby providing a structured foundation for deep learning-based application development for weld quality assessment and prediction. The framework improves observability, traceability, and validation of welding process by establishing reliable multisensory fusion through industrial interfacing and the creation of digital shadow and twin representations. This implementation accelerates further research and development and industrial adoption by enabling systematic dataset generation, integration of AI models, future extensions, and control strategies without the need to redesign integration layer.

NEXT STEPS

Ongoing and further steps involve conducting systematic welding experiments to generate labelled multi-sensor datasets covering diverse process conditions, defect types, joint geometries, and quality indicators. In parallel, deep learning model development is under progress, encompassing BNNs for uncertainty-aware weld quality outcome prediction based on setpoint parameters and weld configurations. Subsequently, CNN-based models for visual data analysis targeting defect detection and quality indicators will be developed. Also, GAN-based data augmentation will be carried out to enrich training datasets, particularly involving computationally expensive simulation data such as FEM-generated simulated data. Further development of the XR HMI layer is also planned, incorporating live AI prediction overlays and quality markers to support the welding job execution.

PUBLICATIONS AND THESES

Wali, H., Skriko, T., et al. (2026) Investigating shielding gas effects with multi-sensor robotic welding setup focusing on ultra-high strength steel in the GMAW process. To be submitted (spring 2026).

Lund, H. (2025). Extended reality-enabled smart manufacturing in multi-robot welding applications [Doctoral thesis, LUT University] Accessible: https://urn.fi/URN:ISBN:978-952-412-263-4

REFERENCES

Pires, J. N., Loureir, A., Bölmsjo G. (2006). Welding Robots: *Technology, System Issues and Application*. Springer London. https://doi.org/10.1007/1-84628-191-1

Tarn, T.-J., Chen, S.-B., Chen, X.-Q. (2015). Robotic Welding, Intelligence and Automation. *Proceedings of 2014 International Conference on Robotic Welding, Intelligence and Automation (RWIA'2014)*, Shanghai, 16-18 October 2014. https://doi.org/10.1007/978-3-319-18997-0

5.6 Application of rapid annealing in the production of fossil-free steels

Contributors: **Ali Sabr, Shahroz Ahmed, Lassi Raami, Pasi Peura**, Tampere University
David Penney, Swansea University, UK

Correspondence: **Prof. Pasi Peura**, Tampere University (pasi.peura@tuni.fi), 050-3013884

BACKGROUND

TAU (Tampere University) has concentrated on studies on cold rolled and continuously annealed thin sheet steel grades. The name of TAU's task is "Application of Rapid Annealing in the Production of Fossil Free Steels" (NOFO). There is limited information available on the effects trace elements in formable cold rolled and annealed steel grades, thus in this area there was a clear research gap. All the studied materials were advanced high strength steel grades deliberately alloyed with controlled trace levels of copper and tin additions. The main aim of the study was to define a concept for manufacturing future formable fossil free UHSS/AHSS steels from raw materials containing significant amount of steel scrap. The other aim was to find out if it will be possible to reduce or eliminate harmful effects of trace elements on the properties and structure of the investigated steels grades by rapid annealing process. These can be expressed as a single research question: "What are the principles in the developing future formable fossil free UHSS/AHSS sheet steels?" To solve this question, the following aspects has been taken into consideration; 1) increasing use of scrap and the resulting higher levels of scrap derived residual elements in future steels, and 2) the effect of rapid heating rates and trace elements on microstructure and properties of AHSS grades.

METHOD

The studied materials included multiphase and press hardening steels deliberately alloyed with controlled trace levels of copper and tin additions. The steel grade used as base was DP800, which was alloyed with up to 0.6 wt-% of copper and up to 0.1 wt-% of tin either solely or in combination. In addition, mechanical behavior of an aluminum rich medium manganese steel alloy was also investigated. Two different heating methods were applied for the samples; ultra fast induction heating at TAU, and conventional and rapid radiation heating inside a hot dip galvanizing simulator at Swansea University in UK.

For the samples, the following investigations were performed; 1) characterization of the microstructure using optical microscopy (OM), scanning (SEM) and transmission (STEM) electron microscopy. EDS, EBSD and TKD methods were applied. 2) X-ray diffraction, 3) Atomic probe tomography (APT, at KTH), 4) tensile, and 5) bending tests.

RESULTS AND FINDINGS

The main findings of the study are presented below. More detailed results and analysis are available from the dissertations (A. Sabr, 2026, S. Ahmed 2026) and in publications (Shahroz et al. 2025, Shahroz et al. 2026).

Resulting microstructures and location of the trace elements: The main process parameter which was altered was heating rate up to the inter-critical annealing temperature. Slow heating rate of 4 °C/s simulated the heating rate typically applied in industrial continuous annealing lines, high heating rate of 120 °C/s simulated induction heating lines, and intermediate heating rate of 50 °C/s was the highest heating rate possible in radiation heated process simulator.

The microstructural studies were performed on slab, hot rolled, and annealed (after cold rolling) samples. No significant differences in the microstructures related to trace elements were detected. Thus, after that the characterization work concentrated on the location of trace elements. In slab samples traces of copper were found in martensitic areas and on the interphase between slab surface and scale (Figure 34). After cold rolling and annealing APT studies showed three times higher copper levels in martensite than in ferrite. (Sabr et al., 2026) Copper stabilizes austenite and thus this explains why traces of copper are found in martensite. This behavior is enhanced when nickel is added to the steel, as it increases solubility of copper in austenite and this mechanism is known to reduce hot shortness.

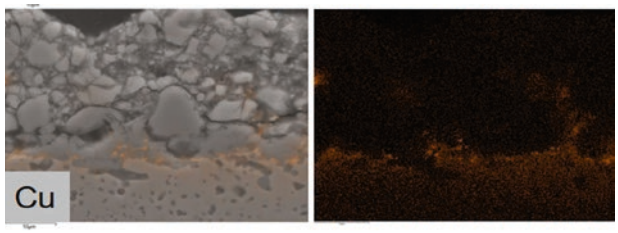

Figure 34. Location of Cu on the interphase between steel and scale in hot rolled DP800 (Sabr et al., 2026).

Effect of copper and tin on the properties of multiphase steels: The effect of deliberately added trace elements on phase transformation temperatures, were not significant, nor no systematic effects of trace elements on the mechanical properties were found. The observed differences in mechanical properties were more related to the different heating rates than on the levels of trace elements. An exception was the samples with copper content of 0.6%, where both yield and tensile strength values were 100-150MPa higher than in other samples after corresponding heat treatments. The same samples got also slightly lower formability indices. (Sabr, 2026)

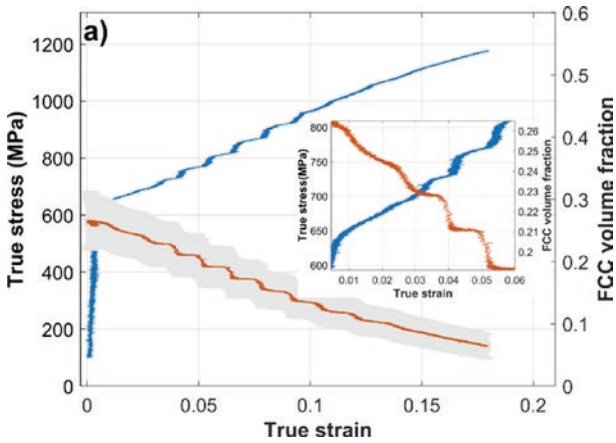

Figure 35. In-situ XRD tensile test results of a medium manganese steels, true stress-strain curve (blue) and corresponding austenite transformation (orange). (Shahroz et al., 2026)

In situ synchrotron XRD testing: In-situ XRD tensile test experiments were conducted at MAXIV synchrotron facility at the DanMAX beamline to investigate the correlation between austenite phase transformation and occurrence of serrated flow in intercritically annealed MMS. The results show that serrations are due to propagating Portevin Le Chatelier (PLC) bands which results from dynamic strain aging (DSA) phenomenon. DSA led to step wise transformation of austenite in this class of steel grades. Location of copper was examined using TKD in intercritically annealed copper containing MMS. The analysis was conducted on thin foil samples using and STEM-EDS. Figure 36 a-d show shows Cu mainly in austenite and at the boundaries of martensite. (Shahroz et al. 2026)

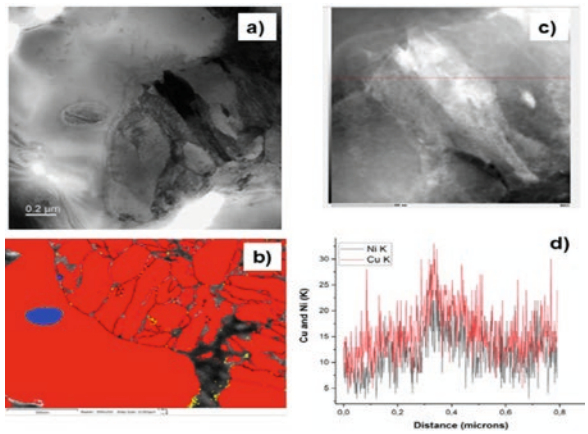

Figure 36. Location of Cu in MMS; (a) bright field TEM micrograph of a sample, (b) phase distribution, red is FCC and blue is BCC. (c and d) STEM-EDS of Cu and Ni (nickel) from the same location. (Shahroz et al., 2026)

IMPACT OF THE WORK

On general level the impact of the work first includes improved scientific knowledge on the function of trace elements in advanced steel grades. This will help to focus coming research on important critical topics. Second, the obtained knowledge will make possible development of trace element tolerant robust future fossil free sheet steels. Previously, there has been limited number of studies on the effects of trace elements and heating rate on the properties of high strength multiphase steels. Thus, the present results are of high scientific novelty and contribute to the aims to achieve fossil free steel production in the future. Especially the steel producers are benefiting from the results when they increase the use of scrap in their steel production. For the steel developers the results are giving guidelines for future steel development projects. For steels used the knowledge obtained and spread during the projects is giving confidence that the properties of the future formable AHSS steels grades will not differ significantly from the present ones.

NEXT STEPS

So far most of the efforts have considered high and ultra-high strength steel. The effects of trace elements and heating rate on mechanical properties and location of the trace elements have been investigated. Despite that, there are still a few research gaps like on the effects of trace elements in formable mild steels, especially in so called interstitial free (IF) steels. There is limited information available how the properties and structure of these steels will change due to trace elements. The same concerns scrap-based press hardening steels. In addition, the role of trace elements in welding of the IF and AHSS steel grades has not yet properly studied. Especially, the effect of copper will be of importance.

PUBLICATIONS AND THESES

Ahmed, S., Oja, O., Kaijalainen, A., & Peura, P. (2025). Effect of cooling practice on the mechanical properties of medium-manganese aluminum-alloyed steels after intercritical annealing quench and partition treatment. *Steel Research International*, 96(2), 2400420. https://doi.org/10.1002/srin.202400420

Raami, L., Valtonen, K., Wendler, M., & Peura, P. (2025). Effect of heat treatments on the cavitation erosion evolution of AISI 420 stainless steels. *Wear*, 206493. https://doi.org/10.1016/j.wear.2025.206493

Raami, L., Wendler, M., Volkova, O., & Peura, P. (2025). The effect of bake hardening on quenched and partitioned AISI 420 stainless steel. *Steel Research International*, 96(5), 2400251. https://doi.org/10.1002/srin.202400251

Ahmed, S., Pun, L., Isakov, M., Raami, L., Hokka, M., Kuokkala, V.-T., & Peura, P. (2026). Investigation of serrated flow in intercritically annealed medium manganese steel by in-situ synchrotron X-ray diffraction. Submitted to *Steel research international*.

Sabr, A., Ahmed, S., Kaijalainen, A., Penney, D., & Peura, P. (2026). Effects of Trace Elements Copper and Tin on Mild and Dual-Phase Steel Properties, to be submitted.

Halonen, H. (2025). *Q&P treatment of a eutectoid silicon steel* [Master's thesis, Tampere University]. Accessible: https://urn.fi/URN:NBN:fi:tuni-2025120511294

Pihlava, E. Press hardening of medium manganese steels [Master's thesis, Tampere University]. To be submitted 2026.

Raami, L. (2026). *Quenching and partitioning of Martensitic Stainless Steels: Heat Treatment, Microstructure, Mechanical Properties, and Cavitation Erosion Resistance*, [Doctoral thesis, Tampere University].

Sabr, A. Effects of Trace Elements Copper and Tin in Dual-Phase Steels [Doctoral thesis, Tampere University]. To be submitted 2026.

Ahmed, S. Microstructural Evolution and Mechanical Response of Medium Manganese Steels Subjected to Intercritical Annealing Quenching and Partitioning [Doctoral thesis, Tampere University]. To be submitted 2026.

REFERENCES

Sabr, A., Ahmed, S., Kaijalainen, A., Penney, D., & Peura, P. (2026). Effects of Trace Elements Copper and Tin on Mild and Dual-Phase Steel Properties, unpublished work.

Ahmed, S., Pun, L., Isakov, M., Raami, L., Hokka, M., Kuokkala, V.-T., & Peura, P. (2026). Investigation of serrated flow in intercritically annealed medium manganese steel by in-situ synchrotron X-ray diffraction, submitted to *Steel research international*.

Sabr, A. Effects of Trace Elements Copper and Tin in Dual-Phase Steels [Doctoral thesis, Tampere University]. To be submitted 2026.

Ahmed, S. Microstructural Evolution and Mechanical Response of Medium Manganese Steels Subjected to Intercritical Annealing Quenching and Partitioning [Doctoral thesis, Tampere University]. To be submitted 2026.

Ahmed, S., Oja, O., Kaijalainen, A., & Peura, P. (2025). Effect of cooling practice on the mechanical properties of medium-manganese aluminum-alloyed steels after intercritical annealing quench and partition treatment. *Steel Research International*, 96(2), 2400420. https://doi.org/10.1002/srin.202400420

5.7 WP2 Business partner contributions

5.7.1 SSAB Europe Oy

Contributors: **SSAB Europe Oy**

Correspondance: **SSAB Europe Oy, Pasi Suikkanen**, (pasi.suikkanen@ssab.com)

Low CO2 steels made from scrap based production as a driver for sustainable growth (SSAB Zero concept and product development)

BACKGROUND

New sustainable low CO2 and fossil free steel products are to a large extent based on scrap based steelmaking. In this route metallic residual elements are always present. They influence processing and final properties. New ways are needed to design chemistry process settings and mechanical performance so that products stay reliable and usable for customers. This task focused on turning that challenge into practical product concepts and new SSAB Zero type steels.

METHOD

SSAB created the concepts and developed new SSAB Zero aligned products across several product groups. This included hot rolled strip and plate products coated and metallic coated products and tubular products. The work was done through a mix of research methods pilot trials and close university cooperation. The aim was to develop sustainable products in a way that supports real value chains and real customer use.

RESULTS AND FINDINGS

The results showed that with the new sustainable production approach it is possible to make high quality sustainable products in hot rolled galvanized and metallic coated categories. The results were validated both in pilot scale and in larger slab scale. Concrete outcomes during the work included SSAB Zero aligned product launches and industrialised deliveries. In hot rolled this included SSAB HR355 MC Zero. In metallic coated and galvanized this included SSAB S280GD Zero, SSAB CR240SLA Zero, SSAB CR300LA Zero, SSAB CR440Y780T-DP Zero. In tubular products this included SSAB Domex Tube Double Grade Zero and SSAB FormTube 220 Zero in tube production and deliveries.

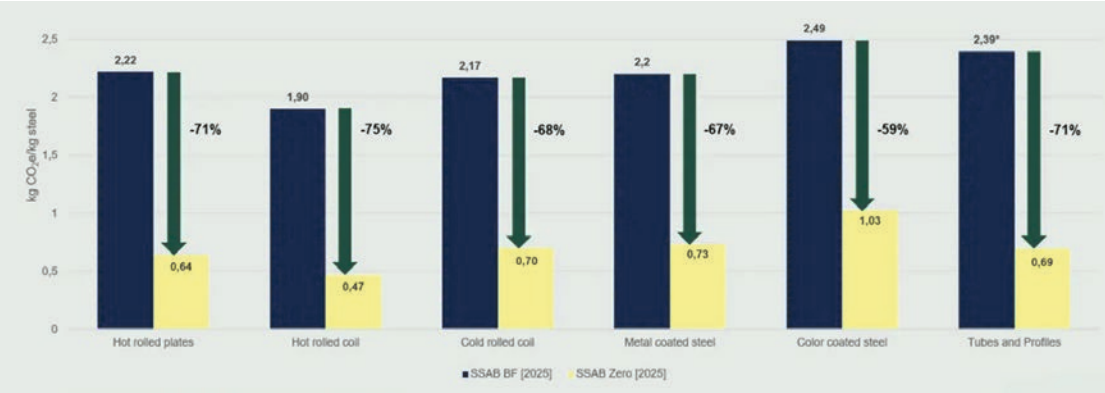

Figure 37. SSAB Zero products deliver significant reductions in CO_2 emissions over the steelmaking life cycle, while still maintaining top-level performance in technical properties.

IMPACT OF THE WORK

This was an important step in the transformation toward fossil free and low CO2 steel products. It strengthened SSAB's ability to develop and industrialise scrap based low CO2 steels across different product families and it created a strong base for further product and application development. Hence SSAB Zero products deliver significant reductions in CO_2 emissions over the steelmaking life cycle, while still maintaining top-level performance in technical properties, Figure 37.

NEXT STEPS

The work continues after the project. SSAB will focus on developing new products processes and applications together with customers through other dedicated projects using the concepts and results created here.

REFERENCES

https://www.ssab.com/en/fossil-free-steel/ssab-zero

5.7.2 Fortaco Finland Oy

Contributors: **Marko Viitala, Ossi Antila, Juha Haapala, Harri Silvola, Anastasia Titievskaja, Petri Hautala, Jussi Kangas, Timo Jyllilä, Jarkko Uusi-Pohjola, Jari-Matti Kallionpää, Valtteri Majalahti, Markus Jouppila, Aki Komulainen**

Fortaco Green Steel Applications for vehicle industry

BACKGROUND

Fortaco's strategy is based on reshaping off-highway industry. Being a leading cabin and steel structure supplier for global brands of off-highway industry, Fortaco's ambition is to be a part of the development of environmentally friendly new product concepts and service development. Many of Fortaco's major customers commit to UN's ambition for 1.5°C to mitigate climate change. Fortaco's goal is to define a list of actions and tangible deliverables leading to fulfillment of the target.

FOSSA2 project is an important complimentary block of Fortaco's sustainability program. Other elements of Fortaco sustainability program are:

- Definition of our sustainability strategy.
- Continuous improvements aiming at reduction of CO_2 footprint and other emissions in our operations by using green, weathering and high-strength steels.
- Development of a new concept of light-weight mobile machinery to reduce CO_2 emissions.
- Research project exploring data-based residual lifetime calculation to enable extension of use, support refurbishment and reuse of steel components.

FOSSA2 project is addressing one of the major gaps in the sustainability program, which is removing CO_2 emissions related to steel manufacturing processes. As such it is a revolutionary step for the whole industry and to be fully implemented into industrial practice it requires involvement of all players of the supply chain.

METHOD

The scope of FOSSA2 project is divided into three main areas:

- Manufacturability study and realization of vehicle cabin with fossil-free green steel
- Simulation study and testing of energy efficient boom solution
- Comparison of corrosion properties between traditional structural steel and corrosion-resistant steels

The goal was to find out green and high-strength steel material performances and behavior and compare the specifications to standard steel materials. An important part of the selection process was the optimization of welding with different materials and welding methods.

RESULTS AND FINDINGS

Fortaco Finland has built a cutting edge ecosystem for green and high strength steel solutions. Together with leading steel producers and research partners, the company has developed the capabilities needed to scale fossil free steel into serial production.

Fortaco now actively promotes structures made from green steel to increase awareness of new technology in the customer interface. The company has also prepared investment plans also for the technologies required to manufacture next generation, fossil free high strength steel cabins and structures.

Manufacturability study and realization of vehicle cabin with fossil free green steel

Key achievements of the reporting period include the successful showcase of the prototype cabin at the BAUMA trade fair. The concept cabin was completed in cooperation with three Fortaco cabin production facilities, and the design and manufacturing phases provided valuable insights into the behavior of green steel during production and testing, as well as its suitability for various customer applications.

Awareness of green steel's potential has been strengthened through active dialogue with customers and suppliers. Presenting the concept cabin at BAUMA is considered a crucial step in promoting green steel solutions. As material availability continues to improve, new customer projects can be launched more rapidly and on a larger scale.

Figure 38. Exhibition cabin built with SSAB Zero™ fossil-free steel material.

Simulation study and testing of energy efficient boom solution (Harri Silvola)

Research project was conducted in cooperation with LUT University and Hiab. Welding deformations can be highly detrimental from both structural performance and functionality, assembly, and manufacturing viewpoints. Conventionally, various tack welding, jig, and clamping technologies are applied to diminish welding deformations.

Computational modeling of welding, i.e., computational weld mechanics (CWM), can be applied to make predictions on thermal fields and temperature histories and subsequently deformations. This diminishes the need for experimentation and prototyping of welding production and can be used for deciding and optimizing the sequence of welds and welding parameters.

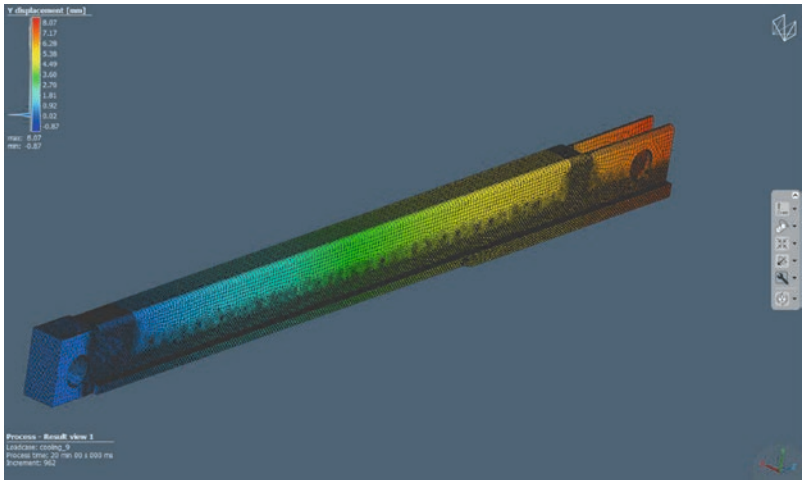

Figure 39. Boom structure simulation study.

Figure 40. Boom structure welding.

This master's thesis work experimentally and numerically studied welding deformations in a representative boom structure. The work was implemented as collaborative work between FOSSA2 partners: LUT University (CWM and related thesis work), HIAB Finland (case boom structure), and Fortaco Finland (materials, welding experimentation, and geometry measurements).

A fully coupled thermal–mechanical finite element model was created to simulate welding using Goldak's double-ellipsoidal heat source model in the Simufact Welding software environment. The test boom assembly, pre-WPS, and welding were implemented at the Fortaco Kurikka site. In

the experiments, different gas metal arc welding configurations were studied: backstep welding techniques and different welding sequences.

The simulation model was validated using experimentally obtained macrographs from the test booms. The conducted measurements showed rather small welding deformations – a maximum of 1.5 mm in the continuous boom structure and 3.2 mm in the connection brackets. These deformations could also be captured by the developed simulation models, indicating that CWM models can be used for assessing welding deformations in large-scale structures.

The tests and related results will be completed by June 2026.

Corrosion durability comparison of different steel materials (Anastasia Titievskaja)

In the cabins of mobile machinery, several factors influence the assessment of the service life of steel structures, such as harsh corrosion environments, material choices, surface treatments and coatings. At Fortaco Finland, stainless steels have been favored in cabins to satisfy the corrosion protection requirements. Economically, it would be a viable option to use weathering steels, which have improved corrosion resistance compared to structural steels and could potentially overcome the issues related to structural steels. On the other hand, the need to use more costly stainless steel could be avoided.

In this work, the corrosion resistance of weathering steels was compared to structural and stainless steels. As part of the project, the performance of SSAB Zero™ fossil-free steel was investigated under similar conditions. Representative welded details in cabin structures were created within a small-scale test specimen made of the four different materials. Different coating configurations were applied: uncoated/unpainted, e-coated, and e-coated, filled, and painted were included in the tests.

The specimens were exposed to a salt-spray chamber Vötsch SC450 for up to 1440 hours to classify different specimen configurations (material and treatments) into protection classes C1 to C5 (as per ISO 9277 standard).

The tests and related results will be completed by June 2026 and will be published in the thesis work available in the LUTPub repository.

Figure 41. Test samples for steel material corrosion durability investigations.

CO-OPERATION IN PUBLICATIONS

Silvola, H. (2026) *Computational modeling of welding deformations in a boom structure* [Master´s thesis, LUT University].

Titevskaja, A. (2026) *Corrosion resistance and mechanical strength of welded weathering steels* [Master´s thesis, LUT University].

5.7.3 John Deere Forestry Oy

Contributors: John Deere Forestry Oy, LUT University, Tampereen yliopisto (TAU)

Correspondence: John Deere Forestry Oy, **Pekka Vesanen** (VesanenPekka@JohnDeere.com)

Industrial utilization of fossil-free steel (FFS) and ultra-high-strength steels (UHSS)

BACKGROUND

The WP2 work package of the FOSSA2 project focused on enabling the industrial utilization of fossil-free steel (FFS) and ultra-high-strength steels (UHSS) in forestry machine structures. The background for the work lies in the growing need to reduce the carbon footprint of heavy machinery while maintaining or improving structural performance, fatigue life, and manufacturability. Previous research has indicated that advanced steel grades and optimized joining methods can significantly reduce weight and emissions, but reliable experimental validation is required before industrial adoption.

METHOD

The work package was implemented through a combination of literature studies, experimental research, and applied industrial testing. Advanced welding techniques were investigated for different joint types and UHSS/FFS materials. Several Master's thesis works were conducted focusing on material joining, weldability, and the carbon footprint implications of fossil-free steel. Mechanical testing included static strength, hardness, impact toughness, and fatigue testing, complemented by component-level and field-oriented evaluations.

RESULTS AND FINDINGS

The results demonstrated advanced welding methods are viable joining technologies for UHSS and fossil-free steel components used in forestry machines. Good penetration, adequate mechanical performance, and competitive fatigue behaviour were achieved for several critical joint types. The studies also provided evidence that the use of fossil-free steel can contribute to a reduced carbon footprint at component level without compromising structural integrity.

IMPACT OF THE WORK

The outcomes of WP2 support the transition towards lower emission forestry machines and strengthen the knowledge base for material and process selection in future product development. The results enable more material-efficient structures, support industrial implementation of advanced welding technologies, and contribute to long term sustainability goals within the forest machinery industry.

NEXT STEPS

The next development phase includes extending the results to additional components, long-term durability follow up, further optimization of manufacturing processes at industrial scale, and tighter integration of fossil-free steel solutions into lifecycle assessment and product development frameworks.

PUBLICATIONS AND THESES

Several Master's theses related to UHSS and fossil-free steel welding and joining.

Lainio I. (2024) *Hiilikädenjäljet kuormakoneen kouran jatkokehityksessä* [Master theses, Tampere University]. Accessible: https://urn.fi/URN:NBN:fi:tuni-202405286375

Harjula, S. (2024). Potential of laser welding technologies in forestry machine manufacturing (John Deere Forestry) [Master´s thesis, LUT University]. Accessible: https://urn.fi/URN:NBN:fi-fe20241220106089

Kittilä E. (2025) *Alumiinin ja teräksen liimaus kantavan rakenteen komponentissa*. [Master theses, Tampere University]

Jussila T. (2025) *Liimaliitoksen numeerinen mitoitus kuormaa kantavaan rakenteeseen metsäteollisuuden työkoneessa* [Master theses, Tampere University]

5.7.4 Hiab Finland Oy

Contributors: **Matti Randelin, Juho Alanko, Johannes Borman, Tuomo Saksa**, Hiab Finland Oy, Demountables & Defence Division

Correspondence: **Matti Randelin**, R&D Manager, Control Systems & Analytics, Hiab Finland Oy, Demontables & Defence Division

Design of fossil-free UHSS applications

BACKGROUND

The implementation of fossil-free steel in hooklift structures was already studied during the FOSSA1 project. The results showed that fossil-free steel is completely interchangeable with conventional steel. The scope quickly shifted from evaluating the properties of fossil-free steel to the hooklift concept itself—specifically, how to utilize higher-strength steel grades in the structure. A new concept for the hooklift structure was developed during the FOSSA1 project. It was noted that with relatively small structural changes, it is possible to simplify the design to reduce manufacturing time and phases, reduce weight, and optimize material usage. All the aforementioned factors directly affect the CO2-emissions of the complete product. The most significant change to the hooklift structure was the tipping body support structure in the middle frame. Now, the work in FOSSA2 has concentrated on other details of hooklift design to create a completely new concept for the steel structure. The main target was to reduce the hooklift weight by 400 kg, thereby reducing CO2-emissions by 20%. Throughout the work, it was planned to continuously evaluate whether small changes could be easily implemented into current products.

METHOD

The study of the new hooklift concept was divided into four tasks: upgrade and lighten, remove welding, simplify, and change manufacturing method. In all tasks, information from WP1 was utilized to determine the effect of actual hooklift usage on specific structural details. The usage data facilitated the design of the new concept by providing the confidence needed to implement new solutions. Examples of tasks included in work are presented in Figure 42.

Figure 42. Example tasks in WP2.

- The "Upgrade and Lighten" task consisted of studying possibilities to upgrade material strength grades while reducing thicknesses to save weight. All large plate materials for the main frames were included, with the target of upgrading S355 or S500 materials to S600, S700, or even higher. Although SSAB cannot yet deliver fossil-free circular section beams, main shafts were also included in the study.
- The "Remove Welding" task included studies on various components to change the design so that welding length is reduced. In the best-case scenario, entire welds would be eliminated. Several large weld areas that could be redesigned had already been identified, and new options were developed during this study.
- The "Simplify" task focused mainly on small details planned to be excluded from the final concept. The target was to identify how the number of items could be reduced and to find additional components to remove from the structure.
- The "Change Manufacturing Method" task included a study on the possibility of replacing smaller welded assemblies with cast or forged parts. In addition, the feasibility of utilizing Wire Arc Additive Manufacturing (WAAM) for component production was investigated.

Lappeenranta University of Technology (LUT) supported the studies with fatigue tests and a Master's thesis by Tuomo Saksa. A new optimized axle concept was developed in the thesis to simplify current axle designs and upgrade materials to higher strength grades. Another Master's thesis was conducted in cooperation with LUT and Fortaco regarding the determination of welding deformation through simulations. These studies were an important part of the work for evaluating changes in the welding process and their effect on manufacturability. Other tasks in this work package related to the implementation of promising new designs, either as improvements to product life-cycle care or as part of new product launches. This allowed Hiab to accelerate the impact of the FOSSA2 project.

RESULTS AND FINDINGS

Multiple design updates were performed for several products in Multilift's portfolio. The most significant achievements were the simplified subframe structure for Ultima and Optima hooklifts and the new body support structure for Optima. The new subframe structure is included in the new Ultima Zero and eUltima products, which were launched during the project. Both products also included smaller design updates based on the studies, the implementation of SSAB Zero steel (recycled fossil-free steel), and readiness for future fossil-free steel. The new body support

structure will be introduced in the next-generation Optima launch in April 2026.Many more development ideas are still pending implementation due to the high volume of work required. These improvements will likely be introduced in the future as part of new product projects. Overall, once all studied improvements are implemented, the calculated total weight reduction could reach 500 kg, and the CO2-emission reduction during the life cycle could exceed 25%. Multilift's eco-portfolio, created during FOSSA, is presented in Figure 43.

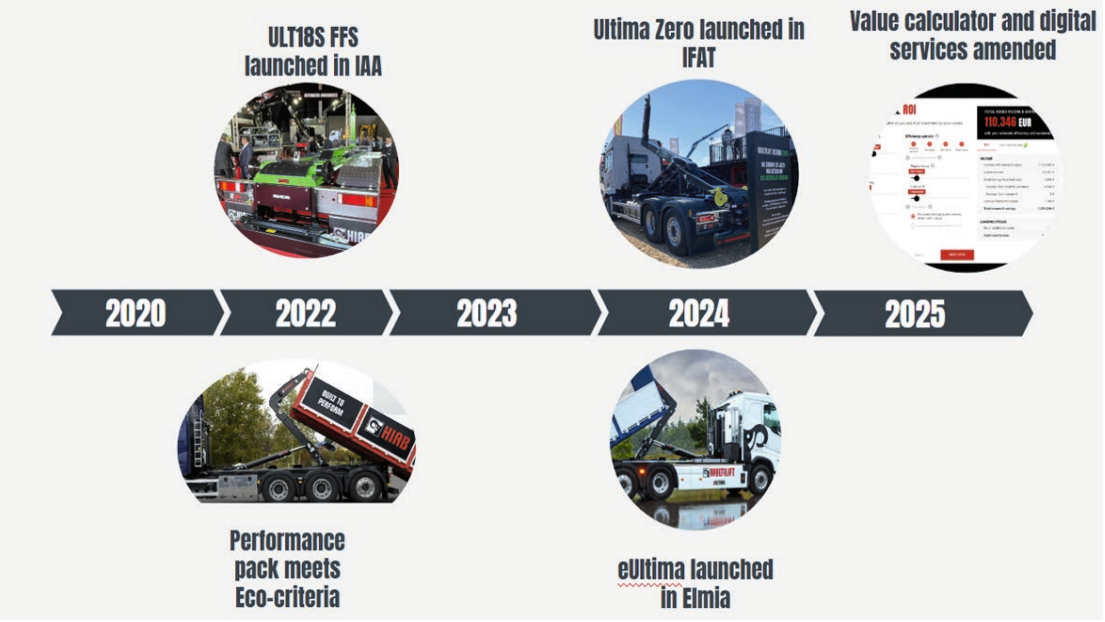

Figure 43. Multilift ecoportfolio.

IMPACT OF THE WORK

The biggest impact of the work has been the launch of the Ultima Zero and eUltima. The mechanical updates and industrialization were completed as part of this work package. Both products received a great reception in the market, and sales of these models have been increasing steadily. New design ideas have also been utilized in products other than eco-products, and the next-generation Optima will incorporate several of these improvements. With the help of improved design, Hiab has been able to achieve significant cost savings alongside environmental benefits.

NEXT STEPS

The next steps will involve continuing the implementation of identified improvements into products. Some improvements will require extensive design work to be utilized in a new hooklift structure. Alongside implementing new designs, new LCA and EPD work must be performed. The work completed will strongly guide Multilift's new products and future fossil-free applications.

THESES

Saksa, T. (2024). *Optimization of hooklift axle joints with high strength steel (HIAB Finland)* [Master´s thesis, LUT University]. Accessible: https://urn.fi/URN:NBN:fi-fe2024111492466

Silvola, H. (2026) *Computational modeling of welding deformations in a boom structure* [Master´s thesis, LUT University]. Publication pending.

5.7.5 Ponsse Plc

Contributor: Kalle Einola, Ponsse Plc, kalle.einola@ponsse.com

BACKGROUND

Based on the earlier project phase, FOSSA Co-Innovation Ponsse was all set to move into practical concepting and testing of SSAB's fossil-free steel materials.

METHOD

Ponsse studied the current availability of early SSAB's fossil free steel sample materials and moved into engineering phase and selected sub assembly of a PONSSE Buffalo forwarder as project scope. PONSSE Buffalo is a productive and popular mid class 8 Wheeled forwarder with load capacity of 14 tons – which often makes a perfect carrier for trying out new concepts at Ponsse.

A forwarder load space material concept was selected as the demonstrator. The load space was chosen as a suitable and well defined application suitable for studying manufacturability, fatigue, and weight effects. The load space was manufactured using SSAB fossil-free steel, explicitly to study cutting, bending, and welding behaviour and to observe how the material behaves through Ponsse's actual manufacturing process and the supply chain. Due to limited availability of rare sample materials, the design differs from standard design. i.e. steel tubes were not available and therefore the stakes of the load space were made of steel plate – however a very functional shape was achieved.

RESULTS AND FINDINGS

SSAB's fossil-free steel has performed flawlessly in both manufacturing phase at Ponsse's supply chain as well as in Ponsse's own production – and also in final product on a PONSSE Buffalo forwarder in actual field tests.

Basically the only feature of fossil-free steel seemingly needs special attention is a slightly larger bending radius needed in practise due to properties of fossil-free steel.

IMPACT OF THE WORK

This concepting project greatly improved Ponsse's readiness to step into new fossil-free steel materials also in production phase – as these will be available in commercial scale in near future.

NEXT STEPS

Following the availability fossil-free steels and looking for highest added value applications.

PUBLICATIONS

https://www.ponsse.com/fi/news2/-/asset_publisher/ZE4CjSrtQpXR/content/ponsse-to-become-first-forest-machine-manufacturer-to-use-ssab-fossil-free-steel

https://news.ponsse.com/en/aiming-for-a-fossil-free-future/

5.8 WP2 Key takeaways

Welding performance and welded-joint behaviour

- **Welding studies provided new knowledge on low-temperature performance in offshore and AHSS steels and on tailoring TMCP steel properties through cooling control.**

  University of Oulu and partners showed that the studied offshore welds met the required CTOD levels for arctic applications, that beam-welded martensitic-austenitic AHSS showed very high fracture toughness at low temperatures, and that multiple steel grades can be produced from a single chemical composition by adjusting the cooling process. The work also provided valuable information on weld metal behaviour and on the influence of tramp elements from scrap-based steelmaking on microstructures and mechanical properties of base metal and heat-affected zone. **These results support the development and use of weldable steels and welded joints in arctic applications, while also showing how cooling control and understanding of scrap-related residuals can be used to tailor steel properties for different grades and support future steel development.**

- **Studies on high-strength and ultra-high-strength steel joints clarified the factors governing fracture behaviour and improved fatigue assessment in welded components.**

  The work showed that dissimilar HSS/UHSS joints can fail from different critical locations depending on base-metal properties, HAZ softening and weld-bead geometry, and that multi-pass welding can alleviate residual stresses near the fusion line. It also showed that weld extension techniques further enhance fatigue strength, that the 4R method improves fatigue assessment under variable-amplitude loading, and that the ktb correction improves fatigue assessment in bending-loaded joints. **These findings support safer and more reliable design of lightweight welded high-strength steel structures by improving failure prediction and fatigue assessment, and help use steel more efficiently in lightweight, lower-emission applications.**

- **An industrially applicable platform for adaptive robotic welding was developed for high-strength steel applications.**

  LUT University developed a layered system architecture integrating multisensor real-time process monitoring, digital shadow/twin functionality and an AR-based user interface. The platform enables unified multisensory data acquisition, synchronized logging and streaming, and real-time process monitoring and control within a single architecture. It also provides a structured foundation for future deep-learning-based weld-quality assessment and prediction tools. **These results support more systematic monitoring, traceability and control in robotic welding, while also creating a practical basis for further development and industrial adoption of data-driven welding solutions.**

Formability and processing of AHSS and UHSS sheet steels

- **Processing and microstructure studies showed how formability and performance can be improved in high-strength steels.**

  University of Oulu and partners showed that, in hot-rolled AHSS, the uniformity of the grain structure has the strongest connection to high HER values. In the studied medium-manganese steel variant, the best combination of strength and ductility was achieved only within a narrow

intercritical annealing temperature range. The work also showed that, within the studied processing window, rapid induction processing can create a hardened surface layer while retaining a softer core. **These results help in developing high-strength steels that are easier to form in manufacturing, while also showing that rapid induction processing can offer an industrially feasible, energy-efficient way to improve bendability without reducing the overall strength of the steel.**

- **Rapid annealing studies improved understanding of how residual elements affect future high-strength sheet steels in scrap-based production.**

  Tampere University and partners showed that copper tends to accumulate in martensitic regions, while copper and tin had only limited overall effects on phase transformation temperatures and mechanical properties in most cases. However, the 0.6 wt-% copper condition showed higher yield and tensile strength than the other similarly processed steels. The work also identified the mechanism behind the serrated deformation behaviour observed in intercritically annealed medium-manganese steels. **These results improve understanding of how heating rate and residual elements affect the properties of cold-rolled high-strength steels, helping to reduce the harmful effects of residuals in future steel development.**

Hydrogen-related behaviour in high-strength steels

- **Hydrogen embrittlement studies provided new insight into how retained austenite and carbide structures influence hydrogen tolerance in martensitic-austenitic AHSS steels.**

  University of Oulu and partners showed that cementite and η-carbides affect hydrogen trapping, that highly compressed film-like retained austenite can act as a diffusion barrier rather than a strong trap, and that suitable retained-austenite morphology and alloying improve hydrogen embrittlement resistance in DQP steels. **These results support the development of next-generation ultrahigh-strength steels with improved tolerance to residual hydrogen.**

- **Welding studies on pipeline steels showed that hydrogen tolerance can differ markedly between the base metal and the heat-affected zone.**

  LUT University showed that, in HFI-welded API 5L X70 pipe steel supplied by SSAB, the HAZ exhibited greater resistance to hydrogen-assisted cracking than the base metal. Rapid cooling during welding produced a refined ferrite–bainite lath structure in the HAZ, accompanied by inter-lath cementite films, high dislocation density and carbon vacancies in cementite. These microstructural features modified hydrogen trapping behaviour and reduced the fraction of diffusible hydrogen. **These findings provide a clear strategy for optimizing welding parameters in pipeline steels, supporting the safe and cost-effective repurposing of existing pipelines for hydrogen transport.**

From steel solutions to industrial implementation

- **SSAB industrialised new SSAB Zero products across several product families.**

  SSAB showed that scrap-based low-CO2 steel production can deliver high-quality products in hot rolled galvanized and metallic coated categories. The work was validated in both pilot scale and larger slab scale, and it resulted in SSAB Zero aligned product launches and

industrialised deliveries across multiple product groups. **This work marked an important step toward fossil-free and low-CO2 steel products by demonstrating that scrap-based production can deliver major reductions in steelmaking-life-cycle CO_2 emissions while maintaining the technical performance required for industrial product applications.**

- **Fortaco advanced the practical industrial use of fossil-free and high-strength steels in vehicle and equipment applications.**

  Fortaco developed and presented a fossil-free steel prototype cabin, prepared investment plans for next-generation fossil-free high-strength steel cabin and structure manufacturing technologies, and built capabilities for scaling green steel solutions towards serial production. The work also showed that welding deformations in the studied boom structure remained limited and could be predicted with the developed simulation models. **These results advance future industrial implementation by strengthening Fortaco's manufacturing readiness, supporting investment planning, and enabling the use of simulation models in the development of fossil-free and high-strength steel applications.**

- **John Deere Forestry demonstrated the industrial potential of fossil-free and ultra-high-strength steels in forestry machine structures.**

  The work showed that advanced welding methods can be applied to critical joint types in UHSS and fossil-free steel components while achieving good penetration, sufficient mechanical performance and competitive fatigue behaviour. It also provided evidence that the use of fossil-free steel can reduce component-level carbon footprint without compromising structural integrity. **These results advance lower-emission forestry machines by enabling more material-efficient structures, guiding material and process selection in future product development, and supporting the industrial use of advanced welding technologies.**

- **Hiab used fossil-free ultra-high-strength steel to develop lighter and simpler hooklift structures with lower life-cycle emissions.**

  Hiab developed a simplified subframe structure for Ultima and Optima hooklifts together with a new body support structure for Optima. The new subframe was implemented in the launched Ultima Zero and eUltima products, which also incorporated SSAB Zero steel and preparedness for future fossil-free steel use. Full implementation of all the studied improvements could reduce weight by up to 500 kg and life-cycle CO2 emissions by more than 25%. **These results advanced Hiab's eco-product development by showing that lighter hooklift structures can deliver both environmental and business benefits through lower life-cycle emissions, reduced weight and significant cost savings.**

- **Ponsse demonstrated that fossil-free steel can be used in a forest machine structure and processed through an actual manufacturing chain.**

  Ponsse selected the load space of a PONSSE Buffalo forwarder as a demonstrator for practical concepting and testing with SSAB's fossil-free steel. The work examined manufacturability, fatigue and weight effects, and the load space was produced to study cutting, bending and welding behaviour in Ponsse's supply chain and own production. The results were encouraging: the fossil-free steel performed well in manufacturing and in field tests, and its properties were found to correspond closely to those of conventional steel. **This concepting work improved Ponsse's readiness to introduce fossil-free steel materials into production when they become available at commercial scale.**

Photo: Ponsse Plc

6. WORK PACKAGE 3
Virtual steel production platform

Work Package 3 examines the use of modelling, simulation and virtual tools in steel processing, structural assessment and industrial applications. This work packages studies how virtual methods can support faster, more controlled development of steels and steel products. The reported work covers hot-strip process modelling, bendability, fatigue assessment, arc-welding simulation, and industrial virtual platforms for steel production and equipment applications.

Hot-strip process modelling and strip behaviour	***How can virtual modelling improve understanding and prediction of hot-strip processing conditions and strip behaviour?***

WP3 addresses two process-related issues in hot-strip rolling: the role of induction heating in temperature control, and the difficulty of controlling profile and flatness when strip geometry is measured only at the end of the finishing mill. These issues are examined through induction-heating modelling and data-driven modelling of strip profile and flatness using process data from the SSAB Raahe finishing mill. Together, these studies examine how modelling can be used to describe hot-strip processing conditions and strip geometry.

Bendability of ultra-high-strength steels	***How can air-bending behaviour of ultra-high-strength steels be better understood and predicted?***

Air-bending of ultra-high-strength steels (UHSS) presents challenges because these steels generally have lower formability than lower-strength grades. Their relatively low fracture strains and limited capacity to accommodate localized deformation can restrict their use in manufacturing processes that involve air-bending or other cold-forming operations. WP3 addresses this through studies on UHSS bendability aimed at improving understanding of air-bending mechanics and at developing improved methods for measuring, describing and predicting bending behaviour based on material properties.

Fatigue assessment of welded joints and arc-welding simulation	***How can simulation improve fatigue assessment of welded joints in demanding structural applications and advance prediction of weld geometry?***

In demanding structural applications, reliable use of welded high-strength steels depends on understanding fatigue behaviour under cyclic service loads and the physical phenomena that govern weld formation. Welded joints require more accurate fatigue assessment under different joint and load conditions, while arc welding still requires advanced simulation tools to describe complex process physics and final weld geometry. These topics are examined through simulation-based fatigue assessment of welded high-strength components and development of arc-welding simulation tools.

Industrial virtual platforms and digital services	***How can virtual tools support product development, production and future digital services?***

Company cases address these questions in practical industrial contexts. SSAB reports on virtual rolling and the development of a scalable virtual steel production platform. Indalgo developed a virtual steelmaking system based on industrial data and digital simulations. John Deere Forestry studies how machine data can be used for machine-life estimation and future digital twin development. Hiab develops simulation platforms to support hooklift product design, condition monitoring, life-expectancy estimation and future digital services. Ponsse participated by providing input to the work and contributing practical industrial perspectives.

6.1 Virtual steel processing

6.1.1 Modelling of phenomena of induction heating

Contributors: **Katariina Lehtola, Joonas Ilmola, Jari Larkiola,** University of Oulu

Correspondence: **Katariina Lehtola** (katariina.lehtola@oulu.fi)

BACKGROUND

In this sub-project, induction heating was examined as part of temperature control in hot-strip rolling. The aim of the Master's thesis was to understand the mechanisms of electromagnetic heating and to develop a Finite Element Model capable of representing induction heating during dilatometry. The theoretical framework relied on Maxwell's equations and the Lorentz force to describe the electromagnetic phenomena, complemented by Fourier's equation to solve heat-conduction-related parameters.

METHOD

The work involved developing an FEM model in Abaqus CAE that replicated the induction heating conditions of a dilatometer. The modelling proceeded alongside experimental dilatometry tests, which were performed to generate reference data for validation. Used results from dilatometer are shown in Figure 44. A comprehensive literature review was completed to support the theoretical basis. The FEM model was constructed to mimic the geometry and operating behaviour of the dilatometer's induction coil, enabling direct comparison between simulated and measured temperature responses.

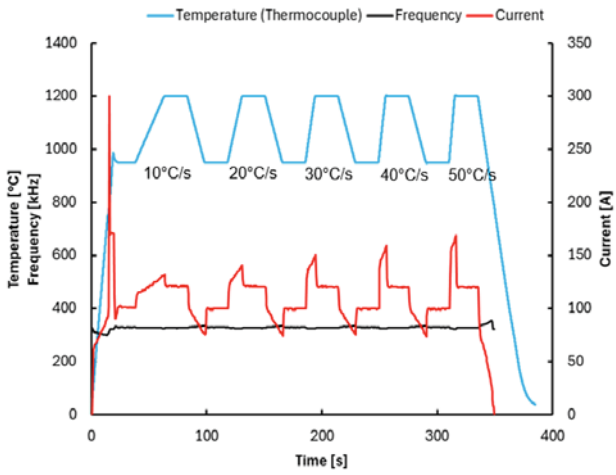

Figure 44. Results from dilatometer.

RESULTS AND FINDINGS

The FEM model was successfully developed and validated against the dilatometry experiments. The model predicted electromagnetic heating behaviour with good accuracy and showed strong alignment with the temperature curves measured during testing. In Figure 45. is shown time-transient heat transfer analysis results of temperature in the sample rod at the time when the model has reached the 1200 °C target temperature in the middle of the sample, where the temperature was measured in the dilatometer experiments.

The comparison between simulated and experimental data demonstrated reliable model performance and confirmed that the key physical phenomena had been captured in the modeling. The compared results are shown in Figure 46.

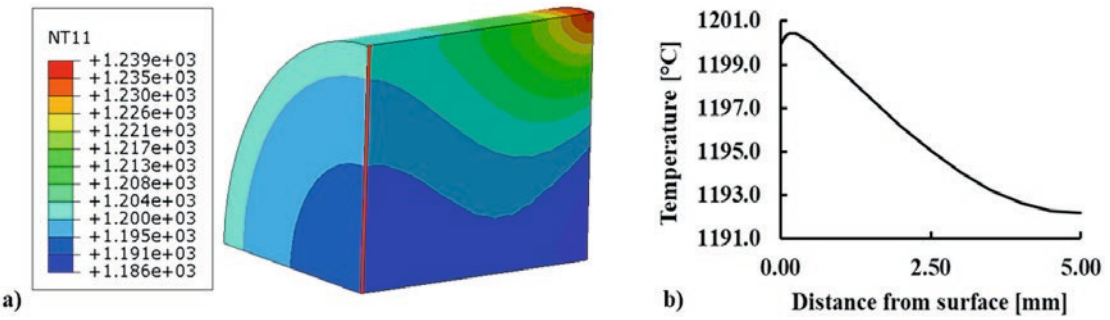

Figure 45. a) Results of temperature from the heat transfer analysis. b) Temperature distribution in the sample rod.

IMPACT OF THE WORK

The completed model provides a solid foundation for continued development of induction heating simulations within hot-strip rolling processes. Its ability to accurately reproduce dilatometer heating behaviour indicates strong potential for applying the model to more complex industrial scenarios. The results enhance the understanding of electromagnetic heating mechanisms and support future process optimization, contributing to improved control of temperature-dependent material behaviour in hot-rolling applications.

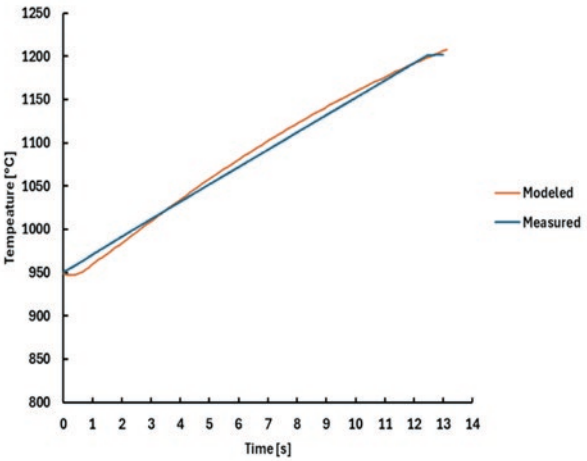

Figure 46. Compared results from dilatometer and model.

NEXT STEPS

Future development of the model should focus on improving the accuracy of the assumptions made in this work. The induction coil was simplified and should be modelled more realistically, including its hollow structure and internal cooling. The current data used for validation was limited by the dilatometer's display, which did not allow direct data export; therefore, more reliable current measurements with shorter intervals than 0.5 s are needed. In addition, heat radiation—particularly between the coil and the conductor—should be modeled more comprehensively to reduce potential sources of inaccuracy.

PUBLICATIONS AND THESES

Lehtola, K., Ilmola, J., & Larkiola, J. (2025). Finite element modeling of electromagnetic heating. *Materials Science Forum*, 1174, 39–46. https://doi.org/10.4028/p-cR2Wo5

Lehtola, K. (2024). *Finite element modeling of electromagnetic heating* [Master's thesis, University of Oulu].

6.1.2 Modelling of surface phenomena

Contributors: **William Meneses, Jari Larkiola**, University of Oulu
Ilmari Juutilainen, Indalgo Oy
Juha Jokisaari, SSAB Raahe Oyj

Correspondence: William Meneses (william.meneses@oulu.fi)

BACKGROUND

The increasing demands to produce steels with higher strengths and thinner gauges and the implementation of mini-mills, require new methods to assure strip geometry. Currently, it is difficult to guarantee good strip geometry because online process controls are hindered by the fact that profile and flatness is measured only at the end of the finishing mill. Therefore, modelling and prediction of strip geometry during hot rolling process is a topic of high importance and relevance both in industry and academia. Predicting strip geometry is a multiple-input/multiple-output problem that involves the understanding of intricate interactions between different process parameters, varying state conditions, and thickness profile and flatness. This complex problem will be addressed using statistical-based (or data-driven) modelling, that will exploit existing process data to extract information on how the different inputs and process conditions contribute to the profile and flatness of the strip.

This report summarises the activities conducted to build a big dataset that includes different process parameter values and strip thickness measurements for more than 1000 coils. This represents the first step to develop statistical-based models using machine learning (ML) algorithms to predict strip profile and flatness during hot rolling.

METHOD

SSAB has shared process data collected from the finishing mill at Raahe, which include many different process inputs (such as strip temperature, rolling forces, thicknesses, strip tension, rolling speed, bending forces, roll shifting, work roll diameters, etc.) and output measurements of strip thickness and flatness. Data processing has been conducted using Python packages.

Data include process parameters for all the six stands in the finishing mill, whereas thickness and flatness are measured at the exit of sixth stand. Additionally, some of these process parameters were used to compute other values based on metallurgical phenomena theories. Following are the equations used to compute them (Mielnik, 1991):

$$R'(\textit{Roll flattening/Hitchcock radius}) = R\left(1 + \frac{16P(1-\nu^2)}{\pi E w (h_0 - h_f)}\right)$$

$$\dot{\bar{\varepsilon}}_{st}\ (\textit{mean strain rate}) = v\left[\frac{1}{R'(h_0 - h_f)}\right]^{1/2} ln\frac{h_0}{h_f}$$

$$\textit{Shape Factor} = \frac{2\sqrt{R(h_0 - h_f)}}{h_f + h_0}$$

$$\bar{\sigma}\ (\textit{mean yield stress in plane strain}) = \frac{P}{w\sqrt{R'(h_0 - h_f)}}\left(\frac{4h}{3{,}2h + \sqrt{R'(h_0 - h_f)}}\right) + \bar{t}$$

Where:

- P: Roll force measured at each stand
- ν: Poisson's ratio of the work rolls
- E: modulus of elasticity of the roll material
- w: width of the strip
- h_0: strip entry thickness
- h_f: strip exit thickness
- v: work roll speed
- h: average strip thickness, $(h_0 + h_f)$ / 2
- $\bar{t}$: mean strip tension (front and back tensions)

RESULTS AND FINDINGS

One single strip thickness profile consists of 200–400 measurement points, depending on the width of the strip. To be able to predict thickness profile, these data must be transformed into a simpler format. Strip thickness data have been reconstructed using Chebyshev orthogonal polynomials, which allow to represent the strip profile using only 5 coefficients (T0–T4). For all the coils in the dataset, Chebyshev polynomials can approximate the original thickness profiles with an average goodness of fit higher than 95% (R2 value). Additionally, Chebyshev coefficients provide a direct quantification of the profile asymmetry (T1 and T3), the parabolic shape (T2) and the nonquadratic look (T4) (Judin, 2011). Figure 47 shows two examples of thickness profiles randomly selected from the dataset. It can be appreciated that the approximated curve (orange dotted line) fits very well the original profile (blue line).

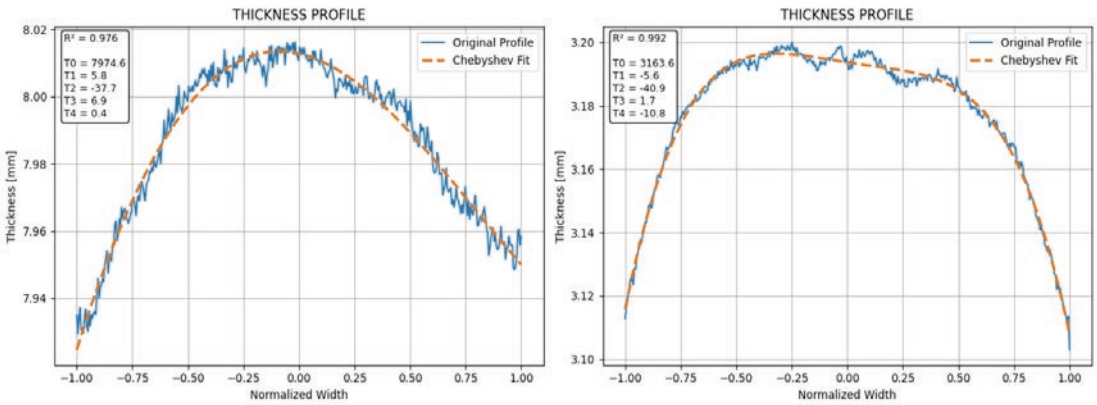

Figure 47. Strip thickness profiles: Original and Chebyshev approximation. Corresponding R2 values and Chebyshev coefficients (T0-T4) are indicated in the plots.

The variables that will be used to predict strip thickness profile are different process parameters collected from different points at a given/fixed frequency and often stored in separate databases. These time series data have been consolidated, filtered to remove outliers, and then analysed to engineer features that capture the process behaviour and can be used as predictors in statistical-based models. These predictors consist of averages, standard deviation, rate of change between consecutive observations, and overall trend (upward or downward) of the process parameters. Some features have been normalized to increase the models' ability to generalize across different rolling campaigns. Furthermore, variables that were highly correlated with others have been removed to improve models parsimony and interpretability.

IMPACT OF THE WORK

Using data from more than 1000 coils, a dataset with strip thickness profiles as response variable and 80 different process parameters as independent variables (predictors) has been created. Process data from SSAB Raahe finishing mill has been systematically processed, analysed and summarised using different Python scripts. If needed, the dataset can be readily fed with data from more coils in an expeditious fashion.

NEXT STEPS

Now that the dataset has been generated, the next step is to fit models aiming at predicting strip thickness profile. The team has decided to utilize gradient boosted regression trees

models, which are highly capable to capture complex relationships between the input and output variables and have good interpretability. After this, flatness measurements will be included to the dataset, to also fit models to predict strip flatness.

REFERENCES

Mielnik EM. Metalworking science and engineering. New York St. Louis Paris [etc.]: McGraw Hill; 1991. [McGraw-Hill series in materials science and engineering].

Judin M, Nylander J, Larkiola J, Verho M. Quality Parameters Defined by Chebyshev Polynomials in Cold Rolling Process Chain. In Belfast, (United Kingdom); 2011

6.2 Local formability and bendability of ultrahigh-strength steels

Contributors: **Aki-Petteri Pokka, Antti Kaijalainen, Matias Jaskari, Tommi Hintsala**, University of Oulu
Vili Kesti & Lars Troive, SSAB Europe Oyj
Juha Huuki, Aalto University

Correspondence: Aki-Petteri Pokka (aki-petteri.pokka@oulu.fi)

BACKGROUND

Air-bending of ultra-high-strength steels (UHSS) presents challenges because these steels generally have lower formability than lower-strength grades. Their relatively low fracture strains and limited capacity to accommodate localized deformation can restrict their use in manufacturing processes that involve air-bending or other cold-forming operations. Improving the applicability of UHSS therefore requires a more detailed understanding of how these materials behave in these forming processes. The objective of this research task is to improve understanding of UHSS bendability and the mechanics of air-bending. The long-term goal is to develop improved methods for measuring and describing bendability, as well as approaches for predicting bending behavior based on material properties.

METHOD

A broad selection of nine steel grades from 355MPa to 1700 MPa at 6 mm sheet thickness was investigated to cover a wide range of mechanical properties and to enable the study of how different material parameters influence bending behavior. The research has focused primarily on macroscopic mechanical behavior, which made it practical and beneficial to include a large number of materials. The formability of these steels was examined through tensile tests and three air bending setups, with strain measurements obtained using digital image correlation (DIC). In addition, plane strain tensile tests were developed and performed for six materials using a new specimen geometry that produces a stress state closer to that occurring in bending than conventional uniaxial tension. Strains were measured during the tests with DIC, and fracture strains were subsequently determined from the specimen cross sections using a digital microscope.

RESULTS AND FINDINGS

A significant part of the work involved revisiting and refining earlier datasets from the FOSSA I project. Bend test DIC data was reanalyzed to determine fracture strains using a new method based on monitoring the evolution of the maximum surface strain and identifying fracture through abnormal growth in this quantity. Tensile test data were similarly re-examined to extract fracture strain values. Comparisons between bending and tensile test results, as shown in Figure 48, showed that the plane-strain tensile fracture strains correlated better with bending derived fracture strains ($R^2 \approx 0.56–0.73$) than conventional uniaxial tensile test fracture strains ($R^2 \approx 0.30–0.53$). These findings highlight the differences in stress state between the test types, and indicate that the plane-strain bending fracture limit should be regarded as an inherent material property (Pokka et al., 2025).

The effect of surface characteristics on bendability was also investigated in a study presented in the Metal Forming 2024 conference, through comparison of dry electropolished and ultrasonic burnished specimens to as-rolled condition of commercial hot-rolled bainitic-martensitic steel

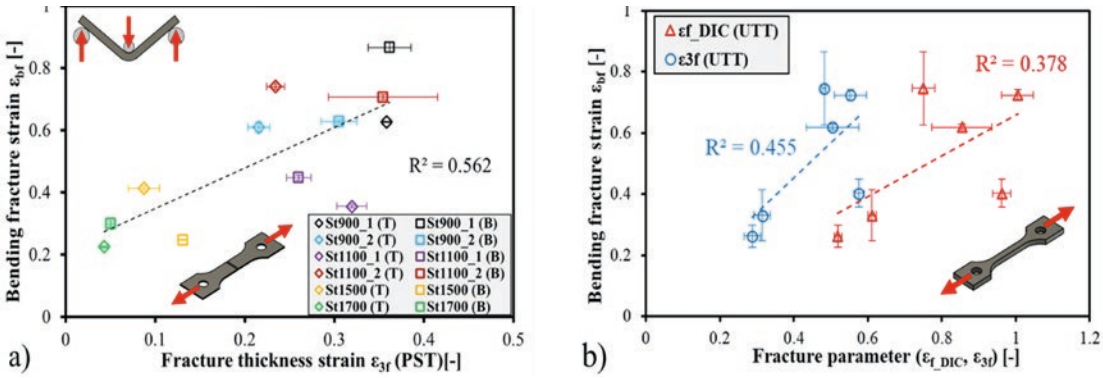

Figure 48. Correlation between the bending fracture strain εbf and a) plane-strain tensile fracture thickness strain ε3f, and b) uniaxial tensile fracture thickness strain ε3f and surface fracture strain εf_DIC. [Combined from original works of (Pokka et al., 2025), licensed under CC BY 4.0]

with thickness of 4 mm. The conclusion was that the strain distribution in air-bending is unaffected by surface treatments, as the strain distribution is mostly determined by the properties of the whole cross-section. The surface treatments decreased the fracture strain, however, indicating that fracture strain in bending is more affected by the properties near the surface. However, surface roughness was not found to affect bending properties at the investigated scale (Ra = 0.56 – 1.62 µm; Rv = 3.63 – 19.90 µm), and the main mechanisms behind the detrimental effects of surface treatment were hypothesized to be increases in hardness, dislocation densities, and residual stresses (Kaijalainen et al., 2024).

Additional research examined the evolution of the cross-section moment during air-bending, and its connection to other phenomena, such as evolution of strain distribution and multi-breakage, as well as material properties. The main observation from the study was that the evolution of the cross-section moment, calculated from punch force–displacement data, is linked to the materials' strain-hardening properties, implying it can be used to predict the evolution of the outer surface strain distribution, bend shape, inner radius, thinning, bend allowance, multi-breakage, and fracture risk. (Pokka et al., 2024)

IMPACT OF THE WORK

This project has substantially improved the understanding of how ultra high strength steels behave in air bending. A large and carefully curated experimental dataset has been generated, covering multiple steel grades, bending configurations and tensile test types. This dataset provides a detailed picture of how material properties, tool geometry and deformation behavior interact in bending operations, and it forms a strong foundation for future modelling and method development.

A key contribution of the work is the development of a new DIC based method for determining fracture strains in bending tests. Since no suitable standardized method existed, a new procedure was created, as illustrated in Figure 49, based on evolution of the maximum surface strain and thresholds calibrated by systematic visual inspection of DIC images. This method now offers a practical, objective, and repeatable way of identifying fracture onset in bending.

NEXT STEPS

Towards the end of the project, effort has shifted toward probabilistic and statistical modeling for predicting material behavior in air-bending. Preliminary model versions have already been created, demonstrating the feasibility of predicting evolutions of peak strain, bend shape and

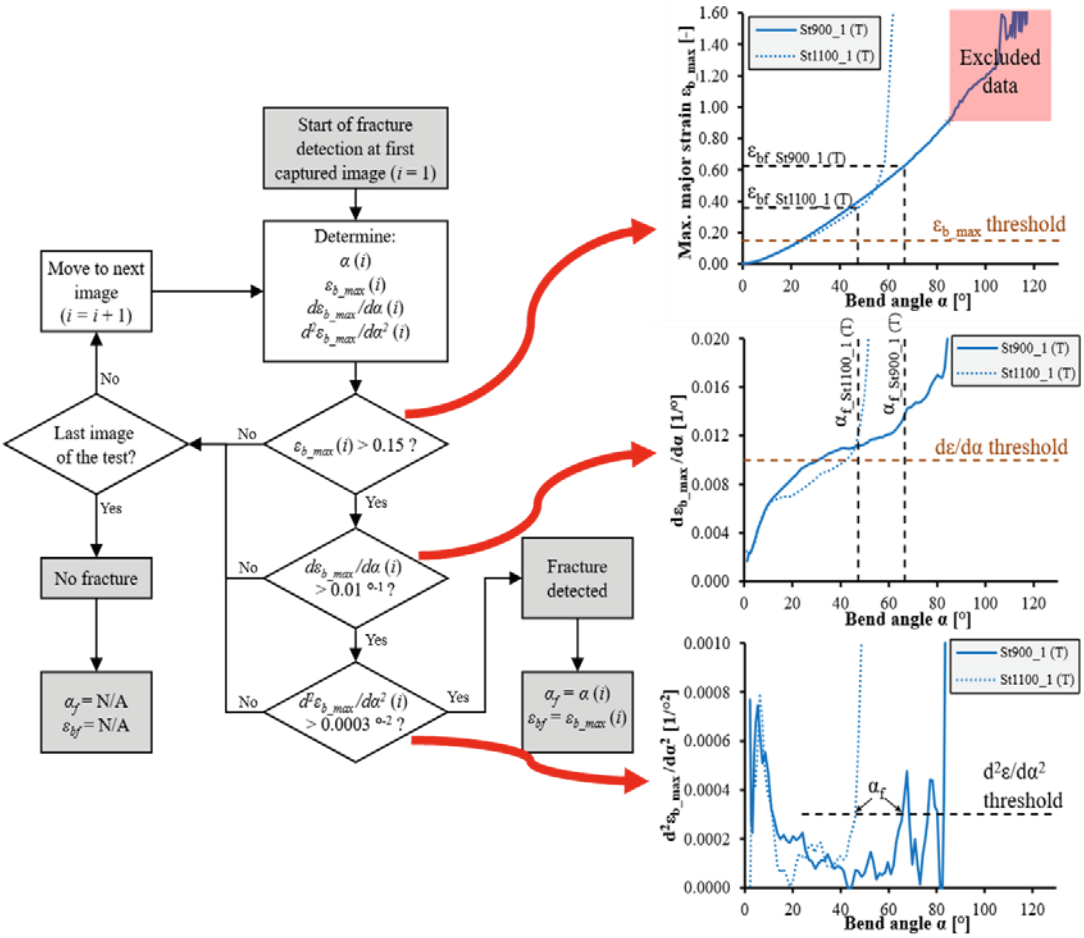

Figure 49. Air-bending fracture identification procedure based on DIC strain measurement. Threshold values "calibrated" by visual inspection, to ensure the fracture detection generally matches the point in time where damage initiation was visually observed. [Combined from original works of (Pokka et al., 2025), licensed under CC BY 4.0]

fracture probability as functions of bend angle and material/tool parameters. The next phase will involve refining these models, validating them with the existing experimental data and exploring their applicability across different steel grades and bending configurations.

Future work will also include extending the probabilistic approach by incorporating uncertainty in material properties and process parameters, with the aim of supporting reliability based design optimization (RBDO) for bending operations. RBDO would allow selection of optimal tool and process settings while maintaining acceptable failure probabilities, offering a more systematic and less conservative approach than traditional safety margin practices.

Another important next step is contributing to the development of bendability characterization and testing standards. Characterizing bendability through a local/global formability framework, using a combination of several parameters instead of relying on a single parameter (such as minimum bend radius Rmin), could offer significantly more information about material behavior, and enable improvements in workshop instructions and product design. The newly developed DIC based fracture strain procedure also provides a foundation for standardization improvements for bendability testing.

PUBLICATIONS

Kaijalainen, A., Pokka, A. P., Jaskari, M., Huuki, J., Hintsala, T., & Kömi, J. (2024). Effect of surface characteristics on strain distribution in air-bending. *Materials Research Proceedings*, 44, 350–357. https://doi.org/10.21741/9781644903254-37

Pokka, A.-P., Kesti, V., Troive, L., & Kaijalainen, A. (2024). Development of the cross-section moment in air-bending. *Materials Research Proceedings*, 41, 1027–1037. https://doi.org/10.21741/9781644903131-113

Pokka, A. P., Kesti, V., & Kaijalainen, A. (2025). Local formability and bendability of UHSS: Correlations between bending and tensile fracture strains. *International Journal of Solids and Structures*, 320(June), 113524. https://doi.org/10.1016/j.ijsolstr.2025.113524

Photo: Hiab Finland Oy

6.3 Simulation-based fatigue assessment of welded high-strength components

Contributors: **Tero Pesonen, Antti Ahola**, Steel Structures, Mechanical Engineering, LUT University

Correspondence: **Antti Ahola** (antti.ahola@lut.fi), +358 50 475 2825

BACKGROUND

Fossil-free lightweight steel designs support low-emission targets by optimizing material use and reducing emissions during the manufacturing phase and throughout the whole product life cycle. Lighter high-strength steel structures also experience higher cyclic stresses, which high-strength steels typically can withstand with higher quasi-static load capacity. However, in-service loads are rarely quasi-static and often fluctuate due to repetitive and cyclic nature of loading or due to vibrations, exposing structures and their joints to fatigue failures. The fatigue performance of welded high-strength steel joints does not improve with the same extent to the increase in the ultimate load capacity. Consequently, cyclically loaded demanding structural applications require more accurate fatigue estimation models to reduce design conservatism and uncertainties, allowing for greater material efficiency and use of lighter structures. Fatigue damage is a highly localized process. In the case of a welded joint, welding-induced factors – such as stress concentrations, material microstructural changes and residual stresses – all significantly influence fatigue resistance, along with acting cyclic loading history. Improving the estimation accuracy of these factors through combined fabrication and loading simulations can enhance fatigue predictions, thereby reducing material use and consequently steel-structure emissions.

METHOD

This task further developed sequential coupled finite-element simulation modeling approach to account for the combined effects of manufacturing (welding and post-weld treatments) and applied load conditions in fatigue assessments. The modeling approach integrates welding simulation, post-weld treatment (optional), and mechanical loading simulation to include fabrication load history into the local material response applied in the fatigue predictions by the 4R methodology (Figure 50).

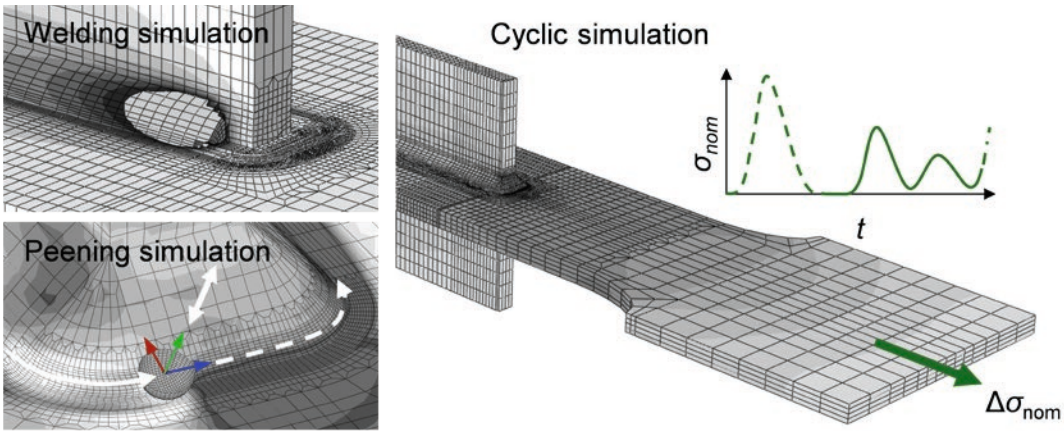

Figure 50. Simulations of the method to assess the material's local response to the combination effect of fabrication and external load.

For the task, the framework (Pesonen et al., 2024) developed in FOSSA Phase 1 was extended to include post-processed welded joints and various complex load conditions, including methodological improvements in the previously-defined framework. Simulation models for combined welding, post-processing (overload and high-frequency impact treatment), and various cyclic load conditions were developed and studied. The numerical results were validated through laboratory experiments by fabricating small-scale specimens based on the simulation model, from which fatigue-related factors were measured at different manufacturing stages. The experimental fabrication data were compared with numerical results for welding- and post-treatment-induced residual stresses and deformations, as well as joint hardness changes. Simulation-based fatigue results were validated through the fatigue tests.

RESULTS AND FINDINGS

Comparing numerical results with experimental findings indicates that various post-fabrication conditions (as-welded, overload, and high-frequency impact treatment) can be simulated with reasonable accuracy for cyclic simulation and further fatigue analysis. Including the effective fatigue stress hypothesis in manufacturing simulations enabled comparison of fatigue-effective results across sequential simulations.

The simulation-based fatigue results showed sufficiently small scatter in the stress range (scatter index of 1.5 within the 90% confidence interval), as shown in Figure 51. The scatter results indicate that the method is applicable for predicting fatigue performance under various joint and load conditions without requiring additional correction factors to the design capacity. The simulation-based fatigue results showed good agreement with experimental data for most load conditions but also revealed the model's limitations under high long-term loading.

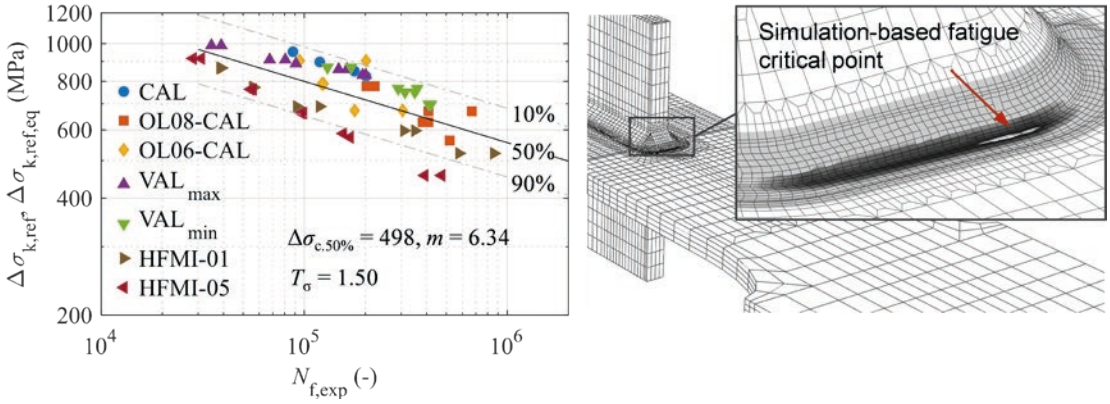

Figure 51. The estimated fatigue capacity curve and experimental data points in the simulated stress range, and an example of the fatigue resistance distribution in the simulation model.

IMPACT OF THE WORK

The simulation offers detailed insight into fatigue-related factors under combined post-fabrication state and cyclic loading, thereby improving estimates of the material's local behavior and thus increasing the accuracy of fatigue life prediction for the welded joint. Lower scatter in estimates across different joint and load conditions reduces conservatism and allows for more efficient material optimization.

The developed simulation process extends the range of methods to assess the fatigue resistance of a welded joint. In addition, it reduces the need for experimental verification, thereby making it a feasible method for studying and evaluating the effects of inputs on fatigue performance.

NEXT STEPS

Future work should extend the method validation to other joint types and post-processing methods, such as grinding or remelting post-weld treatments. Additionally, the wider utilization of nonlinear simulation in fatigue analysis could be investigated.

PUBLICATIONS AND THESES

Pesonen, T., Kozlova, M., Ahola, A., Björk, T., & Moshtaghi, M. (2025). Simulation-based fatigue assessment using the 4R method in different load conditions. *European Journal of Mechanics - A/Solids*, 111, 105600. https://doi.org/10.1016/j.euromechsol.2025.105600

Pesonen, T., Riski, J., Lipiäinen, K., Ahola, A., Leitner, M., & Skriko, T. (2026). Simulation-based 4R fatigue assessment of high-frequency mechanical impact treated welded joints. *Journal of Constructional Steel Research,* 240, 110263. https://doi.org/10.1016/j.jcsr.2026.110263

Pesonen, T. (2026). *Finite element simulation-based fatigue assessment of welded high-strength steel joints* [Doctoral thesis, LUT University] (under pre-examination)

REFERENCES

Pesonen, T., Riski, J., Lipiäinen, K., Ahola, A., & Björk, T. (2024). Framework for a finite element method-based simulation approach to fatigue assessment of welded joints using the 4R method. *International Journal of Fatigue*, 181, 108148. https://doi.org/10.1016/j.ijfatigue.2024.108148

6.4 Simulation tool for arc welding process

Contributors: **Dilip Neupane,** Steel Structures, Mechanical Engineering, LUT University
Antti Ahola, Steel Structures, Mechanical Engineering, LUT University
Tuomas Skriko, Welding Technology, Mechanical Engineering, LUT University

Correspondence: **Dilip Neupane** (dilip.neupane@lut.fi)

BACKGROUND

Welding is the process of joining materials by heating. In this process, a heat source (laser or arc plasma) is used to melt a workpiece, forming a molten pool that solidifies and forms a weld geometry, with or without filler material. This process involves complex physics of mass and energy balance in heat transfer, electric and magnetic fields, electric arc discharge, magnetohydrodynamics, melting, evaporation, and solidification, and multiphase fluid flow. Such a complex process could be better understood only by physics-based simulation models, including prediction of the final shape of weld for fatigue or stress assessment. Currently, the prediction of weld-bead geometry is still heavily reliant on experimental testing, even though geometrical accuracy is one of the governing factors in weld quality and structural performance. A lot of simplified simulations models for welding simulation exits, however, model with complex physics remain limited.

The main aim of this task is to develop simulation tools for arc welding to define the final shape of weld geometry, which can be further used as a basis for the fatigue or stress assessment. The research work is carried out as collaborative work at LUT University and TU Wien, Austria.

METHOD

During project period, firstly, the work focused on a comprehensive literature review of arc welding process simulation, aiming to develop deep understanding of process behaviour and the implementation of software tools. Secondly, the work focused on implementation of the magnetohydrodynamic (MHD) model and development of a physical model for implementing temperature dependent transport properties needed for arc welding simulation. The following figure illustrates the physic of arc welding process for mass and energy balance. In arc welding, the magnetic fields influence both the arc plasma and the weld pool through Lorentz force, altering the molten metal flow and solidification behaviour which ultimately determine the final weld shape, while the joule heating acts as a primary heat source. Electromagnetic fields, arc-plasma behaviour are described by MHD equation together with appropriate interface physics. The MHD equations are solved using either the electric potential or magnetic-induction formulation. From these formulations, the current density and magnetic fields are obtained, which are used to evaluate the Lorentz force and Joule heating. The Lorentz force and Joule heating are represented by a source term added to the momentum and energy equation while solving the multiphysics formulation that couples thermal conduction, fluid flow and electromagnetic fields. Model development utilizes the existing TU Wien laser-solver architecture (Otto & Schmidt, 2010; Otto et al. (2025); Zenz et al., 2024), adapting it to arc welding physic and implementing the full formulation in OpenFoam CFD code.

RESULTS AND FINDINGS

The work in this task is still ongoing. The result presented here are results of the work during the project period. From the review, it was found that the simulation of welding process is governed by fundamental equations of heat and mass flow, the volume of fluid (VOF) equations for tracking the

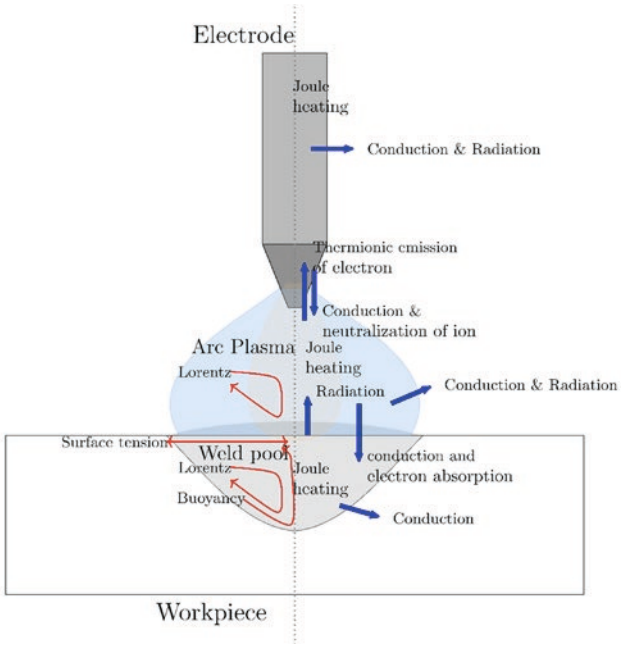

Figure 52. Schematic illustration of physic of arc welding process.

free surface flows or similar and physic of individual welding processes. All governing equations are integrated into a CFD/FEM code; however, the primary challenge lies in accurately modelling the welding process. Various CFD/FEM solvers, such as ANSYS Fluent (e.g., Yujiao et al., 2024), COMSOL (e.g., Traidia et al., 2011), and open-source software like OpenFOAM, can simulate the welding process, with OpenFOAM offering greater flexibility for modifying the solver and other properties. Some researchers have also developed their own in-house codes based on FORTRAN (e.g., Murphy et al., 2009). However, it is difficult to find tools for the simulation of complex physics in arc welding that couples heat transfer and fluid flow, electric and magnetic fields, arc discharge, melting and solidification, and evaporation.

In this work, for implementing MHD, both induction- and potential-based MHD solvers were first developed by extending the interFoam solver, and the results were compared to existing results from the literature and analytical solutions. Then, the implementation was integrated into the TU Wien laser solver architecture. Figure 53 depicts an example of an MHD benchmark with the developed solver, showing the Hartmann flow case and a single bubble rise in a magnetic field simulation, and validation of electromagnetic part of infinite electric rod case.

In Figure 53(a), the numerical comparison of the developed multiphase solver against OpenFOAM's built-in single-phase MHD solver is shown, and the results match with good agreement. Similarly, in Figure 53(b–e), the Argon bubble trajectory is presented for various magnetic field strengths. As the magnetic field strength increases, the bubble trajectory tends to follow a straighter path, which is consistent with the behaviour reported in experimental studies in the literature. Lastly, in Figure 53(e–f), the analytical solution has been compared with the numerical results obtained with the help of the developed solver for the infinite electric rod case with constant radius and a constant current density parallel to the rod axis, and the electric potential iso-lines are presented.

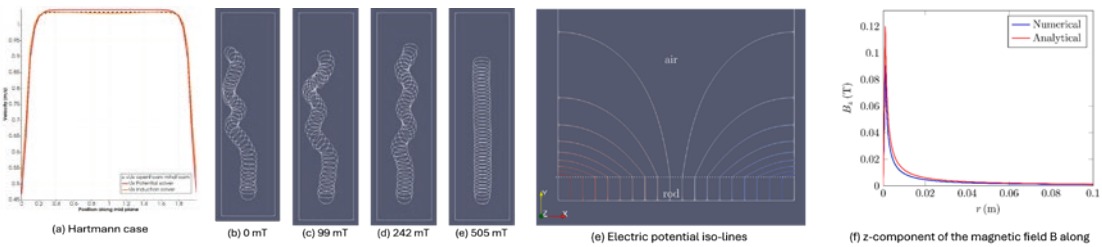

Figure 53. Example of MHD benchmark with developed solver. (a)Hartmann flow case, (b-e) Argon bubble trajectory for various applied magnetic field strength (Bubble rise in a magnetic field), and (e-f) validation of electromagnetic part for infinite electric rod.

IMPACT OF THE WORK

Both induction and potential based MHD solver were developed extending interFoam and the results are validated against literature. The developed simulation tools capable of simulating MHD flow is one of the important physics for arc plasma and weld pool model. The implementation will be integrated in the main tool in future and will deliver a physic-based multiphysics simulation tools capable of predicting weld-bead shape and temperature fields in arc-welded joints.

NEXT STEPS

As future work, the simulation tools will be further developed to 3D arc welding simulation tool for predicting weld geometry considering electrode, arc plasma, workpiece, the arc-plasma behaviour and electrode-workpiece interaction. Validation will be supported through comparison with experimentally measured profiles, temperature fields and molten-pool behaviour.

PUBLICATIONS AND THESES

Publications on the development of the simulation solver is planned and will be included in the doctoral thesis of Dilip Neupane.

REFERENCES

Murphy, A. B., Tanaka, M., Yamamoto, K., Tashiro, S., Sato, T., Lowke, J. J. (2009). Modelling of Thermal Plasmas for arc welding: The role of the shielding gas properties and of metal vapour. *Journal of Physics D: Applied Physics*, 42(19), 194006. https://doi.org/10.1088/0022-3727/42/19/194006

Otto, A., Schmidt, M. (2010). Towards a universal numerical simulation model for laser material processing. *Physics Procedia*, 5, 35–46. https://doi.org/10.1016/j.phpro.2010.08.120

Otto, A., Buttazzoni, M., Durán, C., Florian, T., Zenz, C. (2025). Universal Numerical Simulation Model for Laser Material Processing. *ArXiv pre-print* 2509.22666. https://doi.org/10.48550/arXiv.2509.22666

Traidia, A., Roger, F., ParisTech, E. (2011). A Transient Unified Model of Arc-Weld Pool Couplings during Pulsed Spot Gas Tungsten Arc Welding.

Yujiao, Z., Yinghao, L., Sizhe, N., Hongtao, W., Ran, Z. (2024). Multi-physics coupling simulation of GMAW arc and droplet behaviors based on CFD. *Welding in the World*, 68(10), 2589–2610. https://doi.org/10.1007/s40194-024-01806-5

Zenz, C., Buttazzoni, M., Florian, T., Crespo Armijos, K. E., Gómez Vázquez, R., Liedl, G., Otto, A. (2024). A compressible multiphase mass-of-fluid model for the simulation of laser-based manufacturing processes. *Computers & Fluids*, 268, 106109. https://doi.org/10.1016/j.compfluid.2023.106109

6.5 Industry partner contributions

6.5.1 SSAB Europe Oy

Contributors: SSAB (process & product development, rolling operations, data owners)
Indalgo (PoC implementation team: architecture, integration, UI)
(Optional) model providers / domain experts, as relevant

Correspondence: SSAB: Teemu Peltonen (teemu.peltonen@ssab.com)

Virtual Rolling Mill- Proof of Concept (PoC)

BACKGROUND

The purpose of WP3 was to build a practical foundation for a virtual rolling tool that can support SSAB's product and process development without relying only on production trials. The need is clear: faster product development, better process verification, lower cost of experimentation, and stronger root-cause analysis when deviations appear in production.

METHOD

A Proof of Concept was implemented with a controlled scope to prove feasibility.

- Scope from walking beam furnace (WBF) down to the coilers.
- Historical production data was used as input. A preselected coil set was used.
- One coil was simulated at a time, using a 1D approach (centreline).
- The user could search simulations, view results, and create a new simulation case by changing selected inputs/parameters.
- Results were stored in a simulation database (MongoDB) and visualised in a browser-based UI.
- The architecture was built modular, so that new models and process blocks can be added later.
- In the PoC, results were shown after the run was completed (not streaming during runtime).

RESULTS AND FINDINGS

The PoC demonstrated that a virtual rolling environment can be implemented as a working end-to-end flow:

- production history data can be used as simulation input
- simulation runs can be created and executed in a controlled way
- results can be stored and displayed for analysis
- the modular architecture supports further extension (additional models, broader scope, more use cases)

IMPACT OF THE WORK

The work reduced uncertainty around the concept and created a concrete technical base for a scalable virtual rolling platform. For SSAB, the expected practical value is:

- faster development cycles and fewer costly production trials
- improved process verification for new products and changes
- better tools for analysing deviations and root causes
- a foundation for systematic optimisation work based on simulation

NEXT STEPS

Typical next phases after the PoC are:

- scale from a limited coil set to broader datasets and routine use
- improve multi-run comparison and “what-if” workflows (not only one run at a time)
- enable DOE-style batch runs (many simulations from selected variable ranges)
- extend the scope and fidelity of models where needed
- clarify model assumptions and input requirements for better transparency
- integrate with other SSAB development and quality tools for daily use

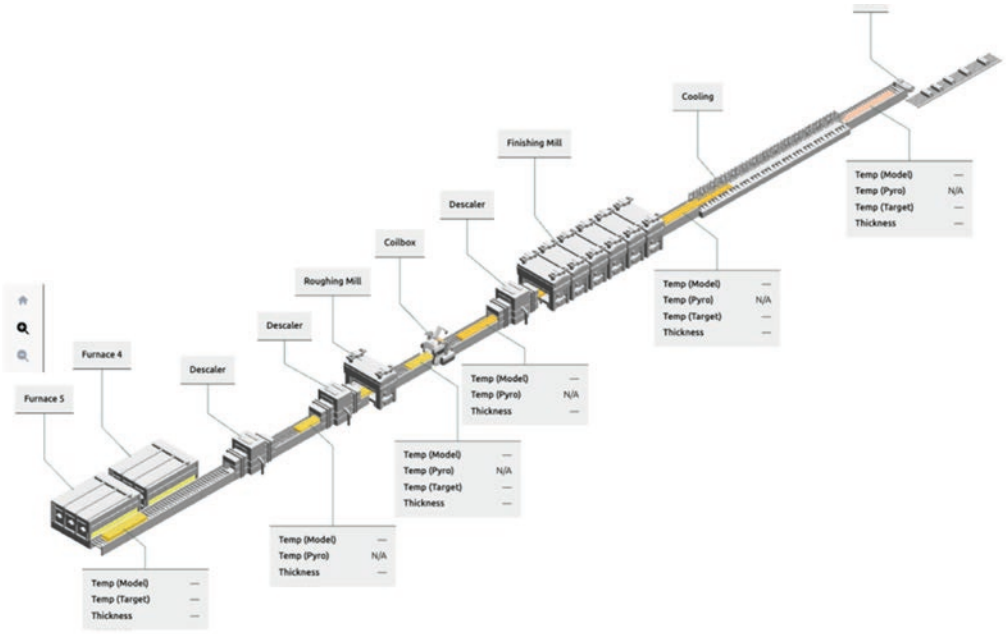

Figure 54. The Virtual Rolling Mill will accelerate new product development and improve its cost-efficiency and overall effectiveness.

6.5.2 Indalgo Oy

Contributors: Indalgo Oy, SSAB, University of Oulu

Correspondence: Perttu Laurinen (perttu.laurinen@indalgo.com)

BACKGROUND

Steel production is going through a major transformation. The industry is moving toward fossil-free production methods to reduce carbon emissions. At the same time, manufacturers must ensure that steel products maintain their required mechanical properties and overall quality while remaining cost-effective.

Traditionally, improving steel production processes or developing new steel products has required physical trials in the factory. These trials can be expensive, time-consuming and energy intensive.

The idea of "virtual steelmaking" is simple but powerful: before making changes in the real factory, test them in a digital environment. Indalgo contributed to the development of this digital simulation environment by combining metallurgical expertise with artificial intelligence–based modelling.

METHOD

During the project, Indalgo worked on building the foundation for a digital "virtual steel plant." In practice, this meant:

- Designing how different digital models and parts of the system connect and work together
- Creating the digital system that allows steel production to be tested and explored virtually
- Using real production data from steel plants
- Testing how well the virtual results match real-world measurements

The goal was to create a system where different production settings can be tested digitally. For example:

- How do changes in processing parameters influence the final properties of the steel?
- How does the chemical composition affect both the production process and the resulting properties of the steel?

Instead of testing these changes directly in production, they can first be explored safely in the virtual environment.

The work was carried out in close cooperation with industrial partners and researchers to ensure that the digital system reflects real factory conditions.

RESULTS AND FINDINGS

The project resulted in:

- A working architecture for a virtual steelmaking system
- Integration of real industrial data into digital simulations
- A foundation that can be expanded to multiple production sites

The concept has already supported a significant customer project. It has opened the door to longer-term collaboration and to scaling the solution to additional factories.

One key learning was that combining knowledge from different fields – production engineering, metallurgy and artificial intelligence – is essential. Close cooperation between experts was critical for making the digital system practical and reliable.

IMPACT OF THE WORK

Virtual steelmaking has several important benefits:

Faster development

New steel grades and process improvements can be tested digitally before implementation. This speeds up innovation.

Better energy efficiency

By optimizing processes digitally, manufacturers can reduce unnecessary energy use and material waste.

Lower risk

Production changes can be evaluated in a safe digital environment, reducing costly mistakes in real factories.

Support for the green transition

As steel producers move toward fossil-free production methods, digital simulation tools help them adapt more quickly and confidently.

In summary, virtual steelmaking helps the steel industry become more efficient, more competitive and more sustainable.

NEXT STEPS

The next steps are to:

- Further validate the system using selected steel grades
- Expand the solution to additional production plants
- Turn the concept into a scalable commercial product
- Support international deployment, especially in Europe and North America

The long-term vision is that virtual steelmaking becomes a standard tool in modern low-carbon steel production.

6.5.3 John Deere Forestry Oy

Contributors: John Deere Forestry Oy, SmartBi

Correspondence: Jouni R Valkila (ValkilaJouni@JohnDeere.com), Engineering Manager, VDV

BACKGROUND

SmartBi conducted a study using data provided by John Deere to assess the viability of utilising low frequency population data for predicting machine life estimates. The research aimed to determine whether such data could be employed to estimate the remaining lifespan of the steel structures in these machines.

METHOD

Data from previous full machine measurements—including CAN, pressure sensors, strain gauges, force transducers, and position gauges—was used and analysed. The CAN (Controller Area Network) system is a network that enables communication between various components within machinery, while strain gauges are sensors used to measure deformation in structural elements. The study aimed to determine whether strain gauge data could be predicted from information already available in the machine's CAN system, and whether it was possible to estimate structural fatigue damage without direct strain data. If this proved unfeasible, the goal was to identify which additional data channels should be added to the CAN system to enable accurate predictions. The research clearly outlined these objectives to provide a focused approach for subsequent investigation.

RESULTS AND FINDINGS

The study demonstrated that accurate predictions are achievable for the specific machine components analysed. Different machine components, such as the motor and gearbox, require distinct data sets for reliable prediction. Notably, the research found that prediction accuracy remained high even when using low-frequency data, provided that machine usage was observed over a sufficiently long period. This suggests that extended monitoring can compensate for less frequent data collection, although some rare usage scenarios may not be captured. Overall, predictions proved generally reliable for the examined parts, highlighting the potential of leveraging existing data for machine health monitoring.

IMPACT OF THE WORK

The significance of the work is to strengthen the idea that such data, that machine is already producing, could be used in monitoring the machine health. Also the future ideas of possible digital twin of forest machine could be done, based on this study.

NEXT STEPS

Producing the more tools to develop the digital twin based on this data.

6.5.4 Hiab Finland Oy

Contributors: **Matti Randelin, Timo Stenvik,** Hiab Finland Oy
Ilkka Mikkonen, EDR & Medeso Oy
Aaro Keskinen, Comatec Mobility Oy

Correspondence: **Matti Randelin**, R&D Manager, Control Systems & Analytics,
Hiab Finland Oy, Demontables & Defence Division
Antti-Jussi Romppanen, Technical Business Developer
EDR & Medeso Oy, Virtual product design

BACKGROUND

A robust simulation platform accelerates product development and enables rapid studies, leading to a shorter time-to-market for new applications. The original concept in the FOSSA1 project was to create a complete virtual platform, spanning from raw material production to the end-user application. In this overarching virtual platform, SSAB is located upstream (steel production), while Fortaco occupies the midstream by processing steel into ready-made components. Hiab's position is downstream, focusing on the end-user by creating usage profiles and defining requirements for the materials used in hooklift structures.

From a core competence perspective, Hiab aims to produce equipment that meets customer needs while ensuring the structure is robust and reliable. The work in the FOSSA2 project focused on further developing the hooklift simulation platform created in FOSSA1. The target was to incorporate more load cases and features to improve simulation accuracy. These simulations facilitate the design of new hooklift concepts and provide ideas for new digital services that support sustainability targets. Furthermore, simulations can operate in the background to calculate life-cycle emissions and provide real-time feedback to help users operate equipment more efficiently.

METHOD

Hiab's virtual platform is built on Ansys and MathWorks products. The primary software used is Ansys Motion (multiphysics simulation), where the hooklift vehicle and its relevant mechanics are modeled. The hooklift's control system—comprising hydraulics, control logic, and electronics—is modeled in Simulink, which is connected to Ansys Motion via a native interface. This setup enables real-time co-simulations, providing results for both controls and mechanics simultaneously. For high-precision structural analysis, Ansys Mechanical was utilized, as its strength analysis tools offer greater depth than those in Ansys Motion. R&D simulation platform is presented in Figure 55.

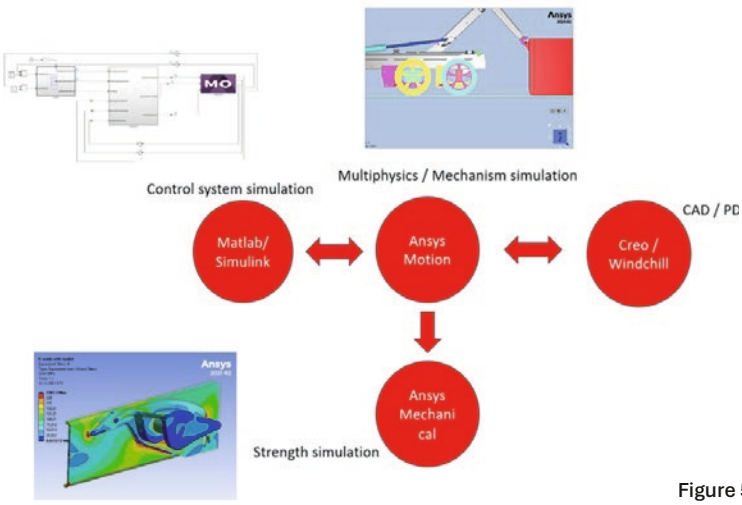

Figure 55. Hooklift R&D simulation platform.

The platform can be extended to other internal Hiab systems for data exchange. During the project, tools were developed to import data from the HiConnect system and export data to the Multilift eco-calculator. Utilizing this platform, design improvements for the hooklift's steel structure were simulated using a full-vehicle model and real user profiles identified in WP1.The full simulation platform is presented in Figure 56.

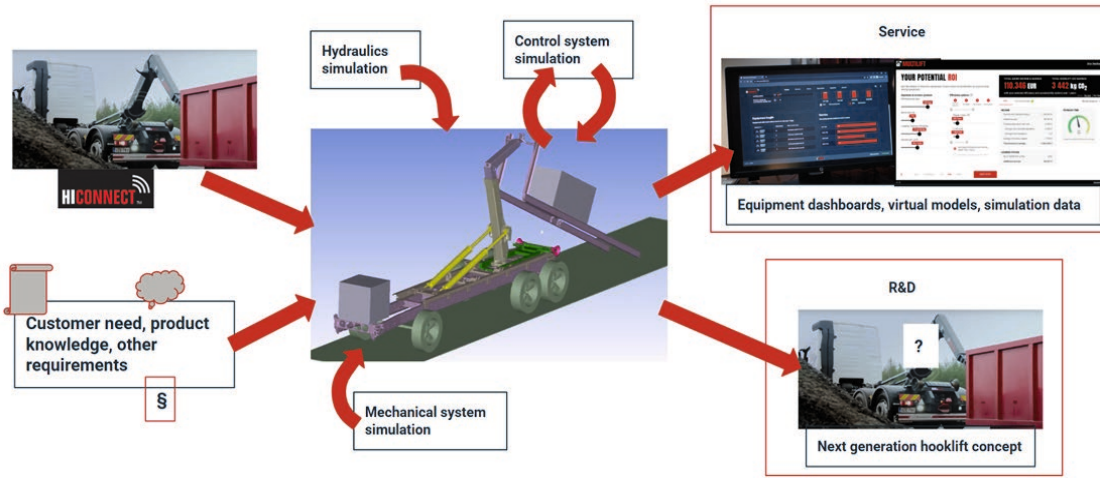

Figure 56. Full simulation platform and its possible connections.

The platform was also expanded to simulate movements beyond basic functionality, loading and tipping. An improved truck suspension model was integrated into the basic simulations, followed by the addition of a tipping stability simulator and a full-vehicle driving simulator. The stability simulator provides critical data on how the hooklift structure affects vehicle stability during tipping—a key safety requirement. The driving simulator represents a significant leap forward; for the first time, Hiab can account for all dynamic forces during driving within the design process.

RESULTS AND FINDINGS

The primary outcome was a simulation platform that surpasses current R&D tools in performance and is scalable across other company functions. The original goal of connecting customer data to the simulation platform and exporting data/applications to the Digital Service team was successfully achieved. HiConnect data can now be used in its raw or processed form to create high-accuracy simulations of actual equipment use.

The resulting simulation data will benefit Hiab's digital services in condition monitoring and sustainability applications, which are sold as part of service packages. Simulation data can also "fill the gaps" where physical measurement data is missing. By utilizing the user profiles created in WP1, accurate estimations for service timing can be determined. Additionally, studies were performed to visualize the life expectancy of the equipment across different user profiles. Evaluation of life expectancy of light hooklift concept with different user profiles is presented in Figure 57.

Hiab's cloud-computing environment for digital services provides an ideal platform for merging measured and simulated data. During the project, the most efficient calculation methods for real-time fatigue analysis were researched. In his Master's thesis, Aaro Keskinen determined a suitable method for fast, cloud-based fatigue analysis derived from high-fidelity simulation results. By combining these findings with FOSSA1 results, Hiab can create small, stand-alone simulation applications that run in the cloud. The Multilift eco-calculator is one such application, capable of utilizing both measured and simulated data as inputs.

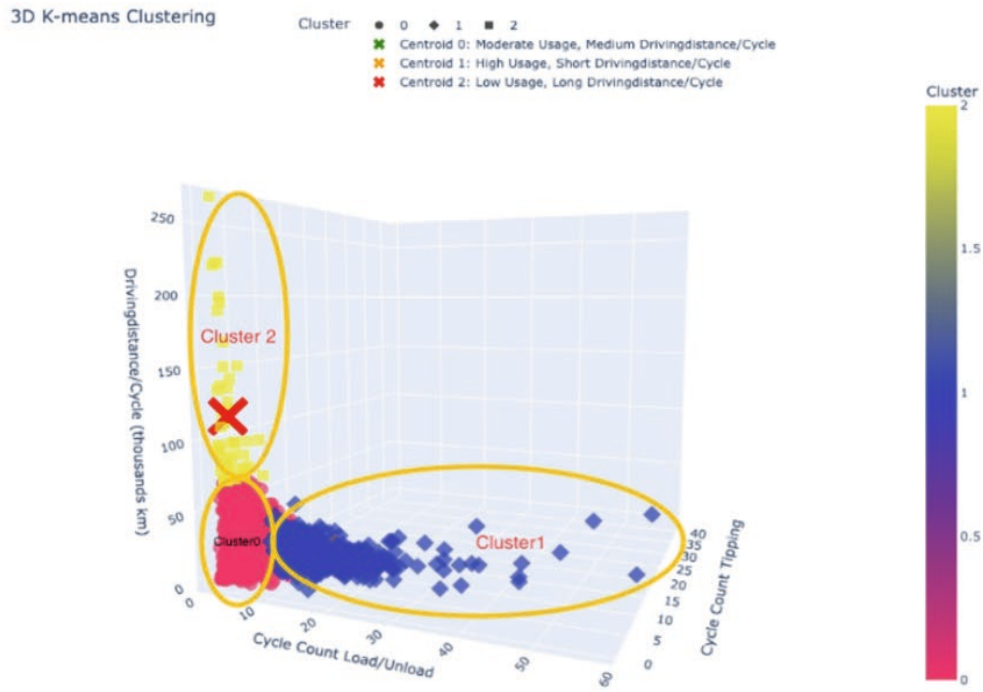

Component	Detail	Model	Cycle	durability [days] 2 cycles/day	5 cycles/day	13 cycles/day
koukku	1	Light	Loading-Unloading	31625	12650	4865
koukku	1	Light	Loading-Tipping	36974	14789	5688
koukku	2	Light	Loading-Unloading	20875	8350	3212
koukku	2	Light	Loading-Tipping	19186	7674	2952
koukku	3	Light	Loading-Unloading	19625	7850	3019
koukku	3	Light	Loading-Tipping	23244	9298	3576
koukku	4	Light	Loading-Unloading	25875	10350	3981
koukku	4	Light	Loading-Tipping	31189	12476	4798
koukku	5	Light	Loading-Unloading	7125	2850	1096
koukku	5	Light	Loading-Tipping	10168	4067	1564

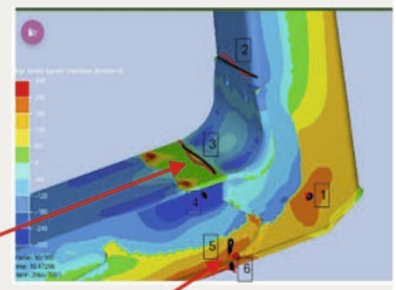

Figure 57. From user profiles (above) to life expectation of light concept of hook frame (below).

IMPACT OF THE WORK

This work significantly impacts Hiab's future digital service offering. With the Multilift eco-calculator and future applications, Hiab can quantify the benefits of eco-options for customers and make their effects visible. Fossil-free steel is one component of the value proposition; it is most effective when combined with functional features. Based on this work, Hiab has created eco-compliant option packages and the sales tools necessary to demonstrate their value.

In the future, Hiab will be able to create more service options and transform existing cloud data into high-value applications. These may range from fleet management dashboards for sustainable operation to real-time user-guidance applications.

NEXT STEPS

Hiab will continue developing its digital service offering by creating new applications for both cloud and local use within hooklift control systems. Simulation platform development will continue by adding more use cases, and the full implementation into R&D processes is scheduled for completion by the end of 2026.

PUBLICATIONS AND THESES

Keskinen, A. (2026) Comparison between different methods for fatigue evaluation of a hooklift for use in real time simulation [Master´s thesis, LUT University]. Publication pending.

Photo: Adobe Stock

6.6 WP3 Key takeaways

- **Induction-heating modelling and industrial data analysis supported hot-strip process modelling and strip profile prediction**

  University of Oulu developed and validated an FEM model for induction heating that showed good agreement with dilatometry experiments, confirming that the key physical phenomena were captured in the modelling. In work carried out with SSAB and Indalgo, data from more than 1000 coils from SSAB Raahe finishing mill was used to build a dataset to predict strip thickness profiles from 80 process parameters, providing a basis for future strip profile modelling.

- **Research on UHSS bendability improved understanding of fracture behaviour in air bending and provided new tools for bendability assessment.**

  University of Oulu generated a comprehensive experimental dataset from tensile and air-bending tests on nine 6 mm steel grades with strength levels from 355 to 1700 MPa. The results showed that plane-strain tensile fracture strains correlated better with bending-derived fracture strains than conventional uniaxial tensile test fracture strains. The work also developed a new DIC-based method for identifying fracture initiation in bending tests.

- **Simulation-based fatigue assessment improved prediction of fatigue performance in welded high-strength steel components under various joint and load conditions.**

  Building on the framework developed in FOSSA Phase 1, LUT University further developed and validated a sequential coupled finite-element simulation approach that integrates welding, post-weld treatment and mechanical loading into fatigue assessment. The results showed that as-welded, overload and high-frequency impact treated conditions could be simulated with reasonable accuracy, and that the simulation-based fatigue results showed sufficiently small scatter in the stress range (scatter index 1.5 within the 90% confidence interval) together with good agreement with experimental data for most load conditions.

- **Physics-based modelling provided a basis for further development of arc welding simulation.**

  LUT University, in collaboration with TU Wien, developed induction-based and potential-based magnetohydrodynamic solvers for arc welding simulation by extending OpenFOAM tools. The solvers were validated against analytical solutions and literature benchmarks, and the work provided a basis for further development of a 3D simulation tool for predicting weld geometry and temperature fields in arc-welded joints.

- **SSAB established a concrete technical base for a scalable virtual rolling platform.**

  SSAB built a proof of concept for the process from walking beam furnace to coiler using historical production data and coil-by-coil simulations. The work showed that simulation runs could be created, executed and reviewed in one environment. This established a practical basis for a scalable virtual rolling platform that can support faster development work, fewer production trials and improved analysis of production deviations.

- **Indalgo built a foundation for a virtual steelmaking system that can be expanded to multiple production sites.**

  Working with SSAB and University of Oulu, Indalgo developed a working architecture for a virtual steelmaking system and integrated real industrial data into digital simulations. The concept has already supported a significant customer project and created a basis for scaling the solution to additional factories. It can support faster development of new steel grades and process improvements, lower-risk testing, and improved energy efficiency in steel production.

- **John Deere Forestry showed that existing machine data can support machine life estimates and future digital twin development.**

  Working with SmartBi, John Deere Forestry studied whether low-frequency machine data could be used to estimate machine life and the remaining lifespan of steel structures. The results showed that accurate predictions were achievable for the analysed components, and that prediction accuracy remained high even with low-frequency data provided that machine usage was observed over a sufficiently long period.

- **Hiab developed a simulation platform that supports both hooklift product design and future digital services.**

  Building on the hooklift simulation platform created in FOSSA1, Hiab expanded the platform with more load cases and features to improve simulation accuracy. The primary outcome was a simulation platform that surpasses current R&D tools in performance, connects HiConnect data with simulation, and can be scaled across other company functions. This provides a basis for condition monitoring, life-expectancy estimation and future digital service applications.

7. Conclusions and next steps

FOSSA2 showed that the transition to fossil-free and low-emission steel cannot be addressed through steel production alone. It requires coordinated development across the value chain, from raw materials, recycling, steel chemistry and processing to manufacturability, product performance and digital development tools. The project examined these questions in practical industrial settings through a combination of research, modelling and pilot work. In this way, FOSSA2 clarified what is needed to move fossil-free and low-emission steel from concept level toward wider industrial use, while also strengthening the cooperation base and competence needed for further development in Finland.

CAPABILITIES AND EXPERTISE DEVELOPED

The project produced high-level scientific expertise on the technical and economic applicability of FFUHSS structures and reinforced national competence in materials science, mechanical engineering, novel thermomechanical processing, and simulation-based design. Capabilities were created in multidisciplinary metallurgical characterization and in the usability assessment of steels in industrial processes, including formability, bendability, weldability, fracture and fatigue behaviour, hydrogen-related phenomena, and the role of residual elements in the development of steel properties. It also created expertise in analytics of fossil-free steel value chains, combining AI with metallurgy and building digital simulation environments. These capabilities produced new engineering tools and process methods for the further development and industrial use of fossil-free steel solutions.

PROJECT SIGNIFICANCE

FOSSA2 made the transition to fossil-free and low-emission steel more practical by reducing uncertainty around where and how new steel solutions can be used. Pilot work showed that fossil-free steel can be taken from concept level into real products and real manufacturing chains, while the economic work created a first basis for later feasibility and sensitivity analysis of fossil-free ultra-high-strength steel applications. Together, these results supported a more concrete path from material development toward controlled industrial use.

The project clarified how the value of lower-emission steel is created in practice. It depends on whether the steel can deliver reliable performance, customer value and clear life-cycle benefits, and whether it can be implemented at product level in ways that are manufacturable and scalable in industry. In practice, this value is shaped by long service life, product design, maintenance and modernization choices as well as by cleaner steel production. The work showed that lower-emission product solutions can deliver clear emission reductions without giving up the technical performance required in industrial use. In some applications, this also included the use of high-strength steels in lighter structures, helping to reduce material use and lower environmental impacts at product level. This created a basis for new product concepts, broader application opportunities and future export-oriented business.

Another important effect was the shift toward more predictive and controlled development. Rather than relying mainly on physical trials, the project combined AI, metallurgical knowledge and industrial production data into practical digital solutions for fossil-free steel development. It

also strengthened model reliability through the controlled generation and use of synthetic data in situations where measured data was limited. Virtual steelmaking and related digital methods made it possible to study new steel grades and process changes before implementation, while advances in adaptive robotic welding and simulation-based fatigue assessment strengthened the basis for weld-quality assessment, improved prediction of the fatigue performance of welded structures, and supported more efficient material use. The project also showed that existing machine data can support life-expectancy estimation and condition monitoring in product use, while creating a basis for future digital twin development and digital services. Together, this work supports faster development, reduces reliance on energy-intensive physical trials, and promotes more resource-efficient development.

The project also improved readiness for future steel applications in demanding conditions. Work on welded joints, fatigue resistance and bendability deepened understanding of how high-strength steels perform in manufacturing and in demanding use, and advanced further steel development for applications where reliability and long-term performance are critical. For the automotive sector, this improved understanding of formability, edge performance and weldability in high-strength steels, while for offshore and arctic applications it strengthened knowledge needed to use welded steels safely in low-temperature and other demanding service conditions. In hydrogen-related applications, the project produced new knowledge on the behaviour of high-strength steels in hydrogen environments and on the factors affecting performance in welded pipeline steels. These results are important for assessing the safe and cost-effective repurposing of existing pipelines for hydrogen transport. The pipeline steel grades and manufacturing methods developed during the project were also shown to perform acceptably in hydrogen atmosphere, enabling the use of domestic alternatives in the construction and operation of hydrogen infrastructure, including transmission and storage networks.

At a wider level, FOSSA2 supported the green transition while also strengthening conditions for industrial competitiveness and industrial renewal. The project strengthened the knowledge base, cooperation structures and practical readiness needed for fossil-free value chains, future investments and new low-emission business opportunities in the Finnish steel and metal industry.

NEXT STEPS

The next phase should build on the areas where the work identified clear needs for validation, refinement and further development:

- **Value-chain and economic theme:** The next step is to improve data reliability and refine the LCC models and their outputs based on validated data, so that feasibility and sensitivity analyses can be carried out on a stronger basis.
- **Welding-related themes:** The work should continue through further studies comparing filler-metal alternatives, identifying local weakest links, optimizing welding parameters, and examining the mechanical failure of welded components under cyclic loads. It should also extend fatigue-assessment work toward thin-walled joints and study the use of HFMI treatments in novel high-strength and ultra-high-strength steel materials.

- **Residual elements:** The next step is to deepen understanding of how scrap-derived residual elements affect microstructure and mechanical properties, and to extend the research to a broader range of steel grades.
- **Formability and bendability:** The work should continue by extending cut-edge and bendability studies to higher-strength steels and by examining damage and fracture behaviour in more detail. In intercritical annealing research, the next steps include carrying out fatigue testing and studying the effect of heating rate, while future formability testing should also give closer attention to material surface quality. Bendability assessment should be advanced through model development based on the available experimental data and through contributions to bendability characterization and testing standards.
- **Hydrogen-related themes:** The work should continue through further study of retained-austenite morphology, interface behaviour and other microstructural features that affect hydrogen tolerance in martensitic-austenitic steels. In welded pipeline steels, the next step is to integrate experimental and simulation results in order to develop predictive models for performance under both hydrogen and air environments and to support optimization of welding parameters and microstructures.
- **Virtual and simulation-based themes:** The next steps include improving the accuracy of the induction-heating model by replacing simplified assumptions with more realistic ones and by strengthening the validation data. In surface phenomena modelling, the next step is to fit predictive models for strip thickness profile. In simulation-based fatigue assessment, the work should extend the method validation to other joint types and post-processing methods. In virtual steelmaking and related industrial digital platforms, the next step is to continue validation, scaling and integration in closer connection with industrial data and practical development work.

Photo: Ponsse Plc

8. List of publications

JOURNAL PAPERS

Afkhami, S., Amraei, M., Javaheri, V., Ghafouri, M., Björk, T., Salminen, A. & Zhao, X-L. (2024). Flow and hardening behavior in the heat-affected zone of welded ultra-high strength steels. *Welding in the World*, *68*, 1001–1016. https://doi.org/10.1007/s40194-024-01703-x

Afkhami, S., Skriko, T., Lipiäinen, K. & Björk, T. (2024). Fracture, deformation route, and mechanical performance of welded cold-formed ultra-high strength steel S1100. *Procedia Structural Integrity*, *61*, 53-61. https://doi.org/10.1016/j.prostr.2024.06.009

Ahmed, S., Oja, O., Kaijalainen, A. & Peura, P. (2024). Effect of cooling practice on the mechanical properties of medium manganese aluminum alloyed steels after inter-critical annealing, quench and partition heat treatment. *Steel research international*, *96(2)*, 2400420. https://doi.org/10.1002/srin.202400420

Ahmed, S., Pun, L., Isakov, M., Raami, L., Hokka, M., Kuokkala, V.-T., & Peura, P. (2026). Investigation of serrated flow in intercritically annealed medium manganese steel by in-situ synchrotron X-ray diffraction. Submitted to *Steel research international*.

Ahmed, S., et al. (2025). In-situ X-ray diffraction analysis of serrated flow in medium manganese steels. Submitted

Ahola, A., Leitner, M., Grönlund, K., Brunnhofer, P., Buzzi, C., Moshtaghi, M. & Björk, T. (2025). Fatigue assessment of as-welded and HFMI-treated high-strength steel joints under variable amplitude loading using local approaches. *Welding in the World*, *69*, 687–700. https://doi.org/10.1007/s40194-024-01919-x

Ahola, A., Lipiäinen, K., Suikkanen, P. & Skriko, T. (2025). Fatigue assessment of welded thin-walled automotive steels using effective stress methods. *Welding in the World*. https://doi.org/10.1007/s40194-025-02292-z

Ahola, A., Salerto, S., Loisa, T., Lipiäinen, K. & Björk, T. (2024). Fatigue strength of single-sided fillet welds in overlapping ultra-high-strength steel sheets. *Welding in the world*, *68*, 1225–1239. https://doi.org/10.1007/s40194-024-01736-2

Alshawwa, O., Mela, K., Ahola, A., Björk, T., Koskimäki, M., Tulonen, J. & Hyvärinen, A. (2025). High-strength steel S700 K-joints: Experimental investigation on ultimate resistance and deformation capacity. *Journal of Constructional Steel Research*, *227*, 109317. https://doi.org/10.1016/j.jcsr.2024.109317

Auvinen, H., Tervo, H., Sainio, J., Kömi, J., & Kaijalainen, A. Microstructure and Toughness Properties of Physically Simulated Heat-Affected Zone of 500MPa Low-Carbon Bainitic Steels. (To be published).

Ayub, H. (2026). Effect of arc welding on microstructure and mechanical properties of S960 MC to S960 QT Ultra-High Strength Steel (UHSS) dissimilar joints (to be published).

Björk, T., Ahola, A. & Kukkonen, O. (2024). On the out-of-plane buckling of RHS X-joints – Analytical and numerical approaches. *Journal of Constructional Steel Research*, *220*, 108836. https://doi.org/10.1016/j.jcsr.2024.108836

Gáspár, M., Kovács, J., Sisodia, R., Sainio, J., Tervo, H., Javaheri, V. & Kaijalainen, A. (2024). Physical simulation-based analysis of multipass welding in S500 shipbuilding steel. *Welding in the World*, *69*, 825–836. https://doi.org/10.1007/s40194-024-01908-0

Gáspár, M., Kovács, J., Sisodia, R. P. S, Sainio, J., Tervo, H., Javaheri, V., Kaijalainen, A. & Lukács, J. CTOD examination of physically simulated heat-affected zones in S500 shipbuilding steel welds. *Welding in the World*, to be published in 2026.

Ghafouri, M., Afkhami, S., Pokka, A., Javaheri, V., Larkiola, J., Moshtaghi, M. & Björk, T. (2025). Hardening behavior and microstructure of S1100 ultrahigh-strength steel at elevated temperatures. *Journal of Constructional Steel Research*. Under review.

Ghafouri, M., Afkhami, S., Pokka, A.-P., Javaheri, V., Larkiola, J., Moshtaghi, M., Björk, T. & Skriko, T. (2026). Plastic deformation and failure of TMCP S1100 ultrahigh-strength steel at elevated temperatures. *Fire Safety Journal, 162,* 104681. https://doi.org/10.1016/j.firesaf.2026.104681

Ghafouri, M., Afkhami, S., Pokka, A.-P., Javaheri, V., Togiani, A., Larkiola, J. & Björk, T. (2024). Effect of temperature on the plastic flow and strain hardening of direct-quenched ultra-high strength steel S960MC. *Thin-Walled Structures*, *194*, 111319. https://doi.org/10.1016/j.tws.2023.111319

Havia, J., Lipiäinen, K., Ahola, A. & Björk, T. (2024). Fatigue design of stress relief grooves to prevent weld root fatigue in butt-welded cast steel to ultra-high-strength steel joints. *Welding in the World*, *68*, 2203–2216. https://doi.org/10.1007/s40194-024-01797-3

Horváth, D., Safyari, M. & Moshtaghi, M. (2026) Hydrogen embrittlement in welded pipeline steels: Fundamentals, mechanisms, testing, mitigation and welding processes. Submitted, under review.

Khedr, M., Elshokrofy, H., Pokka, A.-P., Hamada, A., Jaskari, M., Mustakangas, A., Järvenpää, A., Ibrahim, A. & Elsamanty, M. (2024). Effect of design parameters on auxetic behavior and stiffness of additively manufactured 316L stainless steel. *Journal of Materials Research and Technology*, *30,* 8805–8814. https://doi.org/10.1016/j.jmrt.2024.05.197

Kovács, J., Gáspár, M., Lukács, J., Tervo, H. & Kaijalainen, A. (2024). Comparative study about the results of HAZ physical simulations on different high-strength steel grades. *Welding in the World*, *68,* 1965–1980. https://doi.org/10.1007/s40194-024-01714-8

Latypova, R., Javaheri, V., Claeys, L., Verbeken, K., Depover, T., Kömi, J. & Pallaspuro, S. (2025). Effect of rapid tempering and cementite morphology on hydrogen diffusion and trapping in a medium-carbon advanced high-strength steel. *Engineering Fracture Mechanics*, *326*, 111376. https://doi.org/10.1016/j.engfracmech.2025.111376

Latypova, R., Nyo, T. T., Seppälä, O., Ruoppa, R., Kauppi, T., Singh, H., Huttula, M., King, G., Pallaspuro, S., & Kömi, J. Low-temperature tempering for improving hydrogen embrittlement resistance in direct-quenched steel, Under review.

Leitner, M., Ahola, A., Moshtaghi, M., Björk, T., Brunnhofer, P. & Buzzi, C. (2025). Fatigue strength assessment of HFMI-treated steel joints under bending loading. Welding in the World, 69, 2433–2441. https://doi.org/10.1007/s40194-025-02100-8

Lipiäinen, K., Heinilä, S., Ahola, A., Skriko, T. (2026). Fatigue strength improvement of gusset end detail with welding techniques. Revision submitted to journal (ref. background IIW document: XIII-3163-2025)

Lipiäinen, K., Plosila, P., Kaijalainen, A., Ahola, A. & Björk, T. (2024). Influence of shear cut holes on the fatigue performance of hot-rolled 800 MPa automotive steel grades. *Procedia Structural Integrity*, *57*, 785-792. https://doi.org/10.1016/j.prostr.2024.03.084

Lund, H., Penttilä, S. & Skriko, T. (2025). Advancing smart multi-robot welding through pre-setting and digital twin-based feedback to mitigate angular welding distortion. *Discover Mechanical Engineering*, *4*, 35. https://doi.org/10.1007/s44245-025-00124-4

Meilinger, Á., Javaheri, V., Tervo, H., Abd Al Al, S. Microstructure Evolution in RSW-Welded MS1400 Martensitic Steel: Impact of Pulse Sequencing, *Journal of Manufacturing Processes*. (Submitted)

Nousiainen, O., Hannula, J., Saukko, S., Kaijalainen, A. & Kömi, J. (2024). Comparison of novel 1 GPa low-carbon, low-alloyed steel produced with simulated- and laboratory-scale thermomechanical controlled processes. *Steel Research International*, *96*, 2400481. https://doi.org/10.1002/srin.202400481

Olkkonen, R., Suikkanen, P., Skriko, T., Barsoum, Z. & Ahola, A. (2026). Fatigue design and manufacturing optimization of high-performing welded automotive and structural steel sheets. Submitted.

Pallaspuro, S., Fangnon, E., Aravindh, S.A., Claeys, L., Latypova, R., Yagodzinsky, Y., Aho, N., Kantanen, P., Uusikallio, S., Depover, T., Huttula, M., Dey, P. & Kömi, J. (2024). Mitigating hydrogen embrittlement via film-like retained austenite in 2 GPa direct-quenched and partitioned martensitic steels. *Materials Science and Engineering: A*, *908*, 146872. https://doi.org/10.1016/j.msea.2024.146872

Pesonen, T., Kozlova, M., Ahola, A., Björk, T. & Moshtaghi, M. (2025). Simulation-based fatigue assessment using the 4R method in different load conditions. *European Journal of Mechanics - A/Solids*, *111*, 105600. https://doi.org/10.1016/j.euromechsol.2025.105600

Pesonen, T., Riski, J., Lipiäinen, K., Ahola, A. & Björk, T. (2024). Framework for a finite element method-based simulation approach to fatigue assessment of welded joints using the 4R method. *International Journal of Fatigue*, *181*, 108148. https://doi.org/10.1016/j.ijfatigue.2024.108148

Pesonen, T., Riski, J., Lipiäinen, K., Ahola, A., Leitner, M., & Skriko, T. (2026). Simulation-based 4R fatigue assessment of high-frequency mechanical impact treated welded joints. *Journal of Constructional Steel Research*, *240*, 110263. https://doi.org/10.1016/j.jcsr.2026.110263

Plosila, P., Kesti, V., Hannula, J., Kömi, J. & Kaijalainen, A. (2024). A comparison between tensile and hole expansion properties in 800 MPa tensile strength grade hot-rolled steels. *Materials Today Communications*, *40*, 109521. https://doi.org/10.1016/j.mtcomm.2024.109521

Pokka, A., Kesti, V. & Kaijalainen, A. (2025). Local Formability and Bendability of UHSS: Correlations Between Bending and Tensile Fracture Strains. *International Journal of Solids and Structures*, *320*, 113524. https://doi.org/10.1016/j.ijsolstr.2025.113524

Raami, L., Wendler, M., Volkova, O. & Peura, P. (2025). The effect of bake hardening on quenched and partitioned AISI 420 stainless steel. *Steel Research International*, *96(5)*, 2400251. https://doi.org/10.1002/srin.202400251

Raami, L., Valtonen, K., Wendler, M., & Peura, P. (2026). Effect of heat treatments on the cavitation erosion evolution of AISI 420 stainless steels. *Wear*, 206493. https://doi.org/10.1016/j.wear.2025.206493

Raami, L., et al. (2025). Effect of carbon on the cavitation erosion evolution of quenched and partitioned AISI 420 stainless steel. Submitted

Rohani Raftar, H., Ahola, A., Lipiäinen, K. & Björk, T. (2024). Fatigue behavior of load-carrying cruciform fillet weld joints under variable amplitude load. *Journal of Constructional Steel Research*, *215*, 108559. https://doi.org/10.1016/j.jcsr.2024.108559

Rohani Raftar, H., Ghanadi, M., Hultgren, G., Ahola, A. & Barsoum, Z. (2024). Assessing local stresses in scanned fillet weld geometry using bagged decision trees. *Journal of Constructional Steel Research*, *218*, 108745. https://doi.org/10.1016/j.jcsr.2024.108745

Sabr, A., Ahmed, S., Kaijalainen, A., Penney, D., & Peura, P. (2026). Effects of Trace Elements Copper and Tin on Mild and Dual-Phase Steel Properties, to be submitted.

Safyari, M., Ahmad, M. & Moshtaghi, M. (2026) Insights into gaseous hydrogen permeation behavior in welds of X65 pipeline steel. *Welding in the World*. https://doi.org/10.1007/s40194-026-02362-w

Safyari, M., Horváth, D. & Moshtaghi, M. (2025) Enhancing hydrogen embrittlement resistance in steel pipelines through hybrid welding. *Welding in the World*. https://doi.org/10.1007/s40194-025-02071-w

Safyari, M., Kivimäki, M., Tulonen, J., Virolainen, E., Suikkanen, P. & Moshtaghi, M. (2026) Enhancing fracture toughness of the heat-affected zone in welded X70 pipeline steel under hydrogen gas. Submitted, under review.

Safyari, M. & Moshtaghi, M. (2025) Welding design of API 5L X65 pipeline steel: Effects of robotic hybrid laser arc welding versus GMAW on fracture toughness evaluated by SENT tests in air and hydrogen. *Materials & Design*, *254*, 113950. https://doi.org/10.1016/j.matdes.2025.113950

Seppälä, O., Ilmola, J., Kaijalainen, A. & Larkiola, J. (2026). Simulating thermo-mechanical and microstructural phenomena in a laboratory-scale hot rolling mill. *Materials&Design, 263,* 115694. https://doi.org/10.1016/j.matdes.2026.115694

Wali, H., Skriko, T., et al. (2026) Investigating shielding gas effects with multi-sensor robotic welding setup focusing on ultra-high strength steel in the GMAW process. To be submitted (spring 2026).

Yanchukovich, A., Ahola, A., Björk, T. & Sonsino, C. M. (2024). Comparison of analytical and numerical methods for estimating notch strains. *Materials Science and Engineering Technology*, *55*, 719-732. https://doi.org/10.1002/mawe.202300095

CONFERENCE PAPERS

Abdelghany, A. W., Haiko, O., Järvenpää, A., & Kaijalainen, A. (2026). Revealing the Microstructure and Mechanical Properties of Rapidly Quenched and Tempered 51CrV4 Steel Processed Via a Continuous Induction Line. *Solid State Phenomena* 383 (2026) 7–12. https://doi.org/10.4028/p-69oURO

Afkhami, S., Ghafouri, M., Poutiainen, I., Pokka, A.-P., Javaheri, V., Larkiola, J., Björk, T. & Moshtaghi, M. (2025). Effect of service temperature on the failure of additively manufactured 13Cr10Ni2Al stainless tool steel. *ECF 2024*. Abstract accepted

Ahola, A., Leitner, M., Grönlund, K., Brunnhofer, P., Buzzi, C., Moshtaghi, M. & Björk, T. (2024). Fatigue strength assessment of welded high-strength and ultra-high-strength steel joints in the as-welded and high-frequency mechanical impact (HFMI)-treated conditions under variable amplitude loading (IIW doc. XIII-3057-2024). 77th IIW Annual Assembly and International Conference, 7-12 July 2024, Rhodes, Greece.

Ahola, A., Lipiäinen, K., Suikkanen, P. & Skriko, T. (2025). Fatigue assessment of welded thin-walled automotive steels using effective stress methods. 78th IIW Annual Assembly and International Conference, 22-27 June 2025, Genoa, Italy.

Alatarvas, T., Tervo, H., Kaijalainen, A. & Shu, Q. (2024). Utilizing computational thermodynamics in

characterization and classification of non-metallic inclusions in Ti-deoxidized steels. *Proceedings of SIMS EUROSIM 2024*, 185–191. http://dx.doi.org/10.3384/ecp212.025

Auvinen, H., Tervo, H., Sainio, J., Kömi, J. & Kaijalainen, A. (2026). The effect of alloying contents on impact toughness and microstructure of physically simulated heat-affected zones of 500MPa structural steels. *TIMA 25*. In review.

Elaraby, M., Ali, M., Eissa, M., Kömi, J., Karjalainen, P., Tervo, H., Alatarvas, T., Ghassemali, E., Steggo, J. & Javaheri, V. (2025). Thermodynamic and Algorithmic Optimization of Medium Manganese Steel Composition Design, Non-Metallic Inclusion Analysis, and Microstructural Insights. *Solid State Phenomena*, *383*, 25–32. https://doi.org/10.4028/p-B8yPFf

Gáspár, M., Kovács, J., Tervo, H., Kaijalainen, A., Javaheri, V, Sainio, J. & Kömi, J. (2025). The microstructure and fracture mode of physically simulated heat-affected zones of a weld metal used with 500 MPa offshore steel – part 1: impact toughness test results. Procedia *Structural Integrity*, *68*, 500–505. https://doi.org/10.1016/j.prostr.2025.06.088

Gáspár, M., Kovács, J., Sainio, J., Tervo, H., Javaheri, V. & Kaijalainen, A. (2024). The effect of welding thermal cycles on weld properties of 500 MPa grade offshore steel. *32nd Hungarian Welding Conference 2024*, 88-94. https://www.researchgate.net/publication/387997965_The_effect_of_welding_thermal_cycles_on_weld_properties_of_500_MPa_grade_offshore_steel

Hoikkaniemi, A. J. T., Haiko, O., & Kaijalainen, A. (2026). Effect of EAF Impurities on Microstructure and Mechanical Properties of Low-Carbon Steels. *Solid State Phenomena, 383*, 13–18. https://doi.org/10.4028/p-s1q3hn

Kaijalainen, A., Abdelghany, A., Haiko, O., Hoikkaniemi, A., & Pokka, A.-P. Microstructural Modification and Bendability Improvement in 1300 MPa Steel via Induction Surface Heat Treatment. ESAFORM 2026.

Kaijalainen, A., Pokka, A.-P., Jaskari, M., Huuki, J., Hintsala, T. & Kömi, J. (2024). Effect of surface characteristics on strain distribution in airbending. *Metal Forming 2024*, *44*, pp 350-357. https://doi.org/10.21741/9781644903254-37

Kaijalainen, A., Pokka, A., Jaskari, M., Huuki, J., Hintsala, T. & Kömi, J. (2025). The impact of surface properties on strain distribution in air-bending. *THERMEC 25*. Submitted

Kantanen, P., Plosila, P., Javaheri, V., Perkiö, T. & Kaijalainen, A. (2025). Strain-induced martensite formation during punching of a medium manganese advanced high-strength steel. *Procedia Structural Integrity*, *69*, 53–60. https://doi.org/10.1016/j.prostr.2025.07.008

Kesti, V., Grifé, L., Plosila, P., Frómeta, D. & Kaijalainen, A. (2025). The Relationship Between Fracture Toughness and Blanking Performance of 850MPa Hot-Rolled Steels. *MATEC Web of Conferences / IDDRG 2025*, *408*, 1034. https://doi.org/10.1051/matecconf/202540801034

Latypova, R., Fangnon, E., Ghosh, S., Pallaspuro, S., Claeys, L., Verbeken, K., Depover, T., & Kömi, J. (2025) Effect of silicon alloying on hydrogen diffusion and trapping in medium-carbon DQ&P steels, 5th International Conference on Metals and Hydrogen 2025.

Latypova, R., Fangnon, E., Nousiainen, O., Pallaspuro, S. & Kömi, J. (2024). Role of prior austenite grain structure in hydrogen diffusion, trapping, and embrittlement mechanisms in as-quenched martensitic steels. *Procedia Structural Integrity*, *54*, 149–155. https://doi.org/10.1016/j.prostr.2024.01.067

Lehtola, K., Ilmola, J., & Larkiola, J. (2026). Finite element modeling of electromagnetic heating. *Materials Science Forum, 1174*, 39–46. https://doi.org/10.4028/p-cR2Wo5

Leitner, M., Ahola, A., Moshtaghi, M., Björk, T., Brunnhofer, P. & Buzzi, C. (2024). Fatigue strength assessment of HFMI-treated steel joints under bending loading. 77th IIW Annual Assembly and International Conference, 7-12 July 2024, Rhodes, Greece.

Lipiäinen, K., Heinilä, S., Teikari, J., Ahola, A. & Skriko, T. (2025). Fatigue strength improvement of circular hollow section tube-to-gusset plate detail with welding techniques. 78th IIW Annual Assembly and International Conference, 22-27 June 2025, Genoa, Italy.

Nousiainen, O., Hannula, J., Kaijalainen, A. & Kömi, J. (2025). Effect of wire electrical discharge machining on hole expansion ratio of 1 GPa low carbon low alloyed steel. *Materials Science Forum, 1174*, 33-38. https://doi.org/10.4028/p-U6kuph

Nyo, T., Autio, L., Tulonen, J. & Kaijalainen, A. (2025). Effect of Cold-Forming on Mechanical Properties of AHSS Steel. *Materials Science Forum, 1174*, 15-19. https://doi.org/10.4028/p-sSYx8h

Pallaspuro, S., Hesse, A., Tóth, T., Aho, N., Mirshekari, B., Ghosh, S., Lindqvist, S., Dilger, K. & Kömi, J. (2025). Low-temperature fracture toughness of electron-beam welded low-carbon martensitic-austenitic steel. *Procedia Structural Integrity*, 68, 802-808. https://doi.org/10.1016/j.prostr.2025.06.133

Perkiö, T., Kantanen, P. & Kaijalainen, A. (2026). Effect of intercritical annealing temperature to mechanical performance of hot-rolled medium manganese steel. *Materials Science Forum*, *174*, 83–88. https://doi.org/10.4028/p-kG28cH

Plosila, P, Kantanen, P., Hannula, J., Javaheri, V., Kömi, J. & Kaijalainen, A. (2024). Hole expansion performance of a medium manganese advanced high-strength steel after hot rolling and intercritical annealing. *Materials Research Proceedings*, *44*, 358-367. https://doi.org/10.21741/9781644903254-38

Plosila, P., Kesti, V., Nousiainen, O., Tervo, H., Joy, J., Hannula, J., Kömi, J. & Kaijalainen, A. Characterization of microstructural features and their contribution on mechanical properties of hot-rolled advanced high-strength ferritic and complex-phase steels. To be published 2026.

Plosila, P., Vierelä, R., Juntunen, P., Kesti, V., Kömi, J. & Kaijalainen, A. (2025). An investigation on behaviour of 800 MPa grade hot-rolled steels in interrupted ISO 16630 hole expansion testing. *MATEC Web of Conferences / IDDRG 2025*, *408*, 1073. https://doi.org/10.1051/matecconf/202540801073

Pokka, A.-P., Kesti, V., Troive, L. & Kaijalainen, A. (2024). Development of the cross-section moment in air-bending. *Materials Research Proceedings*, *41*, 1027–1037. https://doi.org/10.21741/9781644903131-113

Rohani Raftar, H., Safyari, M. & Moshtaghi, M. (2025). Hydrogen-assisted fatigue crack growth in pipeline steels: a machine learning approach. *Procedia Structural Integrity*, *68*, 1066–1073. https://doi.org/10.1016/j.prostr.2025.06.171

Tervo, H., Gáspár, M., Kovács, J., Javaheri, V., Sainio, J., Alatarvas, T., Kömi, J., & Kaijalainen, A. (2026). Evolution of inclusions in physically simulated heat-affected zones of a weld metal used with a 500 MPa offshore steel. *Key Engineering Materials, 1040*, 47–53. https://doi.org/10.4028/p-KPi3DF

Tervo, H., Gáspár, M., Kovács, J., Kaijalainen, A., Javaheri, V., Sainio, J., & Kömi, J. (2024) Physical Simulation of Heat-Affected Zones in a Weld Metal Used with 500 MPa Offshore Steel. Linköping Electronic Conference Proceedings 212; *Proceedings of the Second SIMS EUROSIM Conference on Modelling and Simulation, SIMS EUROSIM 2024* (Ed. E. Juuso et al.), 236-241. https://doi.org/10.3384/ecp212.033

Tervo, H., Gáspár, M., Kovács, J., Javaheri, V., Sainio, J., Kömi, J., & Kaijalainen, A. Electron Backscatter Diffraction Characterization of Physically Simulated Heat-Affected Zones of a Weld Metal Used with 500 Mpa Offshore Steels, presented in TIMA25 conference in November 2025, to be published by Trans Tech Publications in 2026.

Tervo, H., Gáspár, M., Kovács, J., Kaijalainen, A., Javaheri, V., Sainio,J. & Kömi, J. (2025). The microstructure and fracture mode of physically simulated heat-affected zones of a weld metal used with 500 MPa offshore steel – part 2: fractographies, inclusions and microstructures. *Procedia Structural Integrity*, *68*, 508–512. https://doi.org/10.1016/j.prostr.2025.06.089

CONFERENCE PRESENTATIONS

Ahmed, et al. (2024). Current trends in alloy development. Materials Day 2024, 10.10.2024 Tampere.

Raami, L. (2024). Quenching and partitioning: A novel process to improve the cavitation erosion resistance of AISI 420 stainless steel. Materials Day 2024, 10.10.2024 Tampere.

PROFESSIONAL MAGAZINE

Gáspár, M., Kovács, J., Sainio, J., Tervo, H., Javaheri, V. & Kaijalainen, A. (2024). A többrétegű varratfelépítés hatásának elemzése fizikai szimulációval 500 MPa szilárdsági kategóriájú hajóacélnál. *Hegesztéstechnika*, *XXXV* (2), 37–42.

Kaijalainen, A. & Plosila, P. (2024). Fossiilivapaat terässovellukset Suomen teräsekosysteemissä, FOSSA2 (Fossil-Free Steel Applications: Phase II). *Ohutlevy (1)*, 14–16. https://urn.fi/URN:NBN:fi:oulu-202409266064

Lund, H., Penttilä, S. & Skriko, T. (2024). Moderni hitsausautomaatio. *Hitsaustekniikka*, Vol. 76:6, 10-15.

Martikainen, A., Penttilä, S., Lund, H. & Skriko, T. (2025). Cobotti- ja robottiautomaation tuottavuuden ja laadun tehostamismahdollisuudet hitsaavassa teollisuudessa. *Hitsaustekniikka*, Vol. 77:3, 27-28

THESES

Doctoral theses

Ahmed, S. Microstructural Evolution and Mechanical Response of Medium Manganese Steels Subjected to Intercritical Annealing Quenching and Partitioning [Doctoral thesis, Tampere University]. To be submitted 2026.

Horváth, D. Hydrogen embrittlement of welded steels. [Doctoral thesis, LUT University]. On-going.

Ilmola, J. (2025). *Modeling of a thermo-mechanically controlled virtual finishing rolling mill and coil cooling processes* (Acta Universitatis Ouluensis) [Doctoral thesis, University of Oulu]. Acccessible: https://urn.fi/URN:NBN:fi:oulu-202412187446

Lund, H. (2025). *Extended reality-enabled smart manufacturing in multi-robot welding applications* [Doctoral thesis, LUT University] Acccessible: https://urn.fi/URN:ISBN:978-952-412-263-4

Meneses, W. Modelling of surface phenomena [Doctoral thesis, University of Oulu]. On-going.

Neupane, D. *Simulation-based models for high-quality welds subjected to cyclic loads*. [Doctoral thesis, LUT University]. On-going. .

Pesonen, T. (2026). *Finite element simulation-based fatigue assessment of welded high-strength steel joints* [Doctoral thesis, LUT University] Accepted, public defence 2 June 2026.

Plosila, P. *Effect of microstructure on cut edge formability of advanced high-strength hot rolled steels* [Doctoral thesis, University of Oulu]. To be submitted 2026.

Pokka, A.-P. *Bendability of ultrahigh-strength steels* [Doctoral thesis, University of Oulu]. To be submitted 2026.

Raami, L. (2026). *Quenching and partitioning of Martensitic Stainless Steels: Heat Treatment, Microstructure, Mechanical Properties, and Cavitation Erosion Resistance*, [Doctoral thesis, Tampere University].

Sabr, A. Effects of Trace Elements Copper and Tin in Dual-Phase Steels [Doctoral thesis, Tampere University]. To be submitted 2026.

Seppälä, O. *Simulating the microstructural evolution of TMCP steel* [Doctoral thesis, University of Oulu]. (under pre-examination)

Wali, H. *Welding automation for high-quality* weldments [Doctoral thesis, LUT University]. On-going.

Master´s theses

Autio, L. (2025) *Fracture toughness and crack initiation of welded S420 offshore steels at a low temperatures -80 C* [Master´s thesis, University of Oulu]. Accessible: https://urn.fi/URN:NBN:fi:oulu-202503192100

Auvinen, H. (2026) *Microstructure and toughness properties of physically simulated heat-affected zone of 500 MPa low-carbon bainitic steels* [Master´s thesis, University of Oulu]. Accessible: https://urn.fi/URN:NBN:fi:oulu-202601211321

Ayub, H. (2026). *Effect of arc welding on microstructure and mechanical properties of S960 MC to S960 QT Ultra-High Strength Steel (UHSS) dissimilar joints* [Master´s thesis, LUT University]. (To be published).

Devkota, J. (2025). *Mechanical performance and fracture behaviour of dissimilar welds made of thermo-mechanically rolled steels: a study of dissimilar steel grades weld joint between S700 MC Plus, and Domex 500 D* [Master´s thesis, LUT University] Accessible: https://urn.fi/URN:NBN:fi-fe2025061871725

Forsman, J. (2024). *Utilization of high-strength fossil-free steels in ship hull structures* [Master´s thesis, LUT University]. Accessible: https://urn.fi/URN:NBN:fi-fe2024112696828

Ghasemi, A. (2026) *Simulation of hydrogen TDS peaks and ML-based prediction of desorption energies (SimuTDS) from experimental data* [Master's thesis, LUT University]. Accessible: https://urn.fi/URN:NBN:fi-fe2026030718761

Halonen, H. (2025). *Q&P treatment of a eutectoid silicon steel* [Master's thesis, Tampere University]. Accessible: https://urn.fi/URN:NBN:fi:tuni-2025120511294

Harjula, S. (2024). *Potential of laser welding technologies in forestry machine manufacturing* [Master´s thesis, LUT University]. Accessible: https://urn.fi/URN:NBN:fi-fe20241220106089

Hintsala, T. (2025). *Effect of alloying content and cooling parameters on mechanical properties of low carbon bainitic steel* [Master´s thesis, University of Oulu]. Accessible: https://urn.fi/URN:NBN:fi:oulu-202509175890

Hoikkaniemi, A. (2024). *Effect of EAF impurities on microstructure and mechanical properties of low-carbon steels* [Master´s thesis, University of Oulu].

Jussila T. (2025) *Liimaliitoksen numeerinen mitoitus kuormaa kantavaan rakenteeseen metsäteollisuuden työkoneessa* [Master theses, Tampere University]

Keskinen, A. (2026) *Comparison between different methods for fatigue evaluation of a hooklift for use in real time simulation* [Master´s thesis, LUT University]. Publication pending.

Kittilä E. (2025) *Alumiinin ja teräksen liimaus kantavan rakenteen komponentissa*. [Master theses, Tampere University]

Lainio I. (2024) *Hiilikädenjäljet kuormakoneen kouran jatkokehityksessä* [Master theses, Tampere University]. Accessible: https://urn.fi/URN:NBN:fi:tuni-202405286375

Lehtola, K. (2024). *Finite element modeling of electromagnetic heating* [Master´s thesis, University of Oulu].

Mikkanen, A. (2025). *Fatigue assessment of welded thin-walled joint using local approaches* [Master´s thesis, LUT University]. Accessible: https://urn.fi/URN:NBN:fi-fe20251204114396

Ojala, J. Finite element analysis for fatigue crack growth assessment using linear elastic fracture mechanics (LUT) [Master´s thesis, LUT University]. On-going

Olkkonen, R. (2025). *Optimal welding parameters for geometrically and metallurgically high-quality thin-walled sheet metal joints* [Master´s thesis, LUT University]. Accessible: https://urn.fi/URN:NBN:fi-fe2025090894868

Perkiö, T. (2024). *Optimizing intercritical annealing treatment for hot-rolled medium-manganese steels* [Master´s thesis, University of Oulu]. Accessible: https://urn.fi/URN:NBN:fi:oulu-202412187424

Pihlava, E. Press hardening of medium manganese steels [Master's thesis, Tampere University]. To be submitted 2026.

Piipponen, V.-V., Trace elements and their effect on properties of hot rolled plate steels [Master´s thesis, University of Oulu]. On-going

Rao, A. Master S-N curve analysis of 4R method using effective stress method (LUT) [Master´s thesis, LUT University]. On-going

Saksa, T. (2024). *Optimization of hooklift axle joints with high strength steel (HIAB Finland)* [Master´s thesis, LUT University]. Accessible: https://urn.fi/URN:NBN:fi-fe2024111492466

Silvola, H. (2026) *Computational modeling of welding deformations in a boom structure* [Master´s thesis, LUT University]. Publication pending.

Titevskaja, A. (2026) *Corrosion resistance and mechanical strength of welded weathering steels* [Master´s thesis, LUT University].

Veijonaho, V. (2025). *Experimental and computational investigation of the bendability of 960MPa ultra-high strength steel* [Master´s thesis, University of Oulu].

Bachelor´s theses

Garabics, B. (2026). Residual stresses in welded ultra-high-strength steels and their correlation with microstructure [Bachelor's thesis, LUT University] (to be published).


SSAB Zero™ steel
Made using recycled steel
and fossil-free energy
Carbon emissions
The fossil carbon emissions in SSAB's
production of SSAB Zero™ steel are
<0.05
kg CO_2e/
kg steel
in Scope 1 and 2 of the GHG Protocol
vs. global average carbon emissions
1.5 kg CO_2e/kg steel
(recycled and iron-ore based)
ssab.com
SSAB

Photo: SSAB

FOSSA2

FOSSA2 - Fossil-free Steel Applications: Final report

Publisher and contact information
Macon Oy
Metsänkuninkaantie 3,
90250 Oulu, Finland
info@macon.fi